STUDY ON ETHYLENE GAS PERMEABILITY OF SEBS/LDPE DOUBLE - LAYERED ZEOLITE COMPOSITE FILM

PORNPAN MONPRASIT

A THESIS SUBMITTED IN PARTIAL FULFILLMENT

OF THE REQUIREMENT FOR THE DEGREE OF

MASTER OF SCIENCE IN POLYMER TECHNOLOGY

FACULTY OF SCIENCE

KING MONGKUT'S INSTITUTE OF TECHNOLOGY LADKRABANG

2010

KMITL - 2010 - SC - M - 014 - 005

หัวข้อวิทยานิพนธ์	การศึกษาการแพร่ของก๊าซเอทิลีนผ่านฟิล์มคอมโพสิตสองชั้นพอลิเอทิลีนชนิดความหนาแน่นต่ำและพอลิเมอร์ร่วมสไตรีนเอทิลีนบิวทิลีนสไตรีนที่ปรับปรุงด้วยซีโอไลต์
นักศึกษา	นางสาวพรพรรณ มั่นประสิทธิ์
รหัสประจำตัว	49067908
ปริญญา	วิทยาศาสตรมหาบัณฑิต
สาขาวิชา	เทคโนโลยีพอลิเมอร์
พ.ศ.	2553
อาจารย์ผู้ควบคุมวิทยานิพนธ์	รศ.ดร.ตะวัน สุขน้อย
อาจารย์ผู้ควบคุมวิทยานิพนธ์ร่วม	ผศ.ดร.สุภารัตน์ รักชลธี
	ดร.อศิรา เฟื่องฟูชาติ
	ผศ.ดร.ชลลดา ฤตวิรุฬห์

บทคัดย่อ

ในงานวิจัยนี้ฟิล์มคอมโพสิตสองชั้นถูกเตรียมขึ้นเพื่อนำไปศึกษาการแพร่ผ่านของก๊าซเอทิลีนเพื่อดูความเป็นไปได้ในการนำไปประยุกต์ใช้เป็นฟิล์มบรรจุภัณฑ์ โดยทำการขึ้นรูปฟิล์มคอมโพสิตสองชั้นด้วยการกดอัดฟิล์มพอลิเอทิลีนชนิดความหนาแน่นต่ำ (LDPE) และพอลิเมอร์ร่วมสไตรีน-เอทิลีน-บิวทิลีน-สไตรีน (SEBS) ที่ผสมซีโอไลต์ชนิด ZSM-5 ในปริมาณ 5 10 20 และ 30% โดยน้ำหนัก จากนั้นทำการศึกษาสัณฐานวิทยา เสถียรภาพทางความร้อน สมบัติเชิงกล และความสามารถในการแพร่ผ่านของก๊าซเอทิลีน ออกซิเจน คาร์บอนไดออกไซด์ และไอน้ำของแผ่นฟิล์มที่เตรียมได้ จากการศึกษาพบว่าฟิล์มดังกล่าวมีความสามารถในการแพร่ผ่านก๊าซเอทิลีนสูงขึ้นเมื่อเติมซีโอไลต์ ทั้งนี้เพราะซีโอไลต์สามารถดูดซับก๊าซเอทิลีนได้ดี จึงทำให้เกิดแรงผลักดัน (Driving force) ที่เพิ่มขึ้นอันเนื่องจากความแตกต่างของความเข้มข้น (Concentration gradient) ของก๊าซเอทิลีน และยังพบว่าความสามารถในการแพร่ผ่านก๊าซเอทิลีนเพิ่มสูงขึ้นเมื่อทำการปรับปรุงการกระจายตัวของซีโอไลต์ อย่างไรก็ตามความสามารถในการแพร่ผ่านก๊าซเอทิลีนของแผ่นฟิล์มไม่มีการเปลี่ยนแปลงเมื่อเพิ่มปริมาณซีโอไลต์มากกว่า 10% โดยน้ำหนัก และเมื่อเปรียบเทียบความสามารถในการแพร่ก๊าซเอทิลีนกับก๊าซชนิดอื่น พบว่าฟิล์มคอมโพสิตสองชั้นที่ผสมซีโอไลต์นั้นมีความจำเพาะเจาะจงในการแพร่ของก๊าซเอทิลีนมากกว่าฟิล์มที่ไม่มีซีโอไลต์ นอกจากนี้ยังพบว่าความสามารถในการแพร่ผ่านก๊าซเอทิลีนไม่ขึ้นกับความเข้มข้นของเอทิลีน แต่จะลดลงเมื่อในระบบมีก๊าซออกซิเจนผสมอยู่ ส่วนสมบัติเชิงกลของฟิล์มคอมโพสิตนั้นมีค่าความแข็งแรงดึง (Tensile strength) อยู่ในช่วง 17-19 MPa ซึ่งมีความเหมาะสมสำหรับการประยุกต์ใช้เป็นฟิล์มบรรจุภัณฑ์

Thesis Title	Study on ethylene gas permeability of SEBS/LDPE double-layered zeolite composite film
Student	Miss Pornpan Monprasit
Student ID.	49067908
Degree	Master of Science
Program	Polymer Technology
Year	2010
Thesis Advisor	Assoc.Prof.Dr. Tawan Sooknoi
Thesis Co-Advisor	Asst.Prof.Dr. Suparat Rukchonlatee
	Dr. Asira Fuongfuchat
	Asst.Prof.Dr. Chonlada Ritvirulh

ABSTRACT

In this work, the composite double-layered film was developed to improve the ethylene permselectivity and tensile properties for the packaging application of fresh fruits and vegetables. The double-layered film was prepared by laminating LDPE and SEBS modified with zeolite ZSM-5. The zeolite loading is 5-30 %wt of SEBS with surface rich zeolite (DB-SR) and with well dispersed zeolite (DB-WD) morphology. The film was characterized by scanning electron microscope (SEM), thermogravimetric analyzer (TGA) and differential scanning calorimeter (DSC). The double-layered film was tested for permeation of ethylene, oxygen, carbondioxide and water vapor. It was found that the ethylene permeability of the films was enhanced from 1,793 to 2,064 cc.mm/m^2.day.atm due to a readily adsorption of ethylene gas by contained zeolite from 0 to 10%wt. This leads to a higher ethylene concentration gradient across the film which becomes a driving force for ethylene permeation. Moreover, the high dispersion of zeolite increased the ethylene permeation up to 2,328 cc.mm/m^2.day.atm. It was also observed that there is no significant difference in ethylene permeation when zeolite contents were higher than 10%wt. As compared to oxygen and carbondioxide, it was observed that the double-layered composite films were more selective to ethylene. It was also found that ethylene permeation is not significantly changed with ethylene concentration. However, the ethylene permeation was decreased in the presence of oxygen due to a competitive adsorption by oxygen. In addition, the films possessed appreciate tensile property for packaging application (tensile strength is about 17-19 MPa).

ACKNOWLEDGEMENT

The author would like to express my profound gratitude to my advisors, Assoc.Prof.Dr. Tawan Sooknoi, Asst.Prof.Dr. Suparat Rukchonlatee, Asst.Prof.Dr. Chonlada Ritvirulh and Dr. Asira Fuongfuchat for their supervisions, helpful suggestion and encouragement throughout this thesis. She is also grateful to Asst.Prof.Dr. Pathavuth Monvisade and Assoc.Prof.Dr. Suwabun Chirachanchai for serving as the chairperson and the committees, and valuable comment.

The author would like to extend this sincere appreciation to all of my teachers, friends and research team for their constant guidance advice, support and encouragement.

The special thank go to Thailand Graduate Institute of Science and Technology (TGIST) for a scholarship. In particularly, the author would like to thank National Metal and Materials Technology center (MTEC) for financial support, help support on blown film and permeability of gas instrument. Thanks are also due to everyone who has contributed suggestion and supports throughout this work.

Sincere thanks to Dr. Doungporn Sirikittikul, Miss Warintorn Booncharoen and Miss Methawadee Thirasat for their advice, suggestion helpful and kindness.

Sincere thanks to the Department of Chemistry, Faculty of Science, King Mongkut's Institute of Technology Ladkrabang for equipment, chemicals and facilities.

Finally, the author dedicates her thesis to parents and family for the constant love and encouragement.

Pornpan Monprasit

TABLE OF CONTENTS

TABLE OF CONTENTS (Continued)

TABLE OF CONTENTS (Continued)

LIST OF TABLES

LIST OF TABLES (Continued)

LIST OF FIGURES

LIST OF FIGURES (Continued)

LIST OF FIGURES (Continued)

CHAPTER 1

INTRODUCTION

1.1 Motivation

Fresh fruit and vegetables need to be stored until their consumption. In order to extend their storage life, it is necessary to reduce rate of biological activities and physiological changes. One of important biological activities is respiration (or metabolism) that normally consumes oxygen and produce carbon dioxide and water vapor. In addition, the postharvest products can also generate the ethylene gas that is a natural growth hormone. Ethylene gas can produce several physiological changes in these produces such as ripening and senescence. Hence, if the fresh produces contact to ethylene gas, their storage time will be shorten. A better preservation of these fresh produces can be obtained by decreasing the ethylene accumulation and the respiratory intensity via control of oxygen, carbon dioxide, water vapor and ethylene contents in the product package. Potassium permanganate is often used to be ethylene removal absorbent, however; it is harmful chemical. Therefore, it is interesting to develop a smart packaging that can provide appropriate storage condition for fresh produces [1-3].

Nowadays, polyolefin has been used in general packaging. This is because it possesses various functional properties including high flexibility, optical clarity, sealability, long shelf life, dimensional stability during sterilization, flex resistance, biocompatibility and environmental compatibility. In addition, it is generally cost effective. However, polyolefin packaging exhibits low water vapor, oxygen, carbon dioxide and ethylene permeability [4]. Hence, it is not suitable as packaging for ethylene sensitive fruits and vegetables. Alternative candidate can be styrene-(ethylene-butylene)-styrene block copolymer (SEBS). This is because it is a non polar polymer with higher flexibility and free volume, as compared to PE. This can be used as a smart packaging with a higher gas and water vapor permeability. In the previous work [5], it was found that zeolite/SEBS composite film showed high ethylene permeability as compared to oxygen and carbon dioxide. However, zeolite/SEBS composite film cannot be fabricated using conventional blown film process. Although, zeolite/SEBS composite film can be prepared by solution casting, it showed poor zeolite dispersion. It is, therefore, of interest to develop double-layered film of zeolite/SEBS and LDPE which can improve the ease of film fabrication and zeolite dispersion. In addition, such film would provide a better mechanical property.

In this research, the fabrication of the double-layered film was attempted to obtain a novel smart packaging with high ethylene permeation. The films were tested for permeability of ethylene, oxygen, carbon dioxide and water vapor and tensile property. The effect of the zeolite dispersion on permeation was also investigated.

1.2 Objectives

1.2.1 To obtain the double-layered films of LDPE-zeolite/SEBS composites with high ethylene permeability which is suitable for fresh produce packaging application.

1.2.2 To understand the effects of zeolite content and dispersion in the films on the ethylene permeation.

1.3 Scope of study

The scope of the study of ethylene permeable zeolite composite double-layered film is as follows:

1.3.1 Preparation zeolite/SEBS composite film using solution casting process with different zeolite dispersion. (The zeolite contents are varied by 5, 10, 20 and 30 %wt in SEBS layer.)

1.3.2 Preparation of composite double-layered film from zeolite/SEBS composite film and LDPE blown film by hot press technique.

1.3.3 Investigation on morphology, thermal stability and tensile property.

1.3.4 Investigation on the effect of zeolite content and dispersion on ethylene, oxygen, carbon dioxide and water vapor permeabilities.

1.3.5 Investigation on ethylene permeability in the mixed gas system.

1.4 Expected results

1.4.1 The developed packaging film can be used to preserve freshness and quality of the produces for exporting.

1.4.2 The knowledge obtained for this interesting can be applied for development of other selective gas permeation films.

CHAPTER 2

THEORY AND LITERATURE REVIEWS

2.1 Zeolite

2.1.1 Zeolite description [6]

Zeolites are a large group of natural or synthetic hydrated aluminum silicates. They are characterized by an aluminosilicate framework structure (complex three-dimensional structure) with large cage cavities that can accommodate sodium, calcium, or other cations (positively charged atoms or atomic clusters), water molecules, and even small organic molecules. Ions and molecules in the cages can be removed or exchanged without destroying the aluminosilicate framework. Nowadays, zeolites are available on a large scale and in a variety of applications. The major use of zeolites is as ion exchangers in laundry detergents where they remove calcium and magnesium from water by exchanging it for sodium present in the zeolite. Furthermore, zeolites are applied as adsorbents in the purification of gas streams to remove water and volatile organic species, and in the separation of different isomers and gas-mixtures, moreover they are applied in the clean up of radioactive waste. However, in this thesis the focus will entirely be on the application of zeolites as selective adsorbent for permeable film.

2.1.2 Structure of zeolite [7-9]

Zeolite structures consist of silica and alumina tetrahedra, that is silicon (Si^{4+}) or aluminum ions (Al^{3+}) surrounded by four oxygen ions (O^{2-}) in a tetrahedral configuration. This is called a primary unit. Each oxygen anion is bonded to two adjacent silicon or aluminum ions. When many primary units are connected together, there are many secondary building units (SBUs) formed. The common SBUs are shown in Figure 2.1. The SBUs are connected to form polyhedra units that are further linked to build up the entire framework (Schematic diagram of framework formation is shown in Figure 2.2).

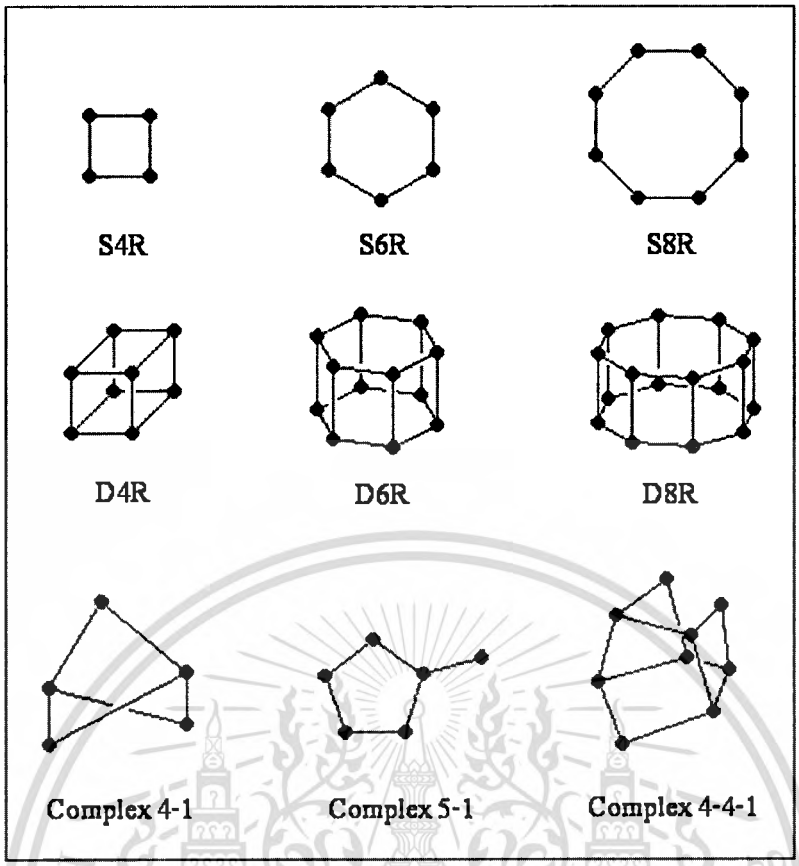

Figure 2.1 Secondary building units (SBUs) in zeolite [10]

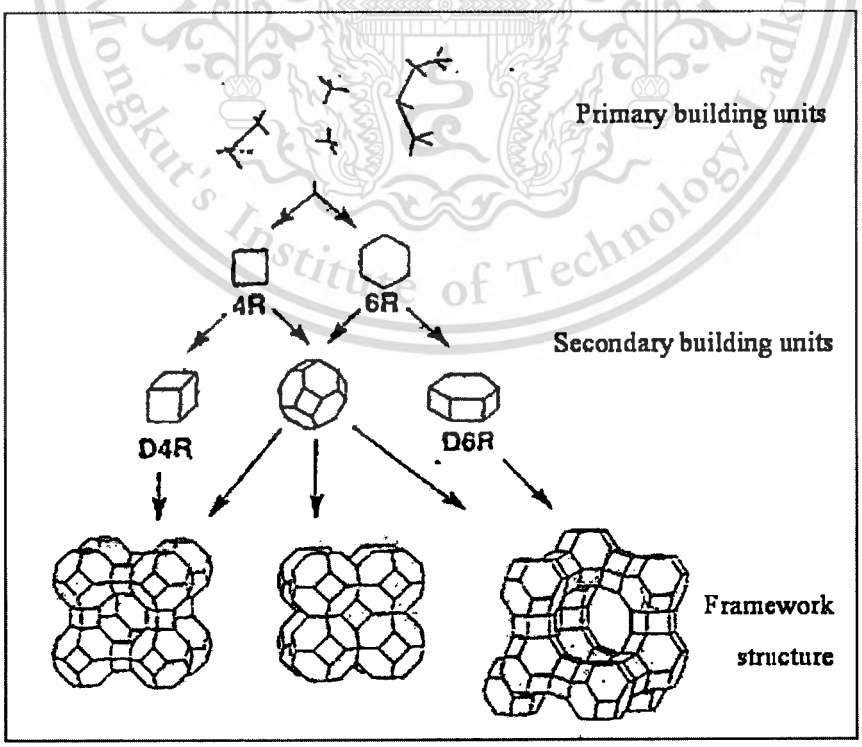

Figure 2.2 Schematic diagram of framework formation

Zeolite structures are a macromolecular aluminosilicate framework (three-dimensional) with net SiO_4^{-4} and AlO_4^{-5} tetrahedral building blocks. This can cause the framework of a zeolite having a negative charge when an alumina tetrahedral is present. So, a cation must be present to balance the charge. Commonly, the negative charge is compensated by additional non-framework cations like sodium (Na^+), which is generally present after the synthesis of the zeolite. Furthermore, charge balancing cations can be exchanged by other cations. In addition, the zeolite structure consists of a pore system that can be classified as cages and channels (one, two or three dimensions). For example, zeolite Y (FAU) is zeolite with cages structure framework having large cavities present while Ferrierite (FER) is zeolite having channels framework with two-dimension. The structures of these different zeolites are displayed in Figure 2.3.

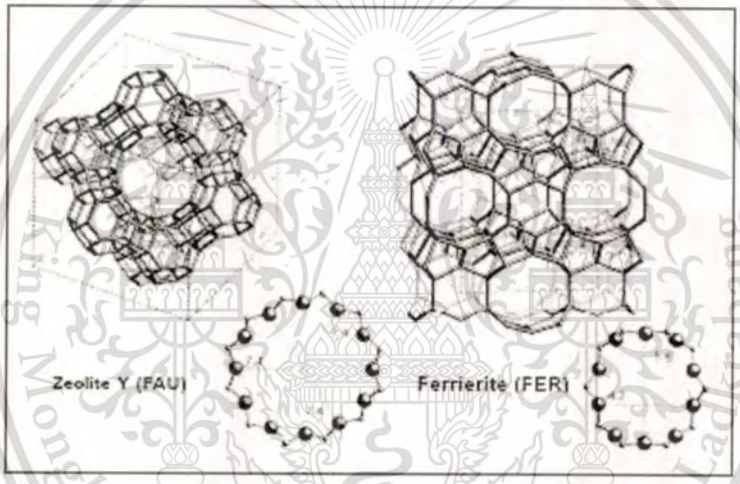

Figure 2.3 Framework structures of zeolite Y (FAU) and ferrierite (FER) [9]

The diameters of the pores and cavities range from 3 Å to 12 Å, which coincides with the dimensions of many hydrocarbon molecules for which they are applied as adsorbents and catalysts. The exact diameter of the pore depends on the coordination and the amount of cations present in the ring. In this thesis the main focus will be on the zeolite ZSM-5.

2.1.3 ZSM-5 zeolite [8,11-13]

ZSM-5 (also known as MFI) is an aluminosilicate zeolite with a high silica and low aluminium content (high Si/Al ratio). It is composed of several Pentasil units linked together by oxygen bridges to form pentasil chains as shown in Figure 2.4. A Pentasil unit consists of eight five-membered rings. In these rings, the vertices are Al or Si and an O is assumed to be bonded between the vertices. The structure of ZSM-5 is a channel framework that provided by 10 membered rings, as represented in Figure 2.5 (a).The pore structure is depicted schematically in Figured 2.5 (b); there are straight and elliptical pores in the cross section intersected by the horizontal pores in a zigzag pattern.

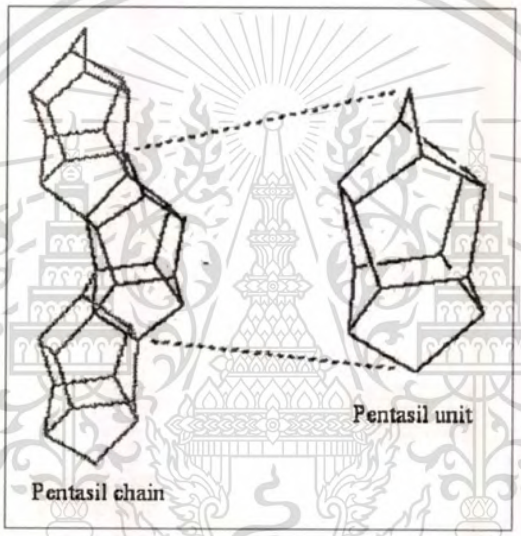

Figure 2.4 Pentasil unit and Pentasil chain [11]

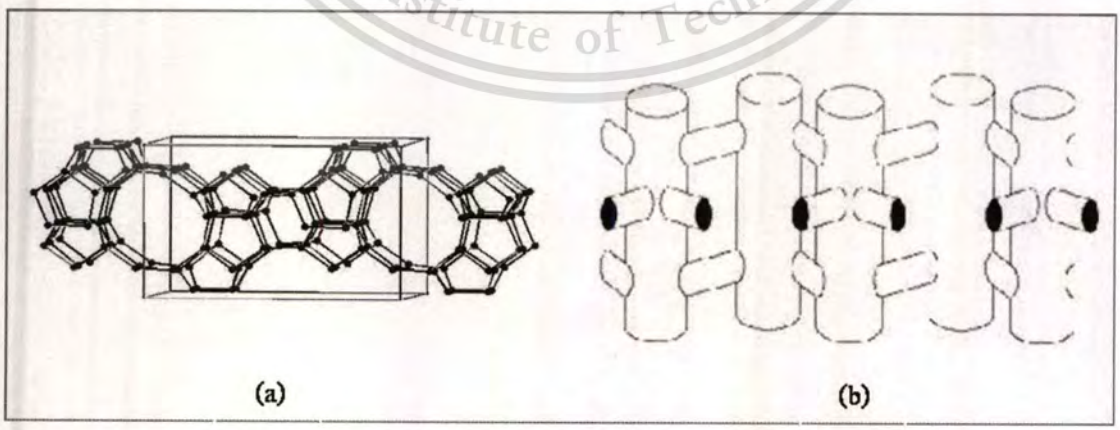

Figure 2.5 (a) Framework structure of ZSM-5 and (b) schematic diagram of the pore structure of ZSM-5 [12-13]

ZSM-5 have an estimated pore size of the channel running parallel with 5.4 – 5.6 Å. This size is approximately in the dimensional range of aromatic molecules, so that ZSM-5 has a high shape-selectivity in catalytic reaction. In additional, its broad range SiO_2/Al_2O_3 (30-100) makes ZSM-5 useful for various applications.

2.1.4 Zeolite as adsorbent [8,14-15]

Zeolite is microporous material having high surface area. The pores of zeolite are precisely uniform in size and molecular dimensions. Their porous structure can be used to sieve molecules having certain dimensions and smaller than that the pores size. Depending on the size of these pores, molecules may be readily adsorbed, slowly adsorbed or completely excluded. The selectivity in sieving is also based on polarity of the zeolite and the sieved molecule; for instance, hydrocarbon is hydrophobic molecule that prefers hydrophobic zeolite (high Si/Al). Due to their unique characteristics, zeolites are commercially used for drying and purifying liquids and gases, and for various industrial separation processes. For example, Zeolite A (LTA) are very effective desiccants and it can remove water from a moist gas with a very low partial pressure. Its adsorption capacity provides more than 25% of their weight in water. Other application of zeolite adsorption is shown in Table 2.1.

Table 2.1 Application of zeolite adsorption [8]

Application	Zeolite
Removal of water from natural gas	NaA
Adsorption of water from organic solvent	KA
Adsorption of VOC from water	Silicalite
Separation of SO_x, NO_x from air	Silicalite
Separation of H_2S from nature gas	CaA
Separation of n-butane/i-butane	MFI

2.2 Polymer

2.2.1 Low density polyethylene (LDPE) [16]

Low-density polyethylene (LDPE) is a thermoplastic made from oil. It was the first grade of polyethylene, produced in 1933 using a high pressure process via free radical polymerization. Its manufacture employs the same method today.

2.2.1.1 Structure of LDPE [17-19]

LDPE is a synthetic polymer that is formed by addition polymerization of ethylene monomer as shown in Figure 2.6. When ethylene molecules are polymerized to form polyethylene, they form long chains of carbon atoms in which each carbon also is bonded to two hydrogen atoms except the end carbon atom (bonded to three hydrogen atoms). LDPE structure and a repeating unit can be represented in Figure 2.7

Figure 2.6 Addition polymerization of ethylene monomer [18]

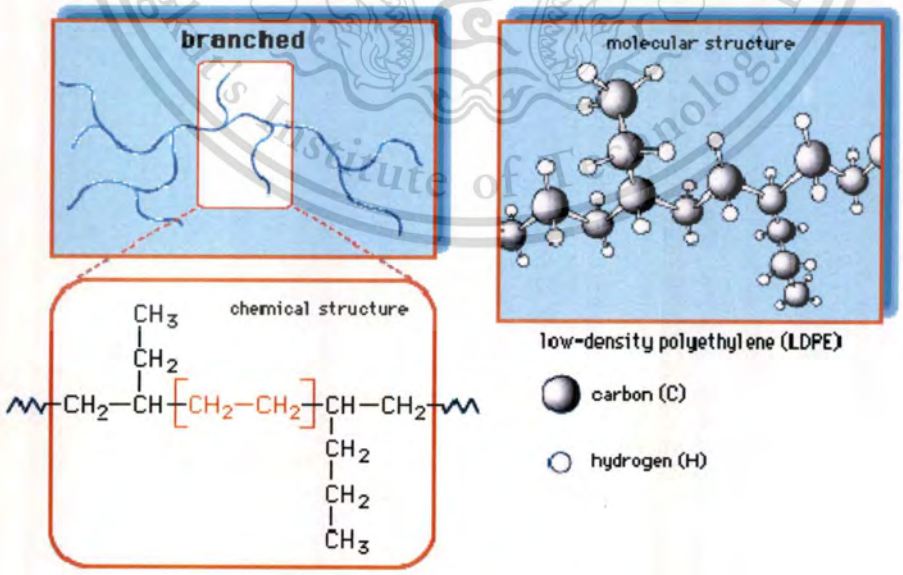

Figure 2.7 LDPE structure [19]

Branching can influence a number of physical properties including tensile strength and crystallinity of polyethylene (PE). LDPE has a high degree of short and long chain branching, which means that the chains do not pack into the crystal structure so well. It has, therefore, less strong intermolecular forces as the instantaneous-dipole induced-dipole attraction is less. This results in a lower tensile strength and increased ductility. The high degree of branching with long chains gives molten LDPE unique and desirable flow properties. In addition, comparing with HDPE, the major difference between LDPE and HDPE is the degree of branching of the polymer chain. HDPE is composed of linear, non-branched chains, while LDPE chains are branched. These different structures are compared in Figure 2.8. This cause leads to some different properties of LDPE and HDPE. Hence, they are suitable for different applications.

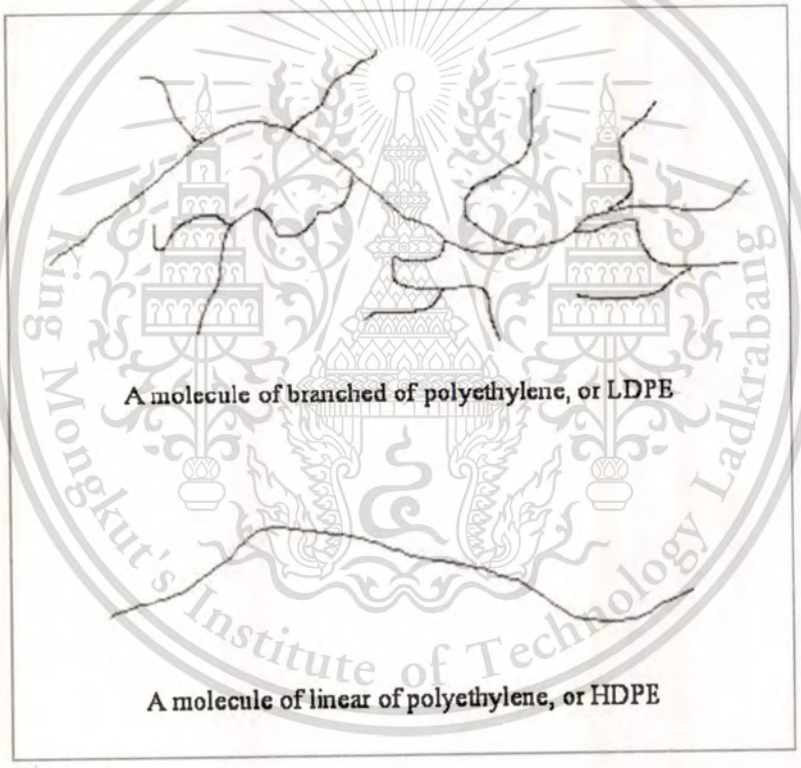

Figure 2.8 Structure comparing of LDPE and HDPE [17]

2.2.1.2 Properties of LDPE [16]

LDPE is defined by a density range of 0.910 - 0.940 g/cm³. This is due to more side chains branching. Melting temperature of LDPE is typically 105 – 115 °C and glass transition temperature is about -120 °C. It is translucent materials with low working temperature. It is unreactive at room temperatures, except by strong oxidizing agents, and some solvents cause

swelling. Chemicals resistance is shown in Table 2.2. It is soft, flexible, tough and low tensile strength while high impact strength. It posses poor temperature resistance which it can withstand temperatures of 80 °C continuously to 95 °C for a short time. LDPE exhibits low moisture permeability. Some of the benefits of the LDPE include its excellent electrical insulation properties, design versatility and low cost.

Table 2.2 Chemical resistance of LDPE [16]

Level	Solvent or chemical reagent
Excellent resistance (no attack)	Diluted and concentrated acids, alcohols, bases and esters
Good resistance (minor attack)	Aldehydes, ketones and vegetable oils
Limited resistance (moderate attack or suitable for short-term use only)	aliphatic and aromatic hydrocarbons, mineral oils, and oxidizing agents
Poor resistance (not recommended for use)	Halogenated hydrocarbons.

2.2.1.3 Applications of LDPE [16]

LDPE is widely used for manufacturing various containers, dispensing bottles, wash bottles, tubing, plastic bags for computer components, and various molded laboratory equipment. Its most common use is in plastic bags. Other products made from it include:

- Trays & general purpose containers
- Food storage and laboratory containers
- Corrosion-resistant work surfaces
- Parts that need to be weldable and machinable
- Parts that require flexibility, for which it serves very well
- Very soft and pliable parts
- Six-pack soda can rings
- Extrusion coating on paperboard and aluminum laminated for beverage cartons.
- Computer components, such as hard drives, screen cards and disk-drives.

2.2.2 Styrene ethylene-butylene styrene block copolymer (SEBS) [20-23]

SEBS is one type of styrenic block copolymers (SBC) which is a tri-block copolymer. Figure 2.9 shows the typical structure of a linear SBC. The styrene end-blocks are hard polymers. The mid-block is composed of rubbery polymer that is ethylene-butylene block).

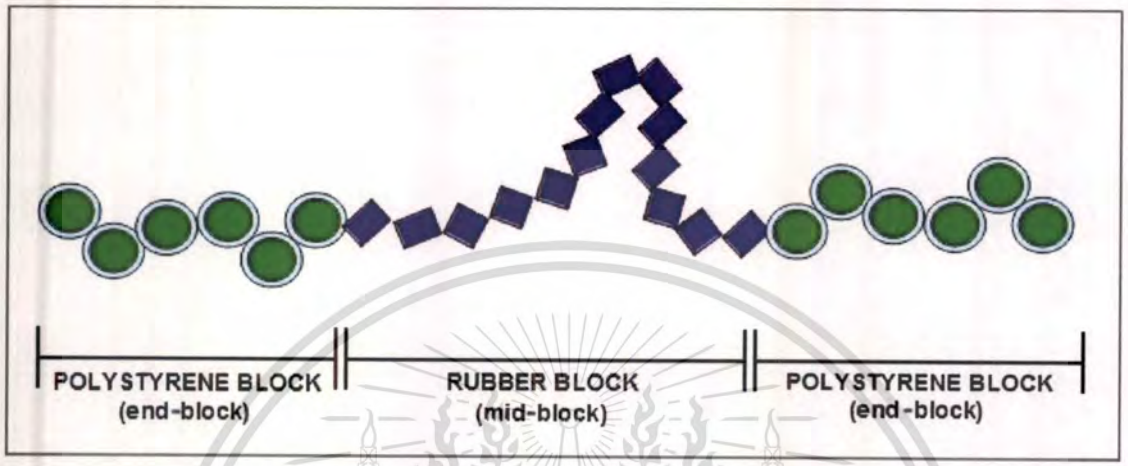

Figure 2.9 Schematic drawing of a linear styrenic tri-block copolymer [21]

SEBS has two glass transition temperatures (T_g), an upper one of about 95°C for the polystyrene domains and a lower one of about -55°C for ethylene-butylene blocks. This two phase structure gives SEBS high strength at end-use temperatures and also provides low viscosity and easy thermoplastic processing at elevated temperatures or in solvent solutions.

SEBS is high performance thermoplastic elastomer (TPEs) designed for use without valcanization. It has fully saturated mid-blocks for the ultimate in stability, which is high resistance to degradation by oxygen, ozone and UV light, and low color. However, it is the most difficult SBC to tackify. SEBS combines high elasticity and low temperature flexibility with resistance to water, acids, and alkalis. It also has a wide range of Shore hardness values. In addition, SEBS is also the highest in tensile strength comparing to other TPEs.

Because of their better thermal stability, SEBS compounds are used for more demanding applications in all market segments. One key application is grips where the soft touch, anti slip properties, good resistance to oil and grease are needed. In addition, SEBS shows major properties including transparency and easy to color, soft touch, room temperature compression set, high tear strength and elasticity, excellent surface appearance, non slip, and low hardness (down to 5 Shore A).

2.2.3 Polymer as packaging film [24-27]

There are numerous packaging materials used to be food packaging including paper, fibre board, glass, tinplate, aluminium and various types of plastics. In this thesis, plastic films are focused.

Plastic films are high performance materials, which play an essential part in modern life. They are mostly used in packaging applications along with some applications in agricultural, medical and engineering fields. Plastic films are perfectly stable, easy to work with and can be lighter than tissue. Moreover, they do not have voids in the surface that allow an ink or coating to penetrate into it. Many packages required transparency because people wanted to see what they were buying. Since then, many plastic films were added to the list of packaging films. Plastic films for packaging are available in the form of packaging pouches, packaging bags, packaging rolls, sheets, foils etc. Food packaging includes bags for bread and rolls, in-store bags for produce and bulk foods, candy wrap and bags, bag-in-a-box, carton liners for cereal and cake mixes, wrappers for fresh food, wrappers for prepared red meat, poultry and fish, milk bags, grocery bags.

The main purpose of food packaging is to protect the food from microbial and chemical contamination, oxygen, water vapor and light. The type of packaging used therefore has an important role in determining the shelf life of a food.

Packaging is described as "active" when it performs some role in the preservation of the food other than providing an inert barrier to outside influences. Active packaging does more than simply provide a barrier to outside influences. It can control, and even react to, events taking place inside the package. Active packaging employs a packaging material that interacts with the internal gas environment to extend the shelf-life of a food. Such new technologies continuously modify the gas environment by removing gases from or adding gases to the headspace inside a package.

Table 2.3 sets out some areas of atmosphere control in which active packaging is being successfully used.

Table 2.3 Use of active packaging [28]

Active Packaging System	Application
Oxygen scavenging	Most food classes
Carbon dioxide production	Most food affected by moulds
Water vapor removal	Dried and mould-sensitive foods
Ethylene removal	Horticultural produce
Ethanol release	Baked foods (where permitted)

2.3 Respiration in fresh produces and ethylene gas as growth hormone [2,29-31]

Respiration of fresh fruits and vegetables is metabolism that consumes oxygen and then, produces carbondioxide gas and water vapor. This respiration activity contributes to aging or senescence of the fresh produces. If this activity is decreased or slow down, the postharvest storage life can be prolonged. Practically, the decreased respiration is obtained from either decreasing oxygen or increasing carbon dioxide. This is a main concept of the modified atmosphere packaging (MAP). In MAP, the oxygen content is decreased to approximately 1-5% (down from 21% in the ambient air). On the other hand, the carbon dioxide content is approximately 5-10% (typically 0.03% in the ambient air).

In addition, fresh produces can also generate the ethylene gas (C_2H_4) that is a natural growth hormone. According to their ethylene production, classification of fresh produces is shown in Table 2.4. The ethylene can effect on the fresh produces in so many difference ways and is biologically active at very low concentration (ppb-ppm range). For example, C_2H_4 is used to promote: ripening of bananas, degreening of oranges, synthesis of pigments in apples, yellowing of broccoli, and senescence of flowers. Although some effects of ethylene are viewed as beneficial, the most of them are detrimental effect that is senescence. In particular, for a climacteric fruit, the ethylene can accelerate unusual fast respiration.

Table 2.4 Classification of the fresh produces that is classified by ethylene production rate [32]

Class	Range at 20 °C (68 °F) ($\mu l\ C_2 H_4$ /Kg-hr)	Commodities
Very low	Less than 0.1	Asparagus, cauliflower, cherry, citrus, grape, jujube, strawberry, pomegranate, leafy vegetables, root vegetables, potato, most cut flowers.
Low	0.1-1.0	Blueberry, cranberry, cucumber, eggplant, okra, olive, pepper, persimmon, pineapple, pumpkin, raspberry, watermelon
Moderate	1.0-10.0	Banana, fig, guava, honeydew, melon, mango, plantain, tomato
High	10.0-100.0	Apple, apricot, avocado, cantaloupe, kiwifruit (ripe), nectarine, papaya, peach, pear, plum
Very high	More than 100.0	Cherimoya, mammee apple, passion fruit, sapote.

When the fresh produces are stored in enclosed areas, the ethylene level is built up. Hence, they have an unusually fast growth when they are contacted with just small amount of this gas. The post-harvest "life" of the product is cut short and it must be discarded as waste. In order to keep produce from ripening too quickly, the inhibition of ethylene action and/or the ethylene removal could be provided. Carbon dioxide, silver, cobalt and 1-methylcyclopropane (1-MCP) are ethylene action inhibitors. While activated carbon, clay and zeolite are used as the ethylene adsorbent. In practical terms, a removal as much ethylene out of the packaging as possible is the best way to cut down on premature ageing and ripening, and prolong the post-harvest life of fruits and vegetables. In addition, during transport, the ethylene sensitive and ethylene producer fruits could be separately preserved.

2.4 Membrane technology

2.4.1 Membrane description [33-34]

Membrane is a thin layer of material capable of separating materials as a function of their chemical or physical properties when a suitable driving force is applied. Membranes are available in different configurations: plate and frame, tubular, hollow fiber and spiral wound. They are made of various materials such as polymer, metal and ceramic.

The basic concept of membrane separation is shown in Figure 2.10. A feed stream enters the system of membrane and a suitable driving force (such as concentration or pressure differential) is applied across the membrane. This leads to preferential transport of one or more components. Certain components (solutes, solvents, or gases) pass through the membrane. Other components do not pass through the membrane or pass through very slowly. The selective transport (called permeation) forms the basis of membrane separations, which generally involve the separation of solutes or fluid. The stream containing the components that permeate through membrane is called the permeate (or filtrate) and the stream containing retained components is called the retentate (or concentrate).

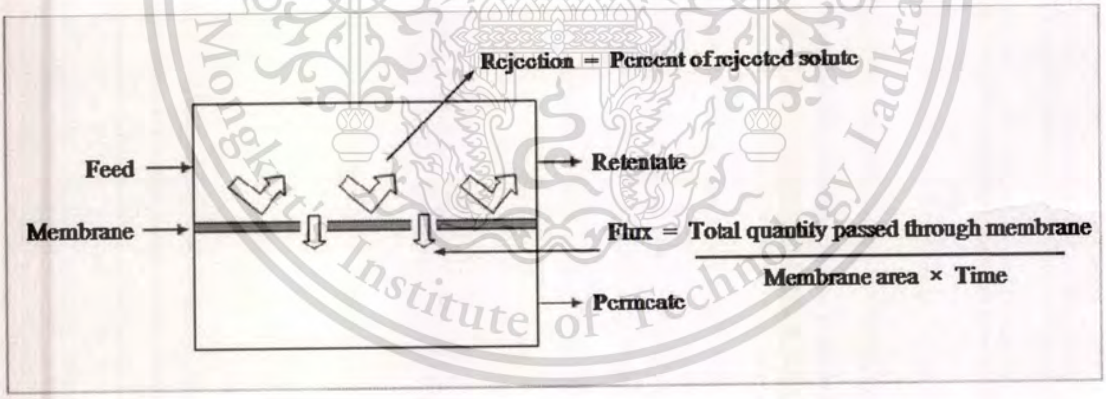

Figure 2.10 Transport of membrane [35]

2.4.2 Applications of membrane [5]

Membrane technology has become a dignified separation technology over the past decennia and is being used increasingly in a broad range of applications. The main force of membrane technology is the fact that it works without the addition of chemicals, with a relatively low energy use and easy and well-arranged process conductions. The important property of membrane, which

is exploited in every application, is the ability of a membrane to control he permeation of a chemical species in contact with it. Applications of membrane is shown in Table 2.5

Table 2.5 Industrial Applications of Membrane Separation Processes [5]

1. Reverse osmosis:
Desalinization of brackish water
Treatment of wastewater to remove a wide variety of impurity
Treatment of surface and ground water
Concentration of foodstuffs
Removal of alcohol from beer and wine
2. Dialysis:
Separation of nickel sulfate from sulfuric acid
Hemodialysis (removal of waste metalbolites, excess body water, and restoration of electrolyte balance in blood
3. Eletrodialysis:
Production table salt from seawater
Treatment of wastewater from electroplating
Demineralization of cheese whey
Production of ultra pure water for the semiconductor industry
4. Microfiltration:
Sterilization of drug
Purification of antibiotic
Separation of mammalian cell from liquid
5. Ultrafiltration:
Preconcentration of milk before making cheese
Recovery of vaccine and antibiotic from fermentation broth
Color removal from Kraft black in paper making
6. Pervaporation:
Dehydration of ethanol-water azeotrope
Removal of water from organic solvent
Removal of organic from water

Table 2.5 (cont)

7. Gas permeation:
Separation of CO_2 of H_2 from methane and other hydrocarbons
Adjustment of the H_2/CO ratio in synthesis gas
Recovery of helium
Recovery methane from biogas
8. Liquid membrane:
Recovery of zinc from wastewater in the viscose fiber industry

In this thesis, gas permeation of polymer membrane is focused to apply in food packaging field.

2.4.3 Gas permeation of polymer membrane [35-37]

Gas permeation is a technique for fractionating gas mixtures by using nonporous polymer membranes having a selective permeability to gas according to a dissolution-diffusion mechanism. In this membrane process, membrane devices for gas or vapor separation usually operate under continuous steady-state conditions with three streams (feed, permeate and retentate stream). Gas is made to pass through the membrane by applying a pressure difference on either side of the membrane. This pressure difference causes a difference in dissolved gas concentration between the two faces of the membrane and hence a diffusional gas flow through the membrane. Membrane selectivity is based on the relative permeation rates of the components through the membrane. Each gaseous component transporting through the membrane has a characteristic permeation rate that is a function of the ability to dissolve and diffuse through the membrane material. The mechanism for transport is based on solubilization and diffusion.

Membranes utilized in separations process need to possess both high selectivity and high permeation (high permselectivity). The selectivity of the membrane to specific gas molecules is the ability of the molecules to diffuse through the membrane. Diffusion of molecules through the polymer is dependent upon a number of polymer properties: crosslinking density (if present), chain stiffness, or glass transition temperature (T_g), crystallinity (if present), crystallite size and distribution, and solubility of the molecules in the polymer membrane.

Chain stiffness and crystallinity affect the free volume of the polymer. Crystallites restrict the free volume, making diffusion more difficult. Increasing the chain stiffness in the amorphous

regions essentially restricts the free volume. Having small, uniformly distributed crystallites in the polymer creates more tortuous pathways for the diffusing molecules. Polarity due to functional groups inside the membrane and Van Der Waals forces due to hydrocarbon fragments can also have a significant influence on separation processes, depending on the nature of the gas molecules.

Permselective polymeric membranes can be divided into two basic categories: glassy and rubbery. Glassy polymers have low chain intrasegmental mobility and long relaxation times, while rubbery polymers exhibit the opposite characteristics, namely high intrasegmental mobility and short relaxation times. Permeation behavior in each type of polymer is shown in Table 2.6.

Table 2.6 Permeation behavior of polymeric materials [37]

Glassy polymer	Rubbery polymer
Diffusion controlled permeation	Solubility controlled permeation
Little movement of polymer segments	Continues movement of holes
Permeation dependent upon size of permeating molecules	Permeation dependent upon ability to dissolve intermolecular interaction and increase moving polymer segment

Membrane separation processes offer numerous industrial advantages over distillation or disposal. Energy requirements are lower, providing for lower overhead costs. The equipment necessary for liquid and gas separations is significantly more compact, simple to build, and reasonably easy to operate. Handling various volumes of separated product is accomplished without having to utilize different equipment because the equipment can be scaled up or operated at partial capacity without problems occurring. Furthermore, permselective membranes have utility in not only industrial processes involving basic chemicals but also in commercial products. Polymer films, such as polyethylene, used in packaging meats, fruits, and vegetables need to have a certain amount of oxygen permeability and diffusion through the packaging while holding back water. This minimum diffusion, especially in meat packaging, allows the meat to retain a more desirable coloring for the consumer.

2.5 Literature reviews

Active packaging was continuously studied over the past 10 years. This is due to a requirement for the extending the storage time of fresh produces, particularly in the food export industry. The concept of extending shelf life of foods by controlling the gases in their immediate environment is not new. In April 1994, there was a report about active packing concept of Food Science Australia [27]. Two concepts are used in food packaging technology; (1) controlled and (2) modified atmospheres. The controlled atmosphere (CA) concept is based on monitoring and control of gaseous composition in the package. On the other hand, the modified atmosphere (MA) concept involves adjusting storage environment by permeation of gases and moisture in the package to retain a gas composition as the initial atmosphere. This latter case depends largely on the gas permeability and selectivity of packaging film. CA is practical with transport container while MA is usually the case for retail packs.

In addition to above, the control of specific gases within a package can be achieved by the use of chemicals to absorb an active gas (ethylene). Activated carbon, clay and zeolite are used to be the ethylene adsorbents [29]. Another concept of ethylene removal is the ethylene scavenging that is based on an adsorption and subsequent decomposition of ethylene. Most of ethylene scavenger is potassium permanganate ($KMnO_4$) that oxidizes ethylene to oxygenate compounds [38-39]. $KMnO_4$ cannot be applied directly to the food packaging, but can be only supplied in the form of sachets because $KMnO_4$ is toxic and shows a purple color. In addition, charcoal containing $PdCl_2$ as a metal catalyst is also used for ethylene scavenging. It is effective for reducing the softening rate of kiwifruits and bananas at 20 °C [29,40]. Other chemicals, for example; 1-Methylcyclopropene (1-MCP or EthylBloc®), silver thiosulphate (STS), nickel (Ni), cobalt (Co) and carbondioxide (CO_2) are effective to delay fruit ripening and extend storage life [31,41]. However, the chemicals in those concepts were generally supplied as sachets, leading to a physical injury of fruits and vegetables during transportation. Furthermore, the fresh produces may be contaminated with toxic chemicals.

Alternatively, an inclusion of finely dispersed minerals such as zeolites, clays and Japanese oya into packaging films can be used for the modified atmosphere packaging (MAP). With MAP technology, low oxygen content in the package leads to a decrease in respiration rate and ethylene synthesis of postharvest product. Furthermore, high carbon dioxide can inhibit the ethylene action [31]. Most of these packaging films, however, are opaque and C_2H_4-adsorbing is not sufficient. Although the incorporated minerals may adsorb ethylene, they also alter the permeability of the

films: C_2H_4 and CO_2 will diffuse out much more rapidly and O_2 will enter the film more readily than the pure PE [29]. Commercially available examples of these mineral containing materials are the Orega plastic film (Cho Yang Heung San Co., Korea), Evert-Fresh (Evert-Fresh Co., USA) and Peakfresh™ (Peakfresh Products, Aus-tralia) [1,29,42-43]. Although this concept can be used for commercial packaging, ethylene removal is not very successful and appropriate for fresh produces. Hence, the development of active packaging is continually studied to obtain a packaging film that possesses high selectivity and permeability of ethylene gas. Recent approach is to incorporate synthetic zeolite into the film.

Ethylene and oxygen permeabilities through polyethylene packaging films were studied [44]. It was found that 3 types of PE film (LDPE, LLDPE and HDPE) exhibit higher ethylene permeability, as compared to oxygen. LDPE showed the highest ethylene permeability and gas permeability ratio of C_2H_4/O_2. Moreover, it became more selective to ethylene at higher temperature. In addition, this ratio was independent of the film thickness but significantly reduced with increasing density of PE (i.e. LDPE > LLDPE > HDPE). The $P(C_2H_4) / P(O_2)$ ratio of zeolite-filled LDPE films (commercial active packaging) was found to be slightly higher than that of the unfilled LDPE film.

In addition to PE film, oxygen and carbon dioxide of wheat gluten film was also studied [45]. It was found that the film showed a wide range of oxygen and carbondioxide permeabilities, depending on relative humidity. The effect of temperature appeared to be less pronounced in comparison with that of relative humidity. The ethylene permeability was also studied and exhibited in range of 1 to 3098 amol.m^{-1}.s^{-1}.Pa^{-1} (or approximately 608 cm^3.mm./m^2.day.atm) [46]. At high temperature and relative humidity (25 °C and 75%RH), the wheat gluten film exhibited a higher ethylene permeation. However, its ethylene permeability was not different from the reference LDPE in the same study.

In the previous work [5], ethylene permeability of zeolite/LDPE and zeolite/SEBS composite films was investigated. It was found that LDPE and SEBS are suitable material for the modified atmosphere. This is because the films facilitate the ethylene permeation but limit the oxygen permeation. Zeolite with high Si/Al can be a good ethylene adsorbent. In addition, adding zeolite into LDPE and SEBS can increase ethylene permeation. For zeolite/LDPE composite film, ZSM-5(280) showed the highest ethylene permeability. Moreover, increasing ZSM-5(280) contents in the composite film can enhance the ethylene permeation. For zeolite/SEBS composite film, SEBS containing silicalite showed the highest ethylene permeability; however, silicalite is

not yet commercially. Furthermore, silicalite/SEBS exhibited higher ethylene permeability than that of ZSM-5(280)/LDPE available.

CHAPTER 3

EXPERIMENTAL DETAILS

3.1 Reagent

1. Styrene ethylene-butylene styrene copolymer (SEBS1652 MFI 5 g/10min, Kraton)
2. Low density polyethylene (JJ4324 MFI 5.5 g/10min, TPI Polene)
3. Zeolite NH_4ZSM5(280) (CBV28014, Zeolyst international)
4. Toluene (Purity 99.9%, Merck)
5. Ethanol (Commercial Grade)
5. Ethylene gas (High purity 99.99%, TIG Co., LTD.)
6. Air zero gas (Purity 99.9%, TIG Co., LTD.)
7. Nitrogen gas (Purity 99.9%, TIG Co., LTD.)

3.2 Apparatus

1. Laboratory glassware
2. Balance
3. Sand bath
4. Magnetic stirrer hot plate with temperature controller system (RCT basic: IKA)
5. Sonicator
6. Glass mold
7. Glass plate
8. Casting blade
9. Vacuum oven
10. Micrometer
11. Laminator (LPD2313 : Fuji Lamipacker)
12. Compression machine (Labtech : LP 20)
13. Viscometer (CT-1000 : Cannon)
14. Scanning electron microscope (LEO 1455 VP : LEO Electron microscope)
15. Thermogravimetric analyzer (Pyris 1 TG : Perkin Elmer)
16. Differential scanning calorimeter (DSC-50 : Shimadzu)
17. Dynamic mechanical thermal analyzer (DMA/SDTA861e : Mettler Toledo)

18. Fourier transform infrared spectrometer (FT-IR spectrum GX : Perkin Elmer)
19. Universal testing machine (LR 5K : LLOYD Instrument)
20. Permeation cell
21. Permeation rig
22. Gas chromatograph with flame ionization detector (FID) (CP-3800 : Varian)
23. Carbon dioxide permeability analyzer (CO_2-TRAN : Mocon)
24. Oxygen permeability analyzer (OX-TRAN : Mocon)
25. Water vapor permeability analyzer (7002 : ILLINOIS Instrument)

3.3 Film preparation

3.3.1 SEBS film

The specification of SEBS is shown in Table 3.1. The neat SEBS film was prepared by a blade solution casting technique.

Table 3.1 Specification of SEBS1652 [47]

Property	Data	Unit
Styrene content	29.0 to 30.8	%w
MFI (230 °C, 5kg)	5	g/10min
Specific gravity	0.91	
Viscosity (Solution in toluene 20%w and at 25 °C)	400 to 525	cP
Elongation at break	500	%
Tensile strength	4500	psi
300% Modulus	700	psi
Hardness (Shore A, 10 s)	69	

Table 3.2 Composition of SEBS film

Formula	Concentration (%wt)	Viscosity* (cP)	SEBS contents (g) / in toluene (g)
SEBS (~ 50 μm thickness)[a]	25	582	16.2 / 48.6
SEBS (~ 80 μm thickness)[b]	30	3051	16.2 / 37.8

* Viscosity of a solution was measured at a casting temperature (around 55 °C)

[a] For preparation as the double-layered film

[b] For preparation as the film with 80 μm thickness

The neat SEBS films were prepared by soaking 16.2 g of the SEBS in 48.6 and 37.8 g of toluene for 24 hr to obtain the polymer solutions with two different concentrations, i.e. 25 %wt and 30 %wt, respectively. The mixtures were heated to approximately 80°C under stirring for 19 hr and then transferred into a sonicater for another 30 min. After that, the solutions were cast onto a glass plate using a casting blade and allowed to dry for a day. The film was then removed from the glass plate by immersing in ethanol. Finally, the film was evacuated in vacuum oven at 60°C until a constant weight was obtained. The films thickness is approximately 50 and 80 μm for 25 %wt and 30 %wt casting solutions, respectively.

3.3.2 Zeolite/SEBS composite film

Two different zeolite/SEBS composite films were prepared by a solution casting containing various zeolite contents. In this work, commercial ZSM-5 with a specification shown in Table 3.3 was used without further modification.

Table 3.3 Specification of ZSM-5 zeolite [48]

Property	Data	Unit
SiO_2/Al_2O_3 mole ratio	280	-
Nominal cation form	Ammonium	
Na_2O weight	0.05	%
Surface area	400	m^2/g
Specific gravity	> 1	

3.3.2.1 Zeolite/SEBS composite film with surface rich zeolite (SR)

The zeolite/SEBS composite film with surface rich zeolite (SR) was prepared as composition shown in Table 3.4.

Table 3.4 Composition of zeolite/SEBS composite film (SR)

Formula	SEBS contents (g)	ZSM-5 (280) contents (g)	Total toluene (mL)
5%ZSM-5 (SR)	1.615	0.085	56
10%ZSM-5 (SR)	1.53	0.170	56

The weight fraction of zeolite/SEBS mixture is 3wt% in toluene (solution viscosity < 10 cP.). For example, 10%ZSM-5 (SR) composite film was prepared by soaking 1.53 g of the SEBS1652 and 36 g of toluene in a 250 flask for 24 hr. The mixture was heated to approximately 60°C under stirring for 2.5 hr. In a separate flask, 0.17 g of ZSM-5 in 20 g of toluene was sonicated for 30 min. While, zeolite was vigorously stirred in toluene at 60°C, the polymer solution was added into the stirring mixture and continued stirring for 30 min. After that, the mixture was transferred into a sonicater for another 15 min. The mixture was poured into a glass mold and allowed to dry for 24 hr. The film was removed from the glass mold while the mold was immersed in ethanol. Finally, the zeolite/SEBS composite film was evacuated in a vacuum oven at 60°C for another 24 hr.

3.3.2.2 Zeolite/SEBS composite film with well dispersed zeolite (WD)

The zeolite/SEBS composite film with well dispersed zeolite (WD) was prepared as composition shown in Table 3.5.

Table 3.5 Composition of zeolite/SEBS composite film (WD)

Formula	SEBS contents (g)	ZSM-5 (280) contents (g)	Total toluene (mL)
5%ZSM-5 (WD)	15.39	0.81	48.6
10%ZSM-5 (WD)	14.58	1.62	48.6
20%ZSM-5 (WD)	12.96	3.24	48.6
30%ZSM-5 (WD)	11.34	4.86	48.6

The weight fraction of zeolite/SEBS mixture is 25wt% in toluene (around 582 cP. in solution viscosity). For example, 10%ZSM-5 (WD) was prepared by soaking 14.58 g of the SEBS1652 and 28.6 g of toluene in a 250 flask for 24 hr. The mixture was heated to approximately 80°C under stirring for 16 hr. In another flask, 1.62 g of ZSM-5 in 20 g of toluene was sonicated for 30 min. The polymer solution was then added into the stirring mixture of zeolite and toluene at 80°C for 3 hr. After that, the mixture was sonicated for 30 min at 50 °C. The mixture was cast on a glass plate using a casting blade and allowed to dry for 24 hr. The film was removed from the glass mold while the mold was immersed in ethanol. Finally, the zeolite/SEBS composite film was evacuated in vacuum oven at 60°C for another 24 hr.

3.3.3 LDPE film

LDPE films with approximately 30 and 80 μm thickness were prepared by colleague at MTEC using blown film process. The LDPE specification and condition of blown film process are described in Appendix A.

3.3.4 Double-layered film

The double-layered film containing LDPE blown film (30 μm) and SEBS film (or zeolite/SEBS composite film, 50 μm) was fabricated via two steps. First, LDPE and SEBS film (or zeolite/SEBS composite film) were adjoined by running through a laminator using supporting papers. A gloss coated paper was used for supporting LDPE side and a photo paper (back side) was used for supporting SEBS side as shown in Figure 3.1) Finally, the adjoined film was compressed using the condition shown in Table 3.6.

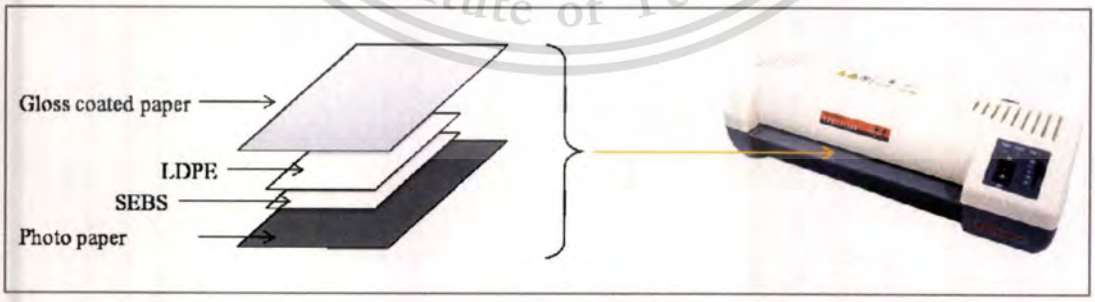

Figure 3.1 The schematic of film layer in adjoining step

Table 3.6 Hot press conditions

Factor	Condition
Temperature of hot pressing	100 °C
Pressure of hot pressing	1800 psi.
Time of hot pressing	12 min.
Temperature of cold pressing	6 °C
Pressure of cold pressing	1800 psi.
Time of cold pressing	6 min.

3.4 Characterization of film

3.4.1 Determination of film morphology using Scanning electron microscope (SEM)

The film morphology was determined by SEM. The sample was immersed for 2 min in the liquid nitrogen then it was immediately cryogenic cracked. The fracture surface of film was coated with gold by ion sputtering. The sample was placed in the sample chamber of SEM and evacuated from ambient pressure to 10^{-4} Torr. The SEM micrograph was taken at the magnification of 700 and 5,000 times.

3.4.2 Determination of zeolite content using Thermogravimetric analyzer (TGA)

The zeolite content in the film was determined by thermogravimetric analyzer. Approximately 10-20 mg of the sample was placed in a platinum pan hanging from a microbalance and nitrogen was introduced as a carrier gas. The sample was heated under air zero (50 ml/min) for %weight loss from 50°C to 700°C at a heating rate of 10°C/min.

3.4.3 Determination of melting temperature (T_m), crystallization temperature (T_c) and % crystallinity using Differential scanning calorimeter (DSC)

The T_m, T_c and %crytallinity of the neat LDPE and LDPE in the double-layered films were determined by differential scanning calorimeter. Approximately 5-10 mg of sample was placed in aluminum pan. The sample was heated from 50°C to 200°C with a heating rate of 10°C/min. Then, the sample was cooled from 200°C to 50°C with a cooling rate of 10°C/min.

3.4.4 Determination of glass transition temperature (T_g) using Dynamic mechanical thermal analyzer (DMTA)

The T_g of the neat SEBS and zeolite/SEBS composite films were investigated by dynamic mechanical thermal analyzer. The specimen was tested in tension mode at constant frequency of 1 Hz. and a temperature range from -120 °C to 130 °C at a heating rate of 4 °C/min.

3.4.5 Investigation on interaction of zeolite particles with polymer matrix using Fourier transform infrared spectrometer (FT-IR)

The FT-IR spectra of thin film samples were recorded in transmission mode (wavenumber of 400-4000 cm^{-1}). An average of 5 scans have been reported for each sample.

3.5 Tensile property testing

Tensile properties of the films were determined by a universal testing machine with a pneumatic grip (size: 2.5 ×2.5 cm). The tensile properties including tensile strength, yield stress, Young's modulus and %elongation at break were measured according to ASTM D882 [49]. The film specimens were cut into a size of 10x80 mm and the tensile testing conditions are shown in Table 3.7.

Table 3.7 Tensile test conditions

Lists	Value	Unit
Load cell	100	N
Test speed	100	mm/min
Gauge length	25	mm

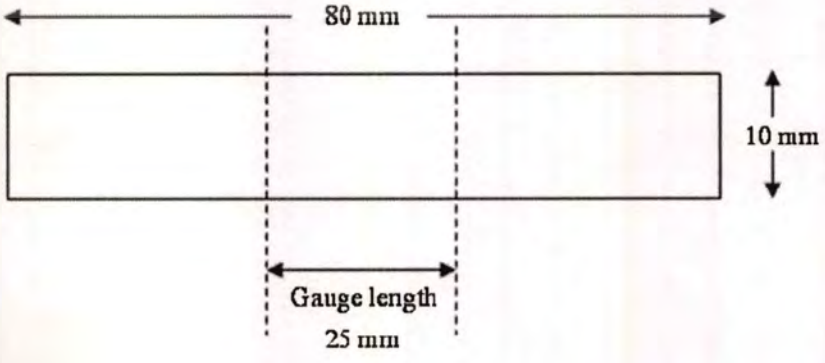

Figure 3.2 Size and shape of a tensile test specimen

Tensile strength, Young's modulus and %elongation at break can be calculated from the following equations.

Tensile strength = F_m/A (3.1)

Yield stress = F_y/A (3.2)

Tensile modulus = Stress / Strain (3.3)

% Elongation at break = $\left(\frac{L - L_0}{L_0}\right)$ x 100 (3.4)

Where F_m = Maximum force (N)

F_y = Force at yield point (N)

A = Initial cross-section area (mm^2)

L = Distance between gauge marks at break (mm)

L_0 = Gauge Length 25 mm

Note: Tensile modulus can be calculated from the slope of stress-strain curve at 2% and 4% elongation.

3.6 Permeation measurement

3.6.1 Ethylene permeation using homemade permeation cell equipped with FID gas chromatograph.

The film was fixed between two metal o-rings with an inside diameter of 100 mm using epoxy adhesive. The component is called a membrane cell, as shown in Figure 3.3.

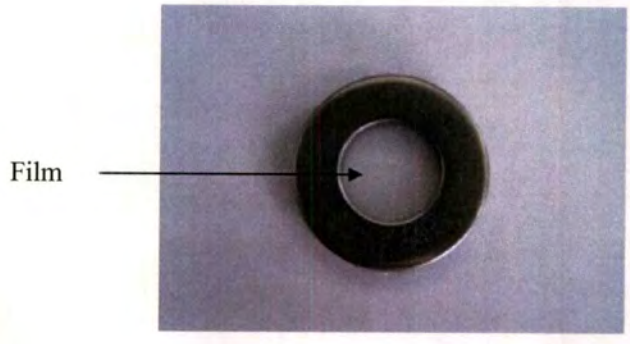

Figure 3.3 Membrane cell: the double-layered film was fixed with the metal rings

The membrane cell was assembled with 4-ways Pyrex glass tube using Viton o-ring. The component is called the permeation cell, as shown in Figure 3.4. The schematic diagram of permeation cell is shown in Figure 3.5.

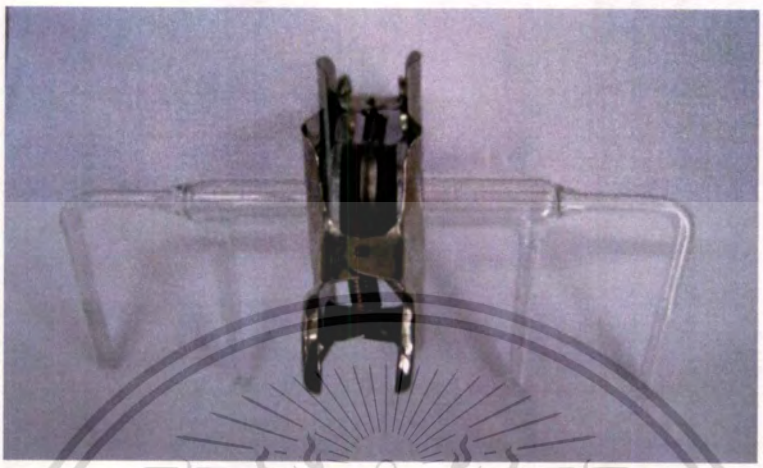

Figure 3.4 Permeation cell

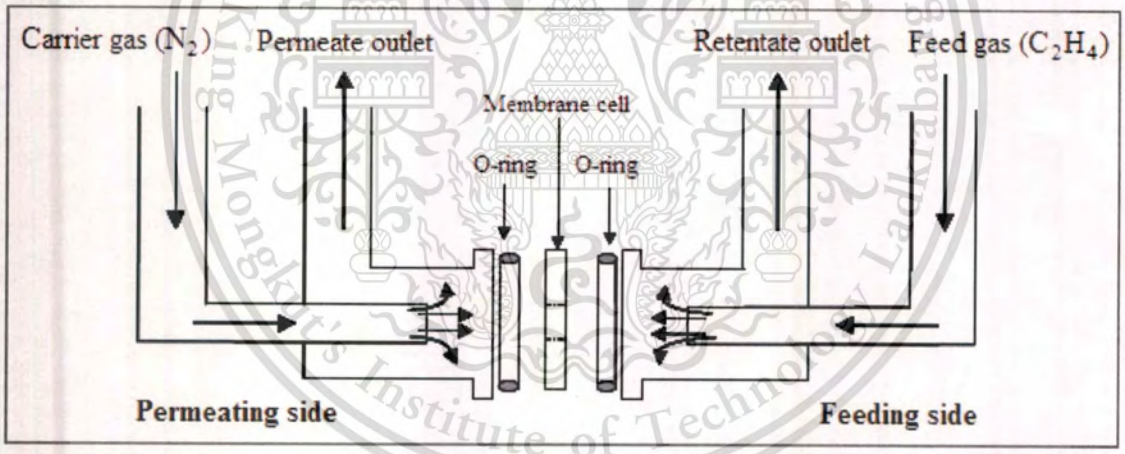

Figure 3.5 Diagram of the permeation cell

The feed gas (ethylene or diluted ethylene) as compositions shown in Table 3.8 and carrier gas (nitrogen) at a flow rate of 30 ml/min was connected to feeding and the permeating sides, respectively.

Table 3.8 Composition of the feed gas

Ethylene concentration (%v/v)	Feed gas Type 1		Feed gas Type 2		Feed gas flow rate (ml/min)
	C_2H_4 flow rate (ml/min)	N_2 flow rate (ml/min)	C_2H_4 flow rate (ml/min)	Air Zero flow rate (ml/min)	
20	6	24	6	24	30
40	12	18	12	18	30
60	18	12	18	12	30
80	24	6	24	6	30
100	30	-	30	-	30

The flow rate of the feed and the carrier gas were controlled by mass flow controllers. As the feed gas flow across the film surface, some of the gas can diffuse through the film to the permeating side. The permeated gas was swept by a carrier gas into the permeate outlet. On the other hand, some of the gas that cannot diffuse through the film was flowed to retentate outlet. The permeate outlet was connected to the sampling valve of gas chromatograph while the retentate outlet was connected to a needle valve and finally, to the vent. The gas flow system for ethylene permeation unit are illustrated in Figure 3.6

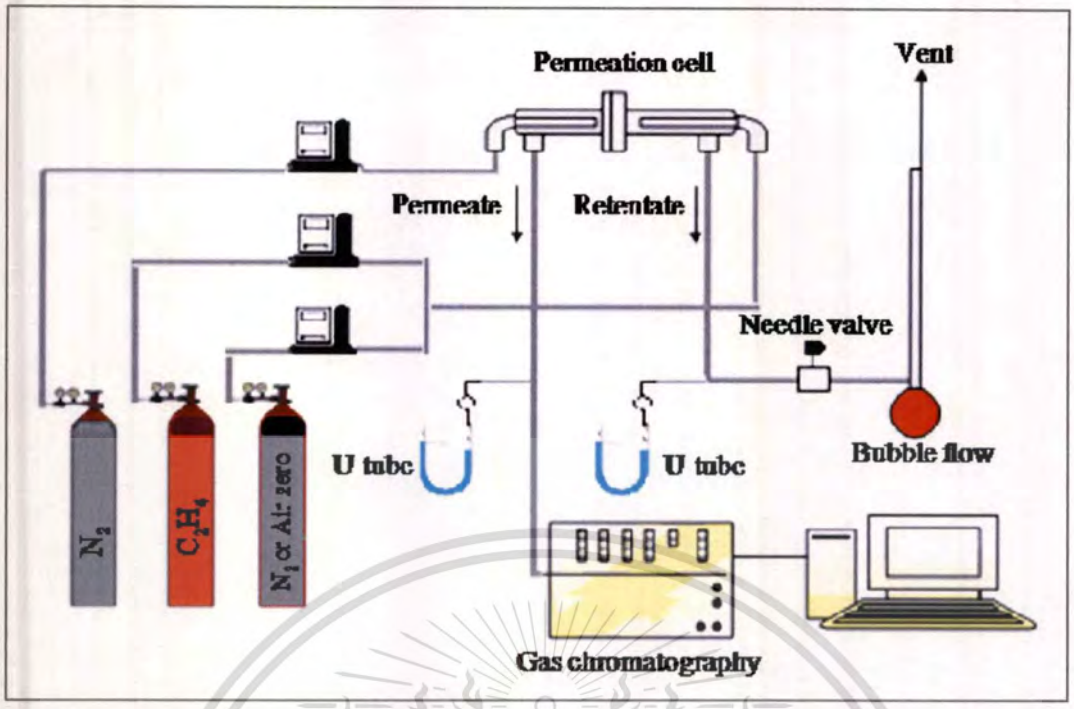

Figure 3.6 Diagram of the ethylene permeation unit

The U-tube glass containing distillation water was connected to both retentate and permeate outlets for measuring the pressure drop. The pressure drop in retentate outlet was adjusted by a needle valve to balance with that of the permeate outlet. During pressure drop adjustment, a dense membrane (aluminum foils) was preliminary used instead of the film in the permeation cell.

For ethylene permeation testing, the dense membrane was replaced by the tested film. The permeate compositions were analyzed by gas chromatograph (Varian model 3800) with Porapak Q column. The injection port, the column oven, and FID detector were set to 200, 40, 200 ^{o}C, respectively. The permeate gas was periodic analyzed by FID detector every 10 min in order to determine permeability at the steady state.

3.6.2 Oxygen permeation using oxygen permeability analyzer

Oxygen permeability of the film was investigated by oxygen permeability analyzer at MTEC. The flat film samples were prepared into a size of 5 × 5 cm^2 and then put in a permeation cell. Oxygen permeation was carried out at 1 atm. and temperature of 23 °C.

3.6.3 Carbon dioxide permeation using carbon dioxide permeability analyzer

The carbon dioxide permeation was determined using a carbon dioxide permeability analyzer at MTEC. Approximately 5 × 5 cm^2 of sample film was placed into the permeation cell.

The carbon dioxide permeability of film was measured at 23°C under atmosphere pressure and obtained from steady state of permeation.

3.6.4 Water vapor permeation using water vapor permeability analyzer

Water vapor permeability of the film was obtained from a water vapor permeability analyzer at MTEC. The water vapor permeation was measured at 38°C under atmosphere pressure (90% humidity). The film sample size is approximately 25 cm^2.

CHAPTER 4

RESULTS AND DISCUSSION

The thickness of the parent films used in this study is shown in Table 4.1. For blade cast SEBS film, the thickness largely depends on the solution viscosity.

Table 4.1 Thickness of the single layer LDPE, SEBS and zeolite/SEBS composite films

Sample	Detail	Solution viscosity (cP.)	Thickness (μm)
LDPE (30)[a]	95 %wt LDPE + 5%wt Anti-blocking agent	-	33 ± 2
LDPE (80)[a]	95 %wt LDPE + 5%wt Anti-blocking agent	-	79 ± 4
SEBS (50)	100%wt SEBS	582[b]	50 ± 6
SEBS (80)	100%wt SEBS	3051[c]	76 ± 7
SE-5SR	95 %wt SEBS + 5%wt ZSM-5	< 10[d]	47 ± 4
SE-10SR	90 %wt SEBS + 10%wt ZSM-5	< 10[d]	45 ± 4
SE-5WD	95 %wt SEBS + 5%wt ZSM-5	> 582[e]	52 ± 2
SE-10WD	90 %wt SEBS + 10%wt ZSM-5	> 582[e]	52 ± 5
SE-20WD	80 %wt SEBS + 20%wt ZSM-5	> 582[e]	50 ± 3
SE-30WD	70 %wt SEBS + 30%wt ZSM-5	> 582[e]	55 ± 4

[a] From blown film process

[b,e] From a blade solution casting with 25 %wt solution

[c] From a blade solution casting with 30 %wt solution

[d] From solution casting with 3 %wt solution

Thickness of the double-layer films, prepared by a hot press technique between LDPE and SEBS (or zeolite/SEBS composite) films, are shown in Table 4.2

Table 4.2 Thickness of the double-layered film with and without zeolite

Sample	Thickness (μm)
DB-0	84 ± 6
DB-5SR	81 ± 5
DB-10SR	76 ± 6
DB-5WD	84 ± 5
DB-10WD	84 ± 3
DB-20WD	79 ± 6
DB-30WD	79 ± 3

From Table 4.2, it can be noticed that the film thickness of the double-layered films are approximately ~ 80 μm comprising of ~ 30 μm LDPE and ~ 50 μm SEBS layers (as shown in Table 4.1). This suggests that the temperature and pressure used for hot press process allows only an adhesion between LDPE and SEBS layers leading to insignificant change in the thickness of each layer. Therefore, the LDPE and SEBS single layers were intentionally prepared with thickness of approximately 80 μm for comparison with the double-layered film. The 76 μm SEBS was obtained form 30 %wt SEBS casting solution. It can be seen from Table 4.1 that when the casting solution viscosity was increased (from 582 to 3051 cP.), the SEBS film thickness was also increased.

4.1 Characterizations of the film

4.1.1 Morphology

The cross-section of the double-layered films was observed from scanning electron microscope, as shown in Figure 4.1 to 4.4.

From the cross-section of a double-layered film (Figure 4.1), it can be found that LDPE (lower) and SEBS (upper) were firmly adjoined. It also can be seen that the thickness of LDPE and SEBS layers in the double-layered film retain approximately 0.03 and 0.05 mm, respectively. It is confirmed that there is only adhesion of between both layers interphase. No melting, blending and interfacial void can be observed in the double-layered film.

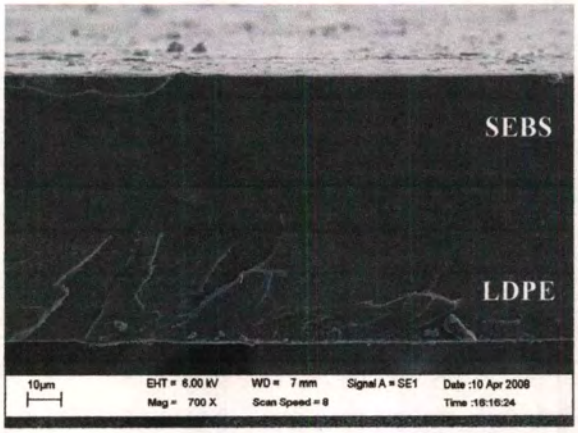

Figure 4.1 SEM micrograph (700X) of the double-layered film without zeolite (DB-0)

For the zeolite composite double-layered film with surface rich zeolite (SR), LDPE was intentionally laminated on the other side of the zeolite/SEBS composite film, as schematic representation shown in Figure 4.2. This would allow the precipitated zeolite layer to expose at the outer surface of the double-layered film and provide the better adhesion of SEBS with LDPE. In addition, a higher interaction of the double-layered film with ethylene in the gas phase can be obtained with this film configuration.

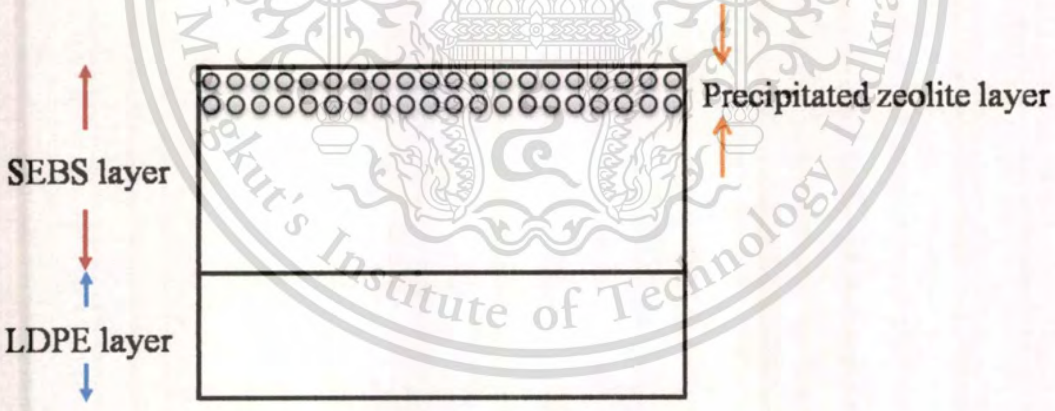

Figure 4.2 Schematic representation of DB-SR film morphology

The film morphology of DB-SR film was shown in Figure 4.3. It can be seen that the zeolite particles agglomerate on one side of the film. This is because viscosity of the 3 %wt casting solution is so low that the zeolite precipitated during evaporation. It can also be seen that when zeolite contents were increased, the thickness of precipitated zeolite layer also increased.

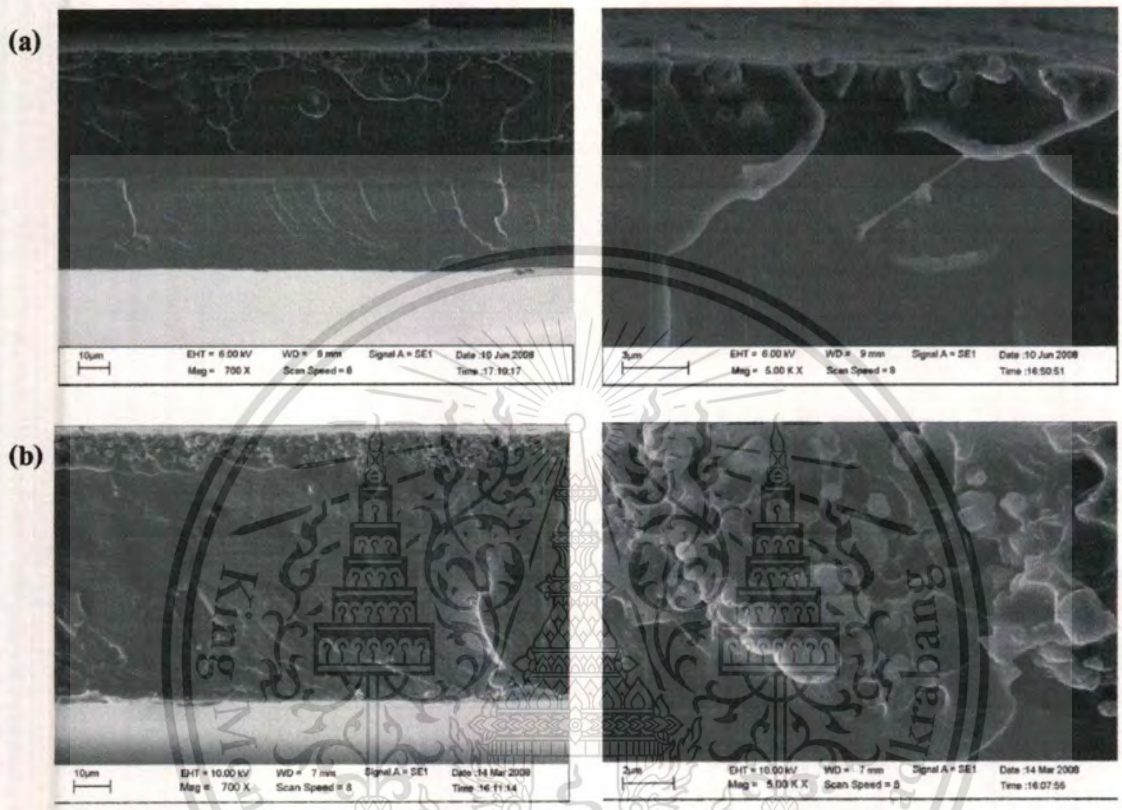

Figure 4.3 SEM micrographs (700X and 5000X) of the zeolite composite double-layered film with surface rich zeolite (DB-SR) : (a) 5% and (b) 10% zeolite loading

For DB-WD film (Figure 4.4), it can be seen that the zeolite particles (5-10%wt loading) were well dispersed in the SEBS layer. This is because the highly viscous media (25 %wt casting solution) can suspend the zeolite particles during evaporation. However, when zeolite contents were increased to 20-30 %wt loading, agglomeration of zeolite particles and interfacial voids of the film can be observed. This is because the particle-particle interactions can develop in composite as well as particle-matrix interactions when the filler content is increased [50].

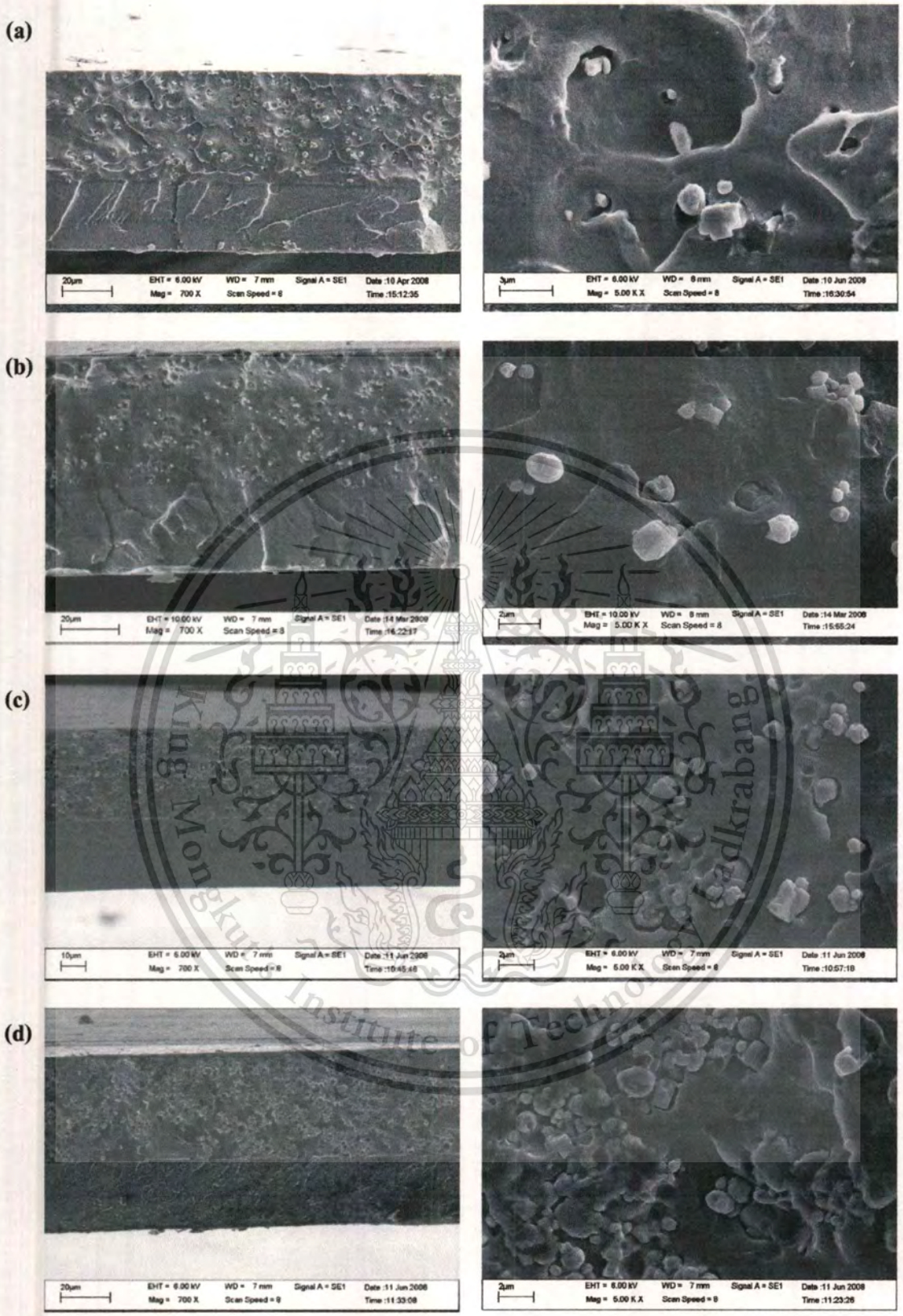

Figure 4.4 SEM micrographs (700X and 5000X) of the zeolite composite double-layered film with well dispersed zeolite (DB-WD) : (a) 5%, (b) 10%, (c) 20% and (d) 30% zeolite loading

4.1.2 %Zeolite loading

%Weight of zeolite in SEBS layer (Table 4.3) was calculated form the %weight remained after 700 °C that was obtained from TGA as listed in Appendix B. Since the double-layered film containing 60-63 %wt of SEBS and 37-40 %wt of LDPE layers as described in Appendix B, %weight of zeolite was be normalized with only %weight of SEBS phase, as the calculation and TGA thermograms shown in Appendix C and D, respectively.

Table 4.3 %Weight of zeolite in the film

%Zeolite loading in SEBS layer	%Weight of zeolite in SEBS layer	
	SR	WD
0	-	-
5	2.10	6.74
10	10.9	9.82
20	-	20.0
30	-	31.3

From Table 4.3, it is found that the %weight of zeolite is relatively closed to that intentionally loaded in SEBS. This confirms that there is no significant loss of zeolite during film preparation. However, there is only 2.10% weight of zeolite in SEBS layer for DB-5SR. This is presumably because small amount of zeolite was loaded in a very low viscosity solution leading to a loss of zeolite during a film casting process.

4.1.3 Thermal properties

Since the film crystallinity can readily affect to gas permeability, the LDPE (30) and double-layered films with and without zeolite were analyzed by DSC. Melting and crystallization temperature and %crystallinity of the film were shown in Table 4.4. Calculation of the %crystallinity and DSC thermograms were shown in Appendix C and E, respectively.

Table 4.4 T_m, T_c and %crystallinity of the LDPE single-layer film and LDPE in the double-layered films

Film	%Zeolite loading	T_m (°C)		T_c (°C)	% Crystallinity
		Onset	Peak		
LDPE (30)	-	99	104	97	34
DB-0	0	101	103	97	39
DB-SR	5	101	104	96	34
	10	100	102	97	30
DB-WD	5	103	105	96	33
	10	102	104	96	32
	20	103	103	96	38
	30	103	105	96	36

It can be seen that the %crystallinity and melting temperature of the double-layered film without zeolite is relatively the same as LDPE film. Generally, the SEBS is highly amorphous [20]. Thus, it is suggested that the observed crystallinity of the double-layered film is contributed only from the LDPE layer. In addition, it can be seen from DSC thermogram of DB-0 (Figure 4.5) that a small hump appeared at relatively lower temperature. This suggests that small crystal may be formed during the lamination and/or hot press processes. However, the similar range of %crystallinity was obtained.

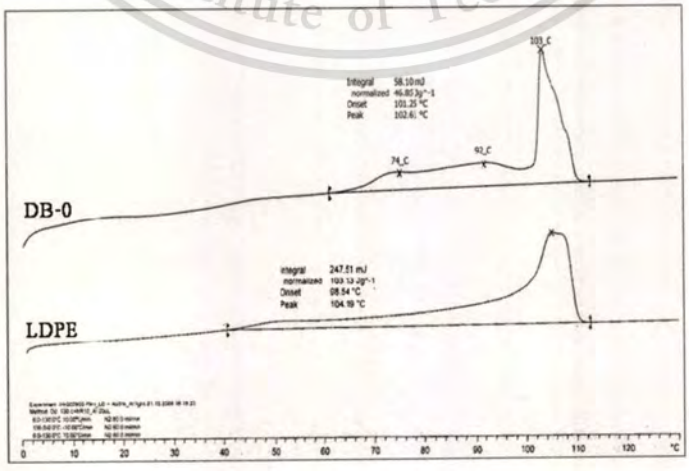

Figure 4.5 DSC thermograms LDPE and the double-layered film without zeolite (DB-0)

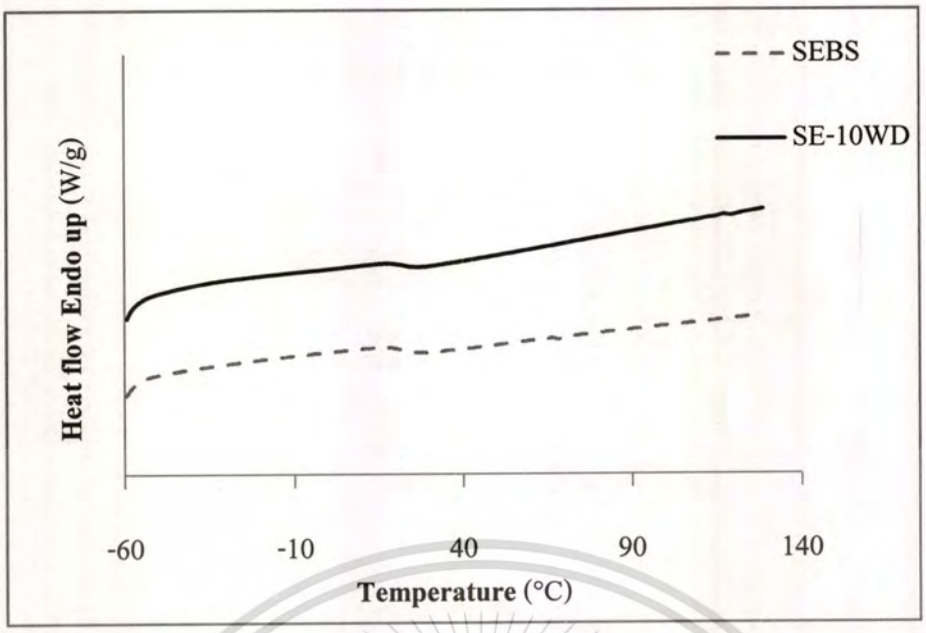

Figure 4.6 DSC thermograms SEBS and SEBS with 10% zeolite loading (SE-10WD)

When the zeolite was added into the SEBS film, it can be seen from the DSC thermogram (Figure 4.6) that no endothermic peak was obtained. This confirms that the zeolite incorporation does not interfere with the arrangement of SEBS chain during film formation. Therefore, when the zeolite/SEBS composite film was laminated with the LDPE film as the double-layered film, %crystallinity and melting temperature of the zeolite composite double-layered film are not different from the double-layered film without zeolite. This is again suggested that no mixing across two layers can be obtained and the incorporated zeolite does not modify LDPE phase. The crystallinity of the zeolite composite double-layered film is solely contributed from the LDPE layer.

Dynamic mechanical thermal analysis (DMTA) was used to measure the glass transition temperatures (T_g) for the neat SEBS and zeolite/SEBS composite (SE-10WD) films since these transitions cannot be clearly observed with the DSC thermograms. DMTA thermograms are shown in Figure 4.7.

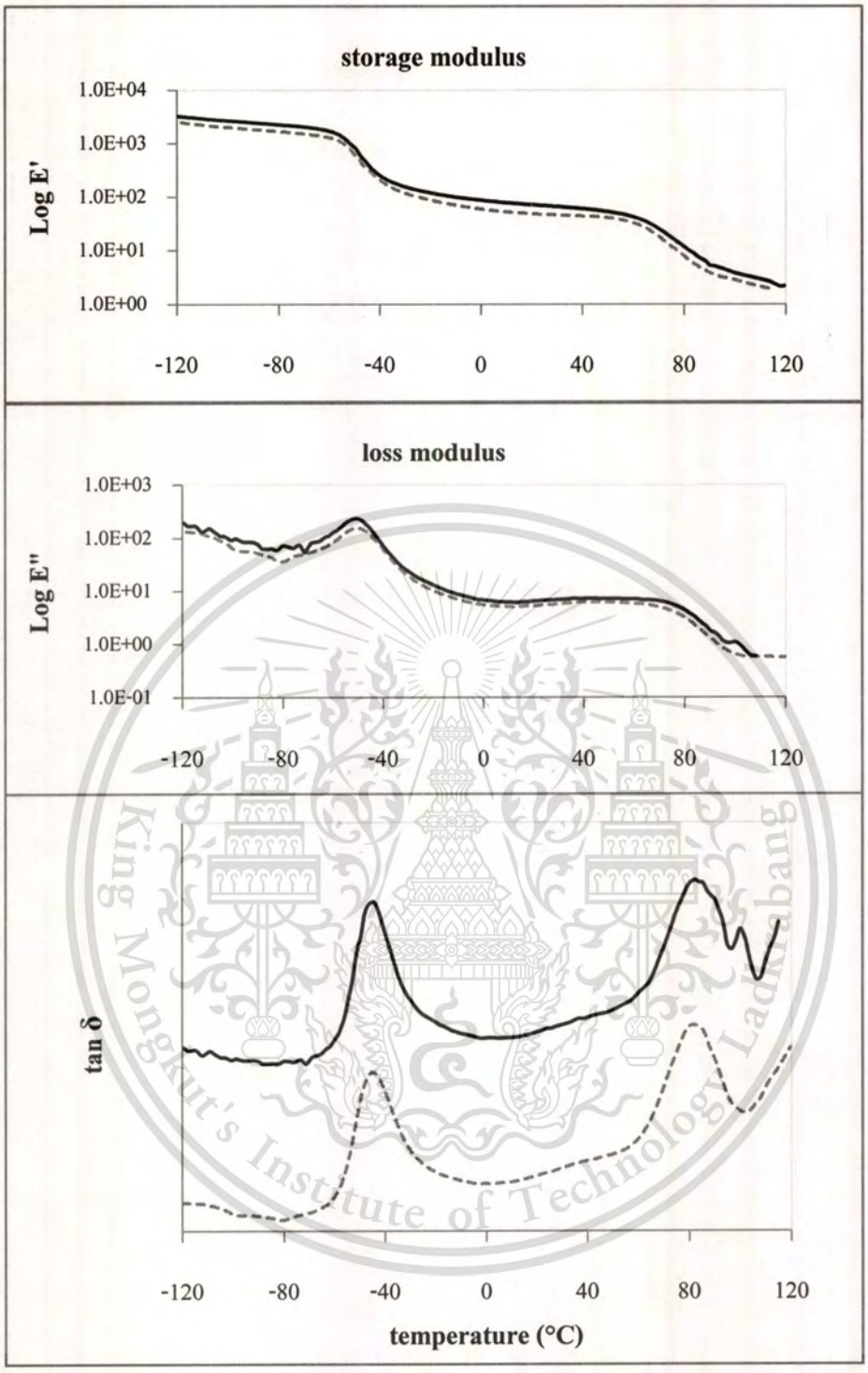

Figure 4.7 Storage modulus, loss modulus and tan δ of (·····) SEBS and (—) SE-10WD films

From Figure 4.7, it can be noticed that both films exhibited two transition stages at approximately -45 °C (EB T_g) and 82 °C (S_1 T_g) corresponding to main relaxation of ethylene-butylene and styrene phase, respectively [51-52]. It is worth noting that the storage modulus (E') of zeolite/SEBS composite film is slightly higher than that of the neat SEBS film. This is

presumably because the presence of rigid zeolite particles would impede the mobility of the polymer chain. Such interference by zeolite, particularly in the styrene segment, can be clearly seen from an additional small relaxation peak in both loss modulus and tan δ of composite film at approximately 100 °C (S_2 T_g). This suggests that some parts of styrene segment possess an interaction with the incorporated zeolite particles leading to higher rigidity of the polymer chains. Hence, the higher thermal energy is required for the chain movement and the pronounced dissipation energy (loss modulus) was then observed at relatively higher temperature. On the other hand, there is no significantly different in glass transition temperature of the ethylene-butylene segment (EB T_g, -45 °C). This is consistent to above observation that the zeolite is presented predominantly in the styrene phase. From these, it is believed that only an interaction between zeolite particle and the styrene segment causes a lower chain flexibility and free volume of the SEBS layer.

4.1.4 Interaction of zeolite particles with polymer matrix

The FT-IR spectra of thin film were provided in order to determine the interaction of zeolite particles with polymer matrix, as shown in Figure 4.8.

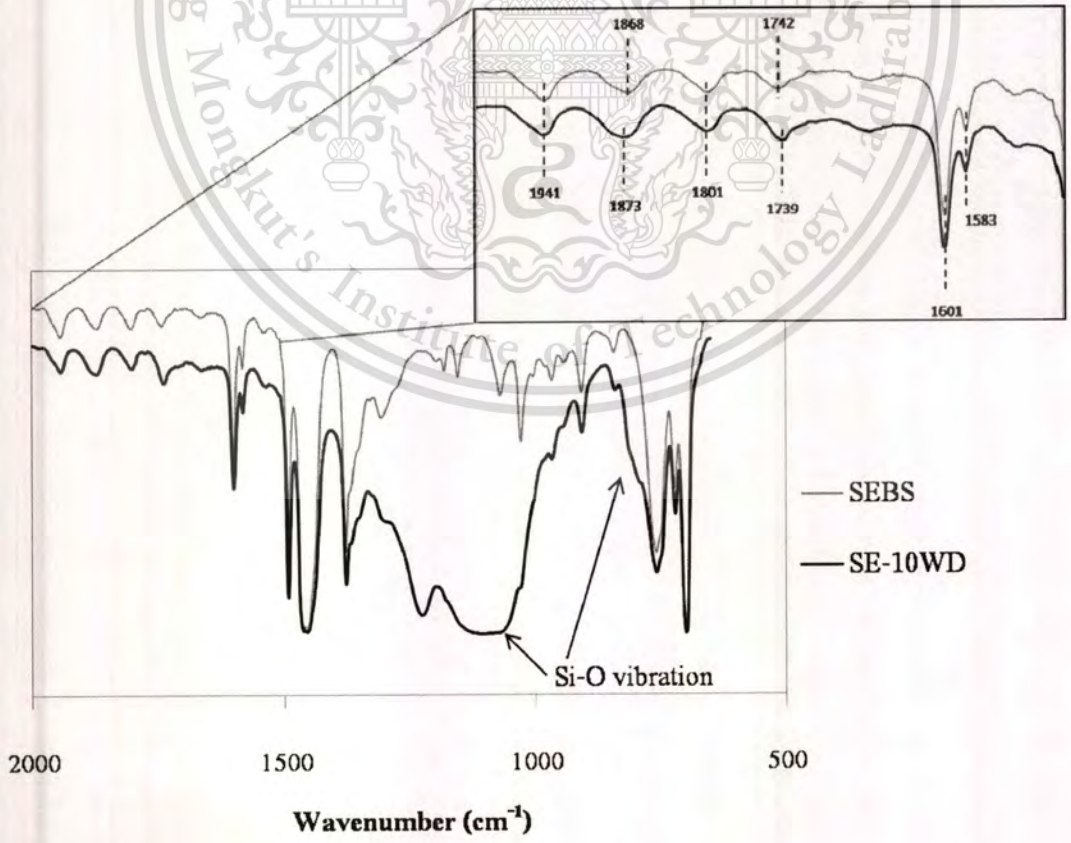

Figure 4.8 FT-IR spectra of SEBS and SEBS and SEBS with 10% zeolite loading (SE-10WD)

FT-IR spectra (Figure 4.8) show only a shift in overtone bands (C-H out of plane bending) which are particularly characteristic of the aromatic moiety in SEBE layer (from 1868 cm^{-1} to 1873 cm^{-1} and 1742 cm^{-1} to 1739 cm^{-1}). This confirms that only the styrene segment was interfered by the incorporated zeolite. It can be seen from Figure 4.9 that SEBS in SE-10WD film was split into small semi-layers with different thickness when zeolite was incorporated. As IR beam pass through this film, it would be perturbed by the dispersed zeolite.

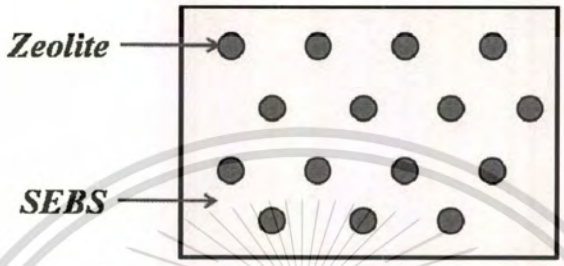

Figure 4.9 Schematic drawing of semi-layer SEBS in zeolite/SEBS composite film

4.2 Tensile properties

The tensile properties of LDPE(80), SEBS(80) and double-layered films without zeolite are shown in Figure 4.10. The LDPE and DB-0 were tested for tensile properties for both transverse (TD) and machine (MD) directions. It was found that the films exhibit somewhat similar tensile properties within the condition prepared and tested for both directions.

(a)

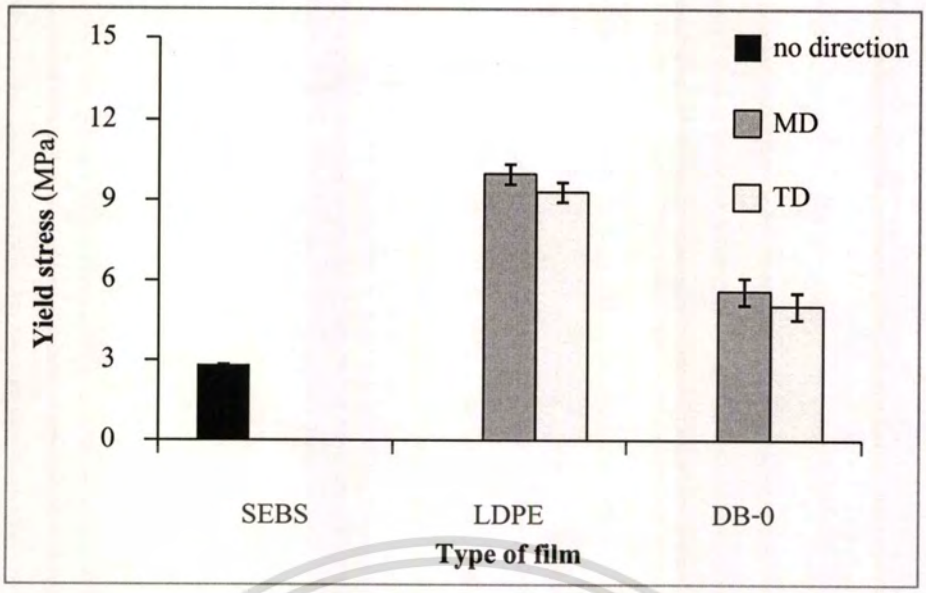

(b)

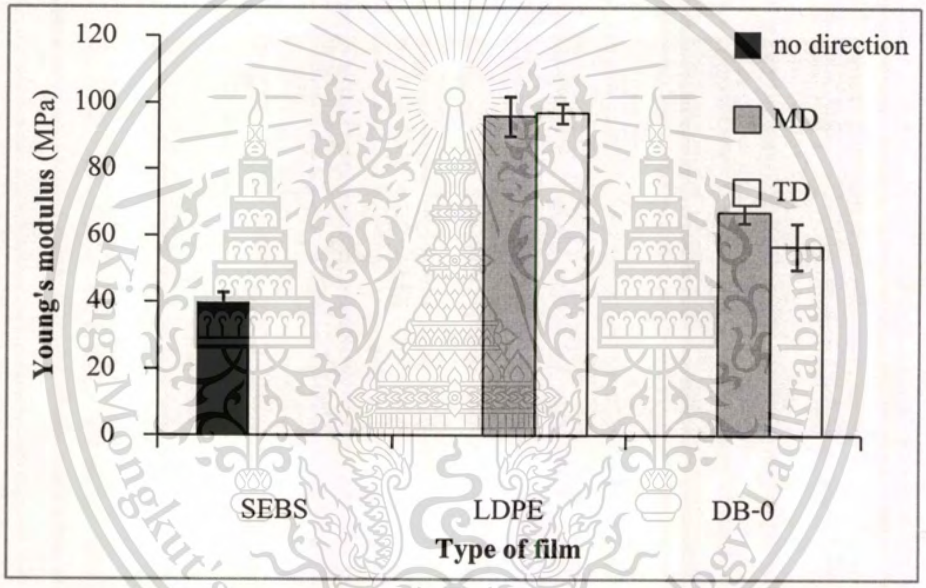

(c)

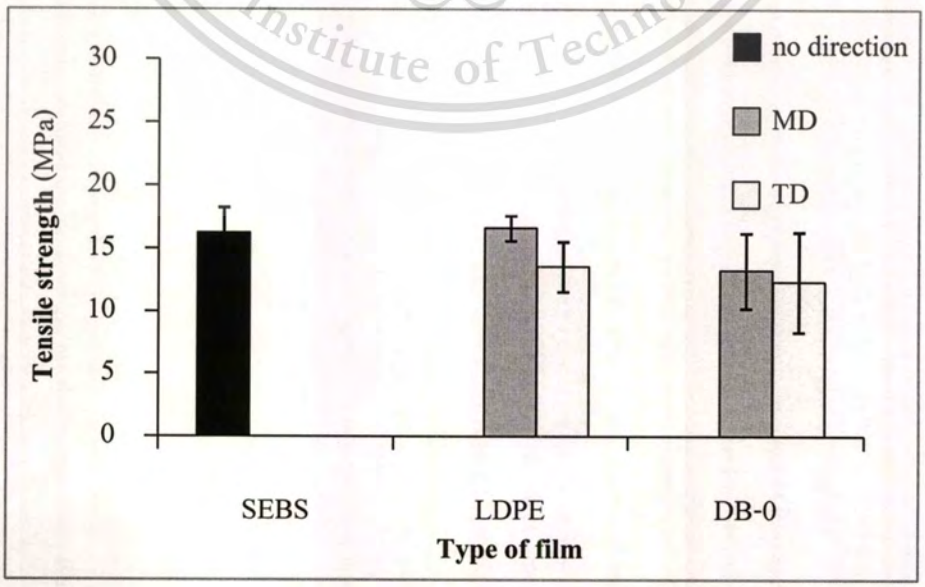

(d)

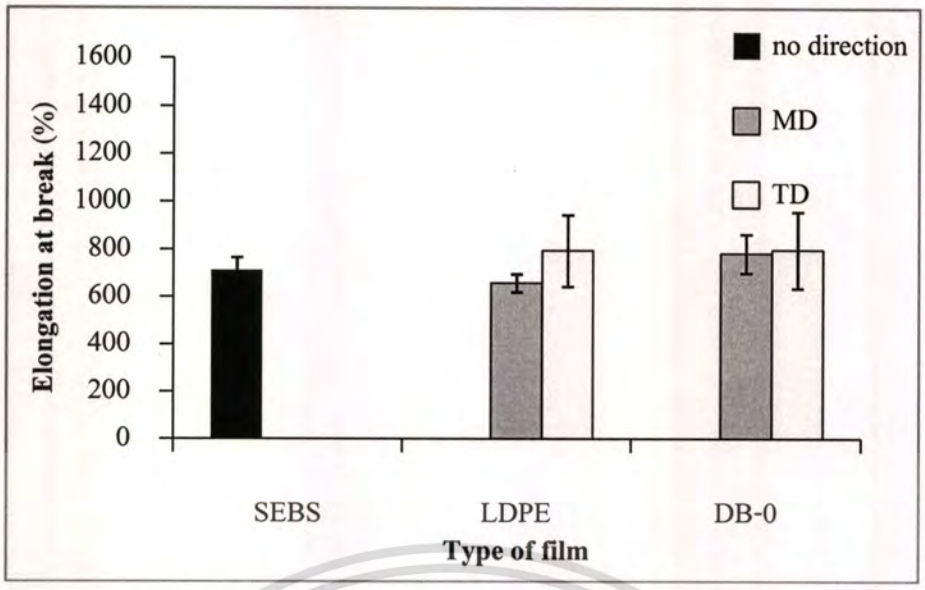

Figure 4.10 Tensile properties of the film without zeolite (80 μm thickness) : (a) yield stress, (b) Young's modulus, (c) tensile strength and (d) elongation at break

It is clearly seen that SEBS can be easily deformed as shown by a lower yield stress when compared with LDPE film (Figure 4.10a). This is because a higher stress is required for deformation of the folded chains of the crystalline region in LDPE at the yield point. On the other hand, there is only physical entanglement of polymer chains in SEBS which requires lower stress for the chain deformation. In addition, it can be seen that Young's modulus of SEBS is lower than that of LDPE. This is because thermoplastic elastomer SEBS (Kraton® G1652) contains 70%wt of ethylene-butylenes units, providing softness and flexibility in its nature. Nevertheless, tensile strength of SEBS is similar to that of LDPE. This is attributed to the polystyrene segment in SEBS acting as a physical crosslink. At temperature below the glass transition state of polystyrene, the styrene segment is agglomerated (as shown in Figure 4.11). These rigid polystyrene domains would be resistant to the movement of polymer chains under stress and act as junction points providing a strong network structure, in a manner similar to that of a vulcanized rubber [20]. Therefore, the high stress is required to a complete rupture of the SEBS film.

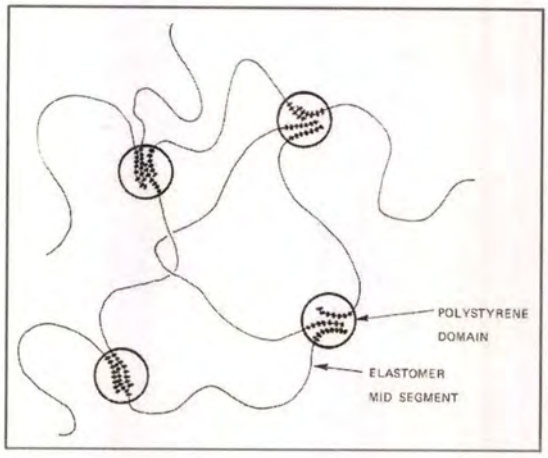

Figure 4.11 Phase structure of SEBS block copolymer

These rigid styrene domains (30%wt) can also inhibit chain elongation leading to a limited strain, as compared to that of typical elastomers. Accordingly, %elongation at break of the SEBS film is not different from that of LDPE film (Figure 4.10d).

Not only weaker tensile properties, SEBS film is also highly sticky. It is difficult to fabricate and handle. Hence, SEBS film alone is not suitable for packaging application. Therefore, the double-layered (SEBS-LDPE) film was prepared using LDPE film as a supporting layer for improving tensile properties, providing less sticky surface and hence eases of processing.

As expected the double-layered film exhibits higher yield stress and modulus, as compared to the SEBS film (Figure 4.10a and b). However, these properties are less than those of LDPE film because the thickness of the LDPE in double-layered film is only 30 μm. Nevertheless, the ultimate tensile strength of double-layered film aligns within the range of LDPE and SEBS films (Figure 4.10c). It is suggested that, during the lamination, there is neither interfacial defect nor additional crystallization of both films at the interphase layer as discussed earlier in the section of 4.1.3.

From the above observation, the obtained double-layered film possesses a better tensile property, as compared to that of the SEBS single layer film. Moreover, it can be easily handled and hence, suitable for packaging application.

When the zeolite was incorporated into the film, tensile properties of the zeolite composite double-layered film were modified as shown in Figure 4.12.

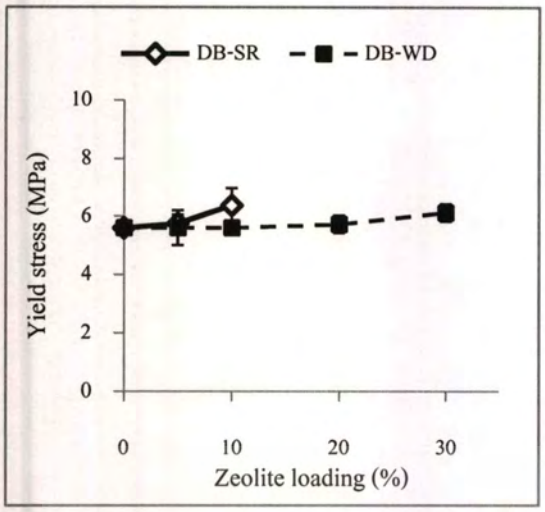

(a1)

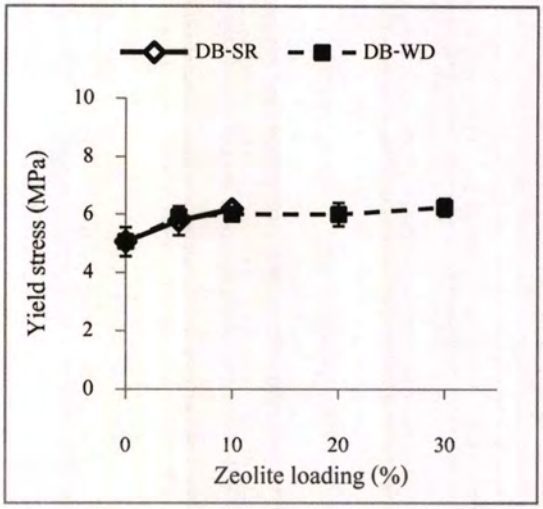

(a2)

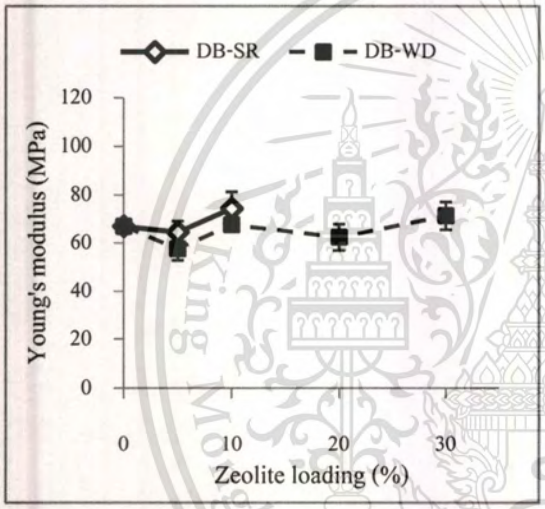

(b1)

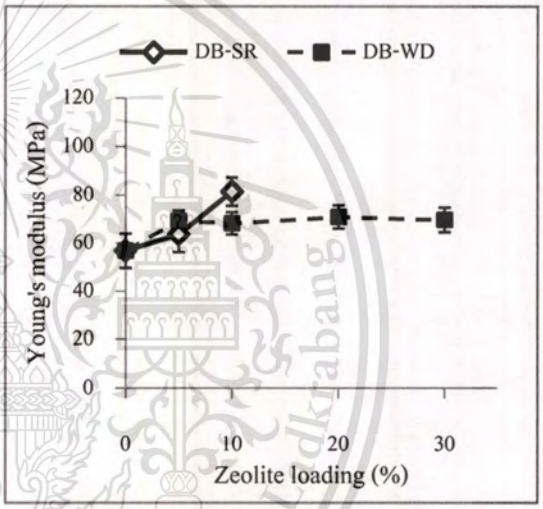

(b2)

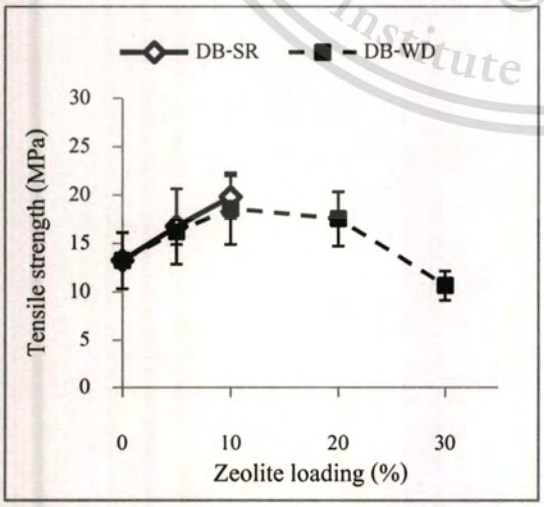

(c1)

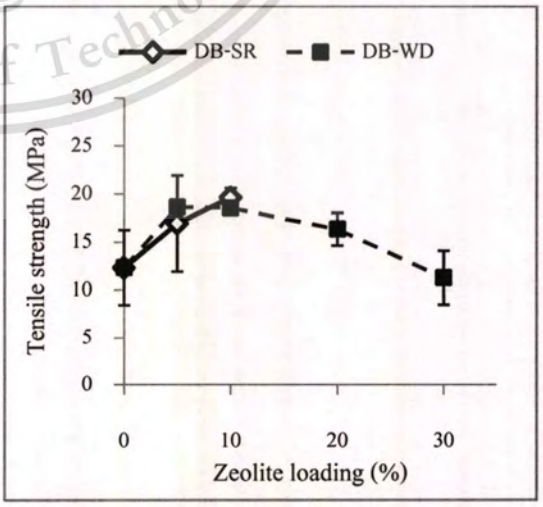

(c2)

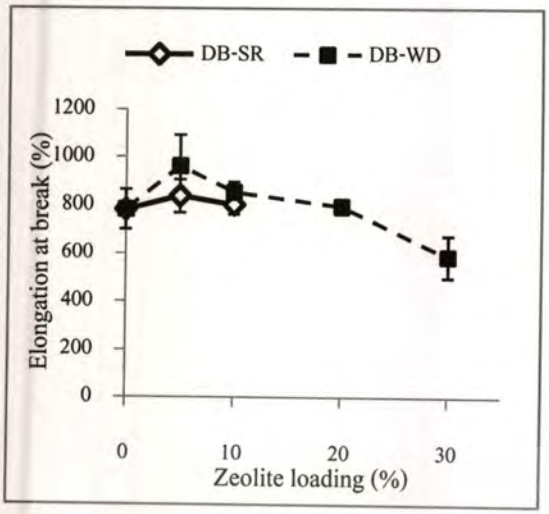

(d1)

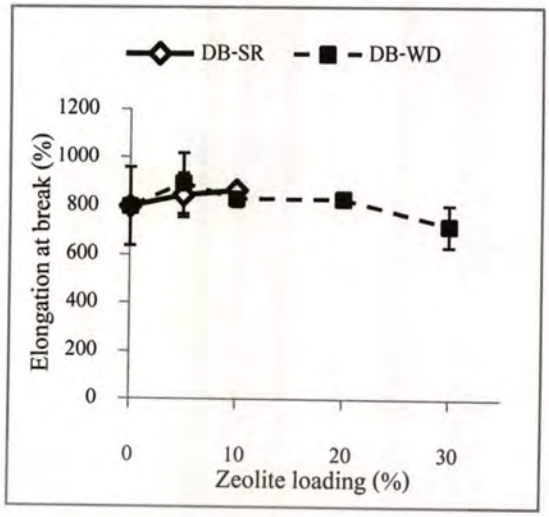

(d2)

Figure 4.12 Tensile properties of the zeolite composite double-layered film: (a) yield stress, (b) Young's modulus, (c) tensile strength and (d) elongation at break as (1) transverse direction; TD (2) machine direction; MD of LDPE layer

From Figure 4.12a, it can be seen that yield stress of the double-layered film is slightly increased from 5 to 6 MPa when zeolite was incorporated. In general, the increase in yield stress arises from the reinforcing effect of the zeolite filler [53-55]. For ZSM-5 in particular, the zeolite is hydrophobic and readily compatible with the SEBS matrix. Together with the small ZSM-5 particles size (approximate 1-2 micron), a strong interfacial interaction and hence adhesion between the zeolite filler and the polymer matrix can be obtained. As the zeolite composite film was stretched, it required relatively higher stress at the yield point to induce the permanent plastic deformation, when compared to the film without zeolite. However, there is no significant change in yield stress when the zeolite content is increased. This is because the zeolite was mainly dispersed only in the rubbery SEBS phase that is supported by the LDPE layer. Since the yield stress of the LDPE support is much higher than that of SEBS, the reinforcing effect of zeolite in the latter phase cannot be clearly observed with increasing zeolite loading.

An addition of zeolite also increases the Young's modulus of the double-layered film. This is because the inclusion of rigid particles in the polymer can increase in rigidity of the film [53,56]. However, no significant change in Young's modulus is shown with increasing zeolite loading (Figure 4.12b). This is again explained by the "buffering effect" of the LDPE supporting layer, which was previously discussed for yield stress.

An increase in tensile strength of the double-layered film is also found when zeolite was added (Figure 4.12c). As the zeolite loading increased from 0 to 10%wt, a corresponding increment of tensile strength from 12 to 19-20 MPa is commonly observed [50]. This is derived from the reinforcing effect, as discussed earlier. However, the tensile strength drops gradually when zeolite loading was increased up to 30%wt. The decrease in tensile strength is resulted from an agglomeration of the zeolite particles, as shown in SEM micrograph (Figure 4.4d). In addition, the interfacial voids are clearly seen in 30%wt zeolite loading. These voids act as stress concentrators and a weaker composite structure is induced by the discontinuity of the stress transfer. Such defects also lead to a lower film extension [50]. Therefore, the elongation is decreased for 30%wt zeolite loading.

In a view of zeolite dispersion, there is no significant difference of tensile properties between the DB-SR and DB-WD films for 0-10%wt zeolite loading. This is because only small amount of zeolite can be loaded in SEBS elastomer matrix. The incorporated particles do not readily affect to the continuity of the SEBS matrix. Therefore, the zeolite can be regarded as reinforcing filler in the DB-SR as well as in the DB-WD.

From the above observations, it is worth noting that all zeolite composite double-layered films exhibit tensile properties (i.e. tensile strength around 11-20 MPa) in a range applicable for those used in packaging industry (i.e. tensile strength 7-22 MPa)

4.3 Gas permeations

The ethylene, carbon dioxide and oxygen permeabilities of the LDPE(80), SEBS(80) and double-layered films without zeolite are shown in Figure 4.13.

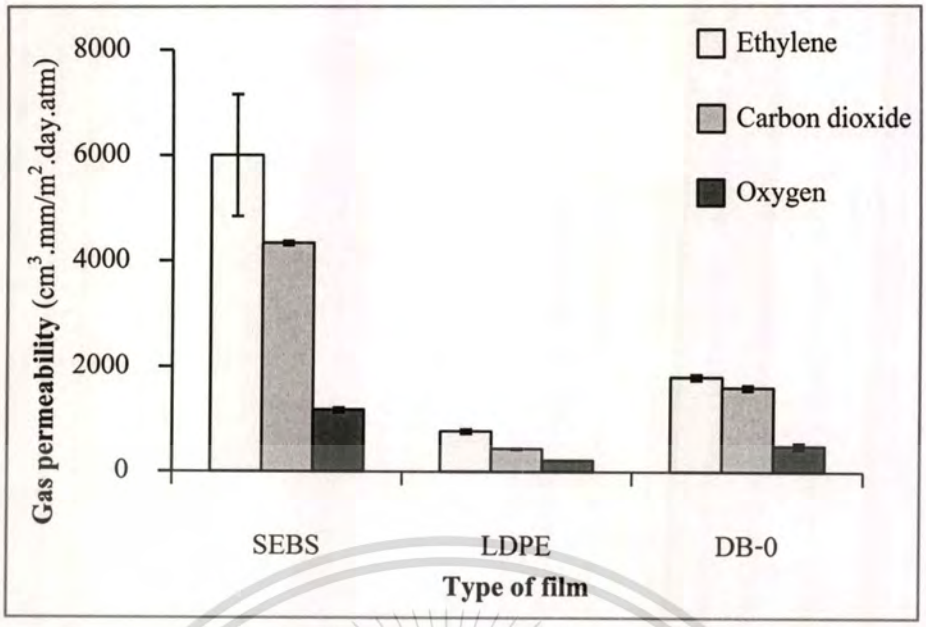

Figure 4.13 Ethylene, carbon dioxide and oxygen permeabilities of the films (80 μm) without zeolite

It was found that gas permeability of SEBS film is much higher than that of LDPE film, especially for the ethylene permeation (Figure 4.13). This is because the SEBS contains ethylene/butylene segments with relatively high free volume and flexibility. Thus the gas molecule can be soluble in the film and readily permeate through this film. Whilst, the crystalline phase in LDPE is generally impermeable for gas molecules [44]. Only amorphous phase of LDPE allows the gas permeation.

As compared to oxygen and carbondioxide, relative higher permeation of ethylene can be observed in all films. This is because both LDPE and SEBS are hydrophobic polymers which allow strong interaction with non-polar ethylene gas. The ratio of gas permeability for ethylene and oxygen (P C_2H_4 / P O_2) was calculated from pure gas permeation experiment to determine the ideal selectivity [57,44], as shown in Table 4.5.

Table 4.5 Permeability ratio of the film without zeolite

Film	$P(C_2H_4)/P(O_2)$	$P(CO_2)/P(O_2)$
SEBS(80)	5.1	3.7
LDPE(80)	3.6	2.0
DB-0	3.6	3.2

It can be seen that SEBS shows ethylene permeability approximately five times higher than that of oxygen, whereas this value is about three times for LDPE. This is indicated that SEBS is a suitable material for a smart packaging. Since, the film can regulate oxygen permeation but facilitate ethylene permeation. In other word, SEBS film readily reduces the ethylene accumulation in the package. This is preferred because, in postharvest, the ethylene gas induces an unusually fast growth e.g. over-ripening, excessive softening and abscission of leaves and flowers. In addition, in the presence of ethylene, the respiration of the fresh produces is also accelerated. Thus, high ethylene permeation of SEBS film is a beneficial property for a smart packaging of fresh produces.

In addition, the permeation of carbon dioxide is higher than that of oxygen. This suggests that the carbon dioxide gas strongly interacts with the film, which is preferred for keeping the fresh produces [58]. The appropriate atmosphere inside the package can be achieved by reducing oxygen concentration and increasing carbon dioxide concentration. Such gas dynamic results in a slow metabolism that allows the products to be kept for a longer period. A diagram of gas exchange is shown in Figure 4.14

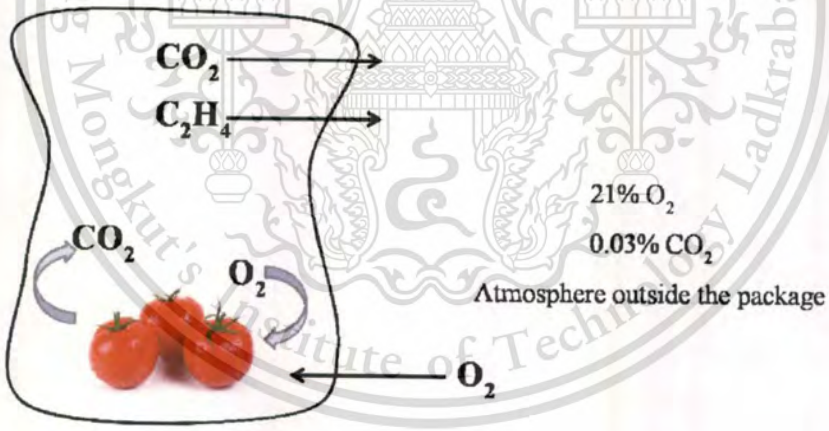

Figure 4.14 Diagram of a gas exchange through the film

Although SEBS seems to be ideal modified atmosphere packaging, it cannot be processed and handle. Thus, SEBS alone cannot be used for a packaging film. To overcome this problem, LDPE supporting layer was incorporated without substantially change in tensile properties as shown earlier in section 4.2.

With LDPE as supporting layer, the gas permeability of the double-layered film is higher than that of the LDPE film, but lower than that of SEBS film, as shown in Figure 4.13. This is

because gas permeability for the double-layered would be readily enhanced in SEBS layer in a manner similar to that of the SEBS single-layer film. In addition, the thickness of LDPE layer, which acts as barrier, is relatively less (30 μm) in the double-layered film. This would allow a faster permeation rate, as compared to LDPE(80) film. The double-layered film still exhibits higher selective for ethylene gas. This is due to the fact that both SEBS and LDPE films possess high selectivity for ethylene permeation. In addition to a higher permeability and selectivity for ethylene, the double-layered film gives good tensile properties as explained earlier. Therefore, it is suitable for application of ethylene removal packaging.

It can also be seen that water vapor transmission rate (WVTR) of all films are so small (Figure 4.15). This is because both LDPE and SEBS are non polar polymers, whereas water is high polar. Hence, water vapor possesses weak interaction with the polymer matrix. This leads to a low adsorption and consequently, low permeation of water in the polymer film [59]. However, the water vapor permeability of SEBS is higher than that of LDPE. This is because SEBS is a highly amorphous polymer with relatively high free volume and flexibility, as discussed earlier. In a similar manner to gas permeation, the double-layered film shows the water vapor transmission rate in between those of SEBS and LDPE films.

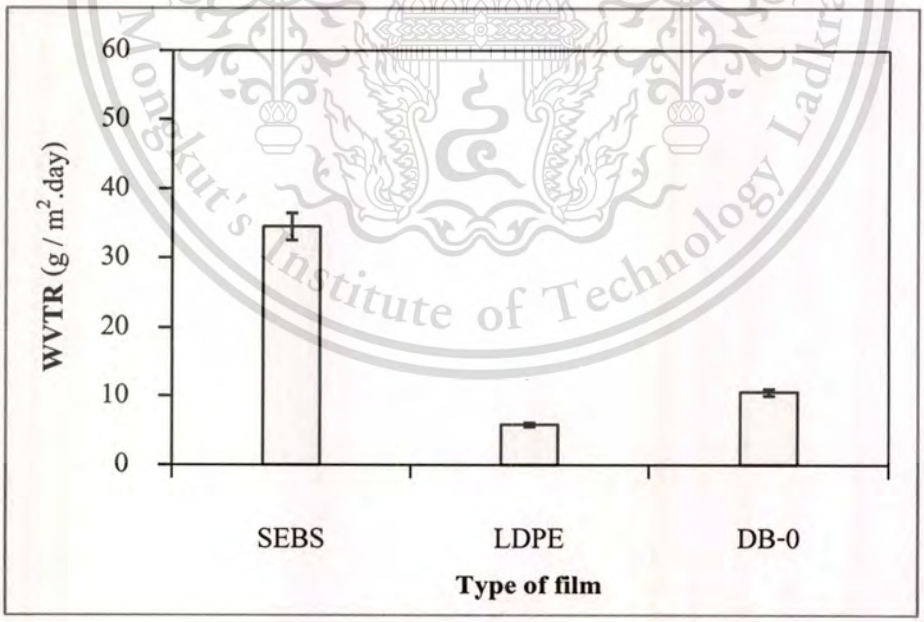

Figure 4.15 Water vapor transmission rate of the films (80 μm) without zeolite

When the zeolite was incorporated into the double-layered film (5-30%wt), the zeolite composite double-layered film exhibits a higher permeability for ethylene, as compared to the double-layered film without zeolite (Figure 4.16).

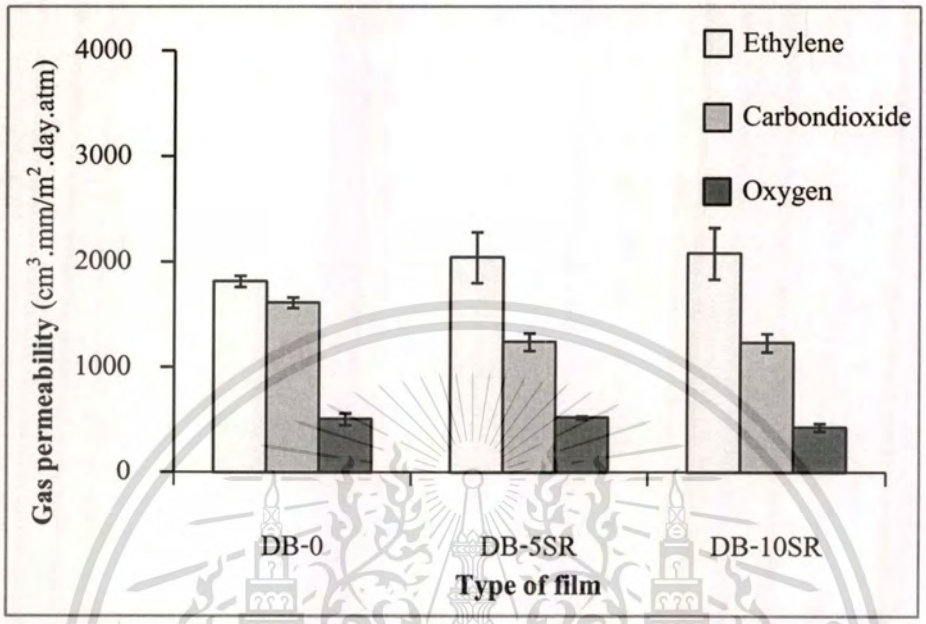

(a)

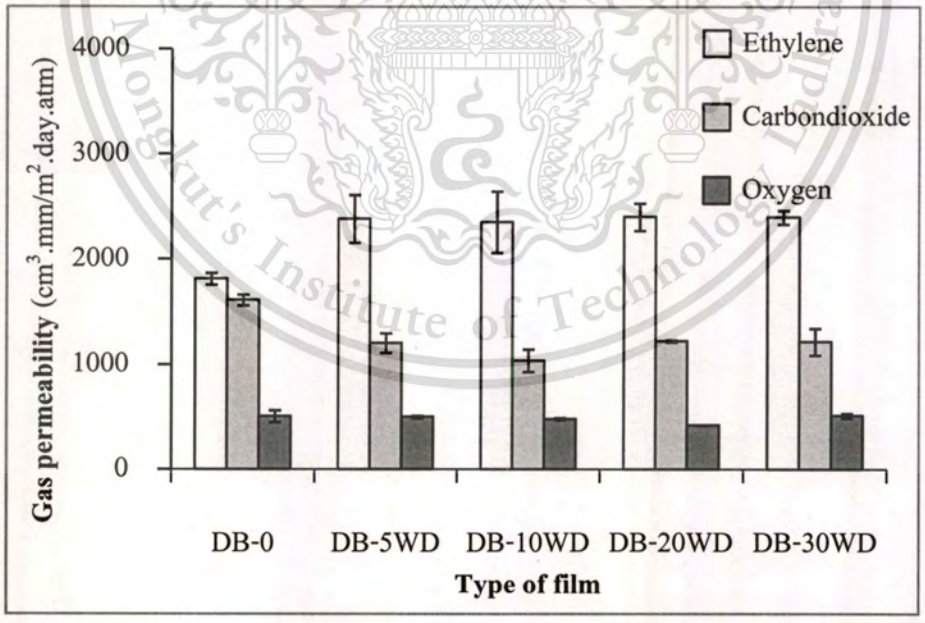

(b)

Figure 4.16 Ethylene, carbon dioxide and oxygen permeabilities of the zeolite composite double-layered film: (a) DB-SR and (b) DB-WD

This is because the ZSM-5 zeolite (Si/Al = 140) possessed 5.5 Å in pore size diameter, is highly hydrophobic. This allows a strong interaction with the ethylene gas, a hydrophobic molecule with 4.2 Å in kinetic diameter [8]. Hence, the incorporated zeolite leads to relative higher ethylene adsorption. This is consistent with the adsorption isotherm of ZSM-5, as shown in Figure 4.17 (ethylene > carbondioxide >> oxygen).

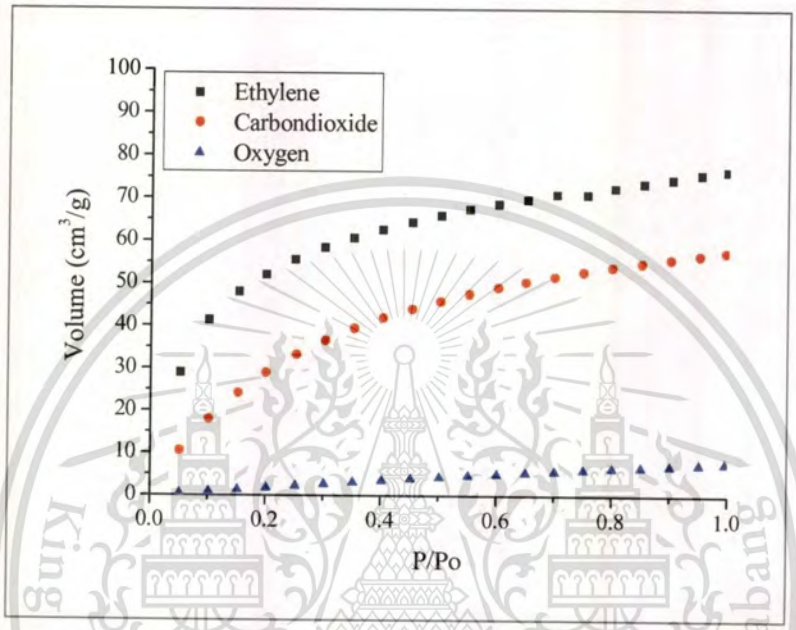

Figure 4.17 Adsorption isotherm by ZSM-5 zeolite [5]

Accordingly, a high concentration of ethylene is expected at the surface of film leading to a higher concentration gradient across the film. This becomes a driving force for ethylene permeation and leads to a greater diffusion of ethylene gas in the film.

However, an increase in zeolite contents does not exhibit a significant improve in ethylene permeation. This is explained by the limitation of ethylene permeation when LDPE is presented in the double-layered film. Although the permeation of ethylene in SEBS phase will be facilitated by an incorporation of the zeolite, the crystalline phase of the LDPE acts as a barrier for ethylene permeation as discussed earlier. Hence, the effect of increasing zeolite in SEBS layer on the total permeability of the double-layered film cannot be clearly observed.

It can be noticed that the ethylene permeability of DB-WD is slightly higher than that of DB-SR. This is indicated that the ethylene permeability also depended on the zeolite dispersion. It is proposed that a short diffusion pathway in the matrix film, between zeolite particles and their neighbors, of the well dispersed (WD) zeolite/SEBS composite layer can assist ethylene

permeation. Since the ethylene gas can be readily adsorbed in zeolite pore, as compared to polymer matrix, the diffusion rate in polymer matrix plays important factor for the ethylene permeation. The ethylene gas is diffused through this shorter pathway of the polymer matrix in the WD zeolite/SEBS composite layer as shown in Figure 4.18. In contrast, zeolite particles accumulate only at the surface of the film, ethylene must diffuse through whole film in surface rich (SR) zeolite/SEBS composite layer. Therefore, the ethylene permeation of DB-SR is lower than that of DB-WD.

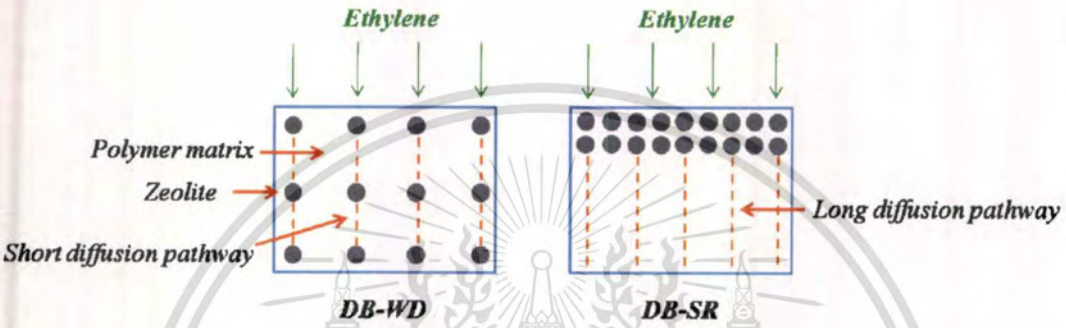

Figure 4.18 Diffusion pathway of ethylene gas in the zeolite/SEBS composite layer

In the presence of zeolite, it can be seen that oxygen permeability of the film is poor and no significant change when zeolite contents are increased. This is because oxygen is an inert adsorbate which possesses weak interaction with zeolite framework on the film. This leads to poor adsorption capacity by zeolite. In addition, oxygen possesses very low boiling point (-183 °C) and high vapor pressure. Thus, it can only be slightly soluble and adsorbed in polymer matrix leading to low permeation for oxygen.

It importantly points out that the increase in $P(C_2H_4) / P(O_2)$ ratio can be observed for the zeolite composite double-layered film (Table 4.6). This is indicated that the zeolite composite double-layered film can readily remove ethylene gas from the package and maintain capability for impeding the permeation of oxygen.

Table 4.6 Permeability ratio of the zeolite composite double-layered film

Film	$P(C_2H_4)/P(O_2)$	$P(CO_2)/P(O_2)$
DB-0	3.6	3.2
DB-5SR	3.9	2.4
DB-10SR	4.8	2.9
DB-5WD	4.8	2.4
DB-10WD	4.9	2.6
DB-20WD	5.4	2.9
DB-30WD	4.7	2.4

For both composite films (DB-SR and DB-WD), carbondioxide permeability is significantly decreased when zeolite was added into the SEBS layer (Figure 4.16). This is because carbondioxide is relatively high polar. Hence, it can only be soluble and mostly diffuse in the styrene segment that possesses relatively high polarity, as compared to the ethylene-butylene segment. In line with this view, it is expected that when zeolite was incorporated in the film, the particles would be mostly dispersed in styrene segment. The interaction between zeolite particle and the styrene segment was evidenced by DMTA and FT-IR as discussed earlier in section 4.1.3 and 4.1.4, respectively. This interaction would lead to a lower chain flexibility and a decrease in free volume. Therefore, the diffusion of carbondioxide gas in the zeolite composite double-layered film was obstructed, resulting in lower carbondioxide permeation, as compared to that in the double-layered film without zeolite. However, there is insignificant change in carbondioxide permeation by varying either zeolite content or dispersion. This is due to the barrier property from LDPE layer as discussed earlier for ethylene permeation. Nevertheless, all zeolite composite double-layered films show P CO_2 / P O_2 ratio $\sim$ 3 which is applicable for modified atmosphere packaging.

With the zeolite incorporation, there is no significant change in water vapor transmission rate of both DB-SR and DB-WD films (Figure 4.19). This is because ZSM-5 is hydrophobic and does not interact well with water vapor, a high polar molecule. However, water vapor transmission rate of all zeolite composite double-layered films are in the range of 10-45 g/mm^2.day, applicable in the postharvest package [60].

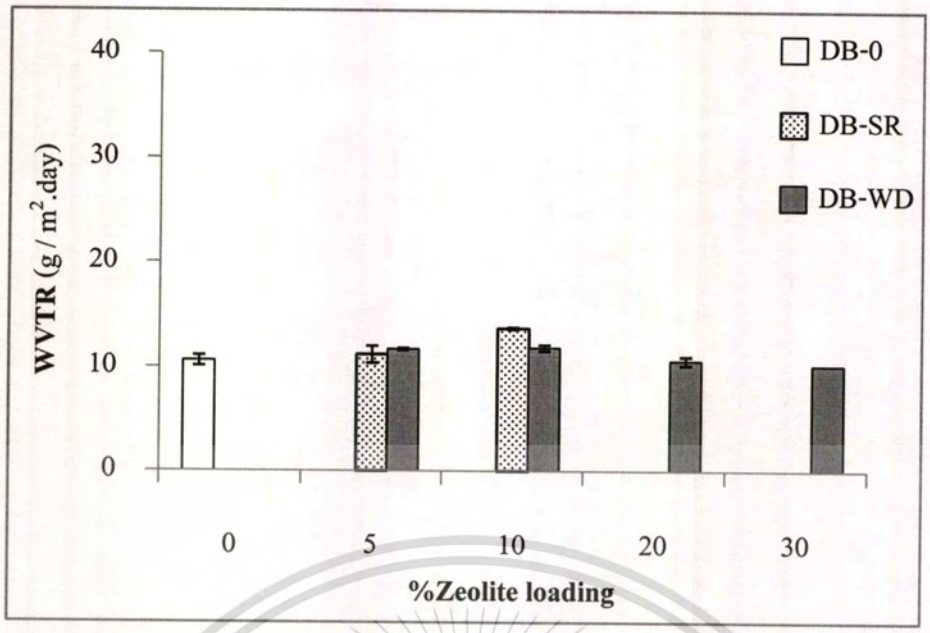

Figure 4.19 Water vapor transmission rate of the zeolite composite double-layered film

The relationship of ethylene flux and feed concentration was studied and shown in Figure 4.20.

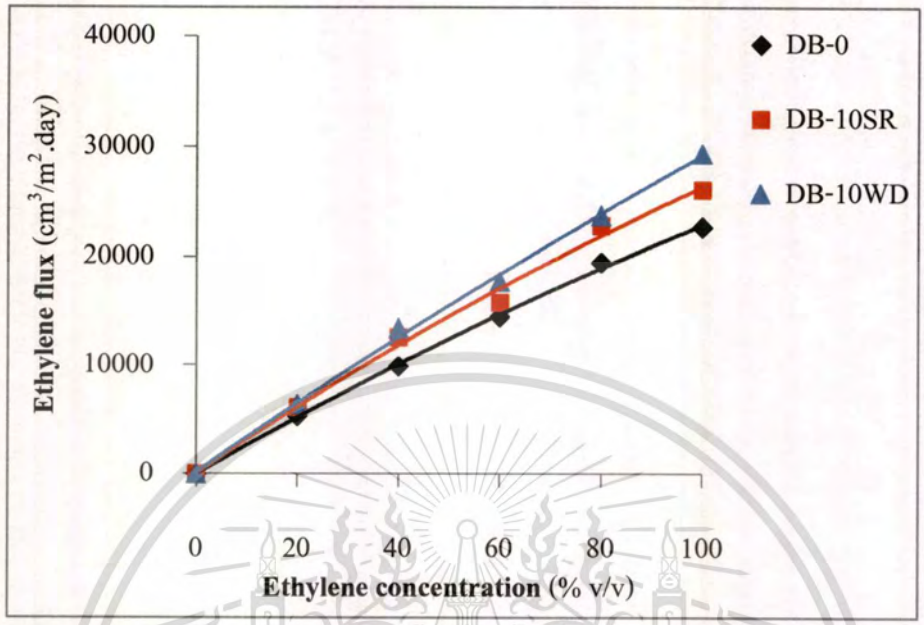

(a) In N_2

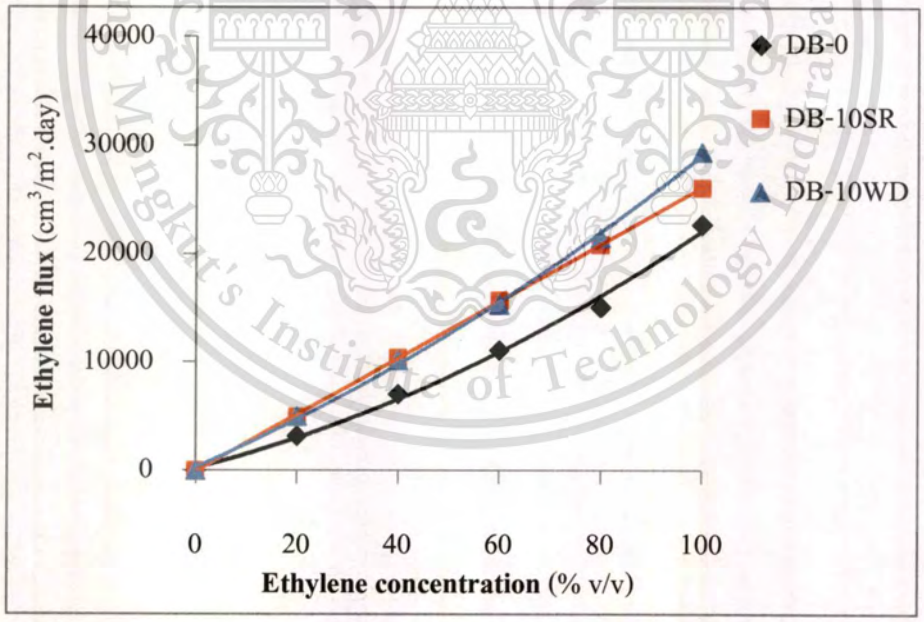

(b) In air zero (80%N_2 / 20%O_2)

Figure 4.20 Relationship of ethylene flux –feed concentration of the double-layered film with and without zeolite : (a) under N_2 and (b) under air zero (mixture of 20%O_2 and 80%N_2) atmosphere

It can be seen that ethylene flux is enhanced when the concentration of ethylene in the gas phase is increased. This is explained by Fick's law of diffusion as follow [61]:

$$J = -D\frac{\partial \phi}{\partial x} \tag{4.1}$$

where J is the diffusion rate of gas through the membrane per a unit area, D is diffusion coefficient or diffusivity, $\partial\phi$ is the concentration gradient of gas on the feed and permeate side of the membrane and ∂x is the distance or the film thickness, respectively. In this study, the constant ambient temperature (25 °C) was used for permeation test. This hence results in a constant diffusion coefficient (D) of the gas in the film [61]. In addition, the film thickness was prepared within the same range and presumably no significant change in the thickness of the film tested. Therefore, the ethylene flux, which relates to permeability, depends only on the ethylene concentration of feed gas. As the ethylene concentration in the feeding side is increased, the higher concentration gradient can be obtained. Accordingly, the ethylene gas molecule can feasibly permeate increasingly throughout the film.

Although flux of the permeated ethylene *(J)* is increased by an increase in ethylene concentration gradient as discussed previously, ethylene permeability is not significantly changed, as shown in Figure 4.21.

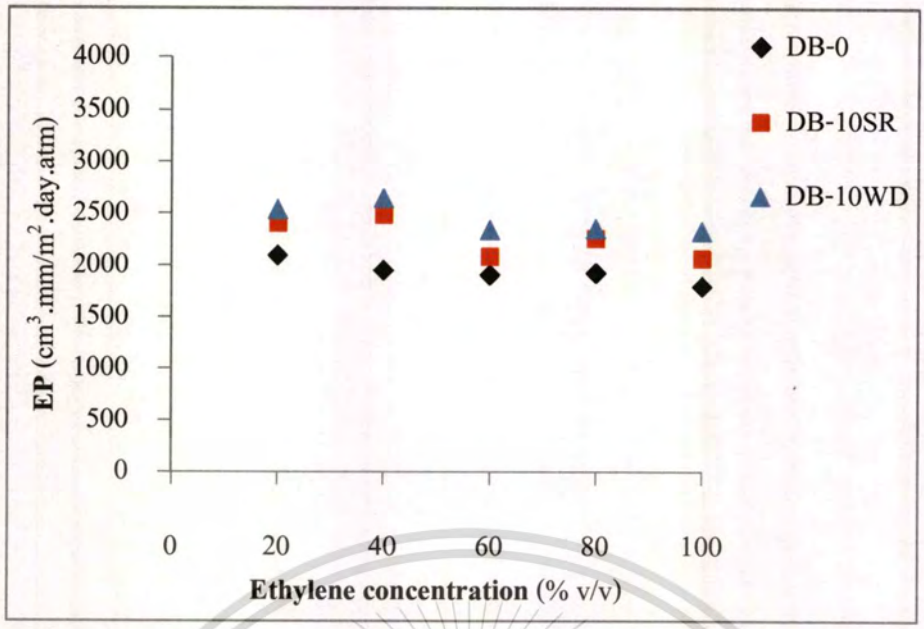

(a) In N_2

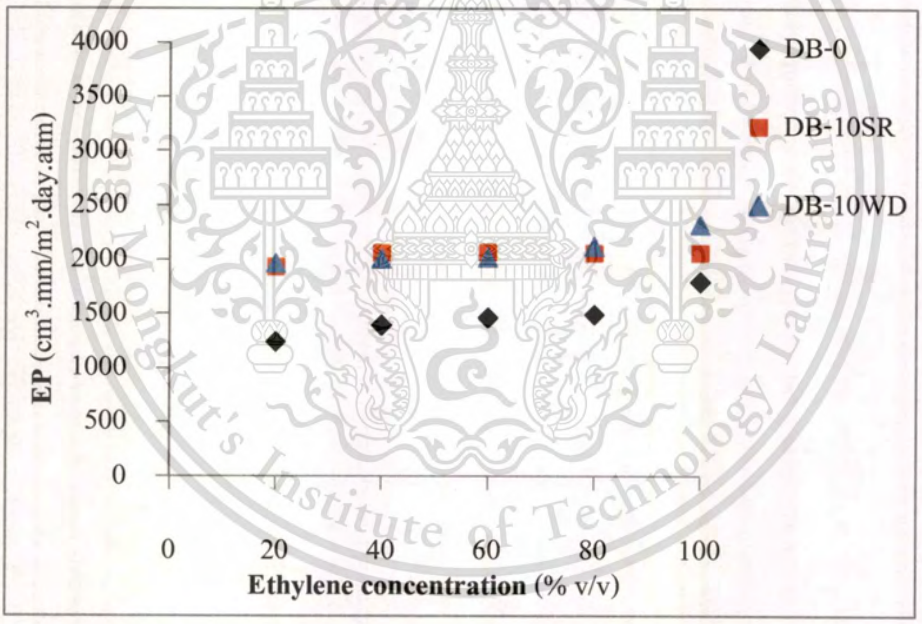

(b) In air zero (80%N_2 / 20%O_2)

Figure 4.21 Relationship of ethylene permeability –feed concentration of the double-layered film with and without zeolite : (a) under N_2 and (b) under air zero (mixture of 20%O_2 and 80%N_2) atmosphere

This is because permeability (P) is inversely proportional to Δp, as shown in Eq. 4.2

$$P = \frac{J \Delta x}{A \Delta p} \tag{4.2}$$

where P is the gas permeability ($cm^3.mm/m^2.day.atm$), J is the transmission rate of the permeated gas (cm^3/day), Δx is the film thickness (mm), A is the surface area of the film (m^2), Δp is the partial pressure difference of the analyte gas across the film (atm). When ethylene concentration in the feed is increased, the partial pressure difference of ethylene across the film is also increased.

From Figure 4.21(a), it can be seen that ethylene permeability of the zeolite composite double-layered film is higher than that of the double-layered film without zeolite. This result can be observed clearly for all ethylene concentrations. In addition, the ethylene permeability of DB-WD film is slightly higher than that of DB-SR film. This is because the short diffusion pathway in DB-WD can facilitates ethylene permeation, as discussed in Figure 4.16.

In the presence of oxygen (Figure 4.21b), ethylene permeation of all films is decreased, especially for the double-layered film without zeolite. This is because the mass transfer of ethylene from gas phase onto such film surface would be inhibited by the competitive adsorption of oxygen. This leads to a notably lower ethylene permeation particularly at low ethylene concentration, as compared to that in the C_2H_4-N_2 mixed gas atmosphere (Figure 4.21a). However, when zeolite was incorporated in the film, the effect by such competitive adsorption is readily decreased. This is because zeolite in the composite film can selectively adsorb ethylene gas, as compared to oxygen. (as discussed earlier by the adsorption isotherm). In other words, the affinity of the film toward ethylene gas becomes significantly improved when the zeolite is present. Accordingly, the interference of oxygen partial pressure would be smaller, as compared to the double-layered film without zeolite. It can be noticed from Figure 4.21b that, in the present of oxygen, the ethylene permeability of DB-WD film is not significantly different from DB-SR film at low ethylene concentration. However, this effect is pronounced particularly at high ethylene_concentration. This is explained that the gas permeation mechanism is taken place via three steps; (I) mass transfer from the gas phase onto the film surface (II) gas diffusion in the film and (III) desorption of gas into permeate side, as shown in Figure 4.22.

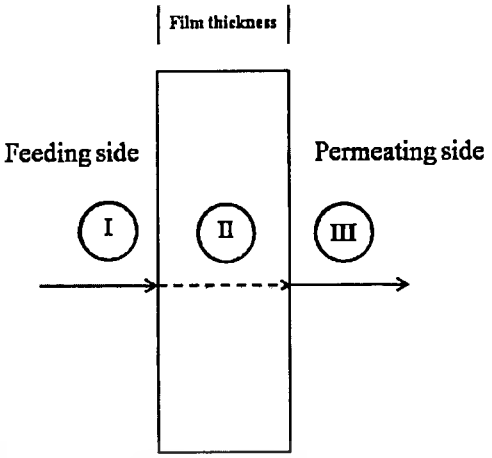

Figure 4.22 Gas permeation mechanism : (I) mass transfer of gas onto the film surface (II) gas diffusion in the film and (III) desorption of gas into permeate side

Due to the competitive adsorption, when ethylene concentration in feeding side is low (high oxygen partial pressure), only small amount of the ethylene molecule can be adsorbed on the film. Hence, the permeation rate is determined by mass transfer of ethylene in the gas phase onto the film surface. Accordingly, the zeolite dispersion in the film does not obviously affect to the total ethylene permeation. It is suggested that the gas molecule can be transferred onto the film surface with a similar rate (rate determining step) for both zeolite composite films (DB-SR and DB-WD). Therefore, no significant difference in the ethylene permeability can be observed at low ethylene concentration. However, when the ethylene concentration is high, ethylene can readily adsorb on the film surface. In this case, mass transfer (I) from gas phase to the film is negligible. In turn, rate determining step for the ethylene permeation becomes the gas diffusion in the film (II). Therefore, the well dispersion of zeolite particles in DB-WD film can somewhat enhance the ethylene permeation as observed.

CHAPTER 5

CONCLUSION AND SUGGESTION

5.1 Conclusion

SEBS is a potential candidate for MAP with high ethylene permeability. This is because the ethylene/butylene segment in SEBS, which is hydrophobic and highly free volume and flexible, allows stronger interaction with ethylene, as compared to carbon dioxide and oxygen. Hence, its free volume can facilitate ethylene permeation. In addition, the permeation of carbon dioxide is higher than that of oxygen. This is also a preferential choice for modifying the gas composition that is suitable for fresh produces packaging. Moreover, its drawback in mechanical properties was successfully improved by the use of LDPE supporting layer.

The incorporated zeolite in SEBS layer readily serves as ethylene adsorbent, and readily improves ethylene concentration gradient across the film which becomes a major driving force of ethylene permeation. The ethylene permeability of the film is also facilitated by a better zeolite dispersion. It was suggested that the short diffusion pathway between the zeolite particles dispersed in the film plays important role on the gas permeability. However, when the zeolite loading is higher than 5 %wt, the ethylene permeability cannot be clearly improved owing to the limited gas permeability of LDPE supporting layer. This is because crystallinity phase in LDPE is generally impermeable for gas molecules. As MAP benefit, an addition of zeolite also decreases the carbondioxide permeation. This is derived from the interaction between zeolite and PS segment that causes an increase in chain rigidity. Oxygen permeability was not readily affected by the incorporation of zeolite.

In the presence of oxygen, the ethylene permeation of the film is decreased. This is because the adsorption of ethylene can be competed by oxygen, particularly at high oxygen concentration. Adding zeolite suppresses the competitive adsorption. This is due to the highly selective adsorption of ethylene by ZSM-5 zeolite.

The incorporated zeolite particles also act as reinforcing filler leading to improved tensile properties of the film when loading is less than 10%wt. However, there is no significant change in yield stress and Young's modulus when the zeolite content is increased. In addition, when the zeolite content is higher than 10 %wt, agglomeration and interfacial voids were created in the composite double-layer film resulting in a significant drop in the ultimate tensile strength. In a

view of zeolite dispersion, there is no significant difference of tensile properties between the DB-SR and DB-WD films. With 5 %wt zeolite content, the zeolite composite double-layered film possesses appropriate mechanical properties and ethylene permeability and selectivity that can be used for MAP with ethylene removal ability.

5.2 Suggestion for future studies

5.2.1 Although the zeolite loading is higher than 5 %wt, the ethylene permeability cannot be clearly improved owing to the limited gas permeability of LDPE supporting layer. Thus, the ethylene permeability would be enhanced by the development of the supporting layer, such as a perforation of the film.

5.2.2 It is well know that gas permeation can be enhanced with a lower film thickness. To increase the ethylene permeation, film thickness of SEBS layer would also be decreased.

5.2.3 This study can provide the zeolite composite double-layered films with high ethylene permeability which is suitable for fresh produces packaging application. It is interest to determine the storage time of the fresh produces (ethylene sensitive fruits and vegetables). Such film would be studied for packing them.

REFERENCES

[1] A.L. Brody, E.R. Strupinsky and L.R. Kline. 2001. **Active Packaging for Food Applications.** USA : Technomic.

[2] M.E. Saltveit. 1999. "Effect of Ethylene on Quality of Fresh Fruits and Vegetables." **Postharvest Biology and Technology.** 15(3) : 279-292.

[3] D. Zagory and A.A. Kader. 1988. "Modified Atmosphere Packaging of Fresh Produce." **Food Technology.** 42(9) : 70-74.

[4] K. Shah, T.K. Ling, L. Woo, G. Nebgen, S. Edwards and L. Zakarija. 1998. **Gas Permeability and Medical Film Products.** [online]. Available : http://www.devicelink.com/mpb/archive/98/09/005.html.

[5] S. Apisittinet. 2007. "Study on Ethylene Gas Permeability of Zeolite-LDPE and Zeolite-SEBS Composite Film." M.Sc. Thesis of King Mongkut's Institute of Thechnology Ladkrabang.

[6] P.B. Leavens. 2007. **Zeolite.** [online]. Available : http://www.chemistryexplained.com/Va-Z/Zeolites.html.

[7] A. Dyer. 1988. **An Introduction to Zeolite Molecular Sieves.** New York : John Wiley and Sons.

[8] S.M. Auerbach, K.A. Carrado and P.K. Dutta. editor. 2003. **Handbook of Zeolite Science and Technology.** New York : Basel.

[9] S.V. Donk. 2002. **Adsorption, Diffusion and Reaction Studies of Hydrocarbons on Zeolite Catalysts.** [online]. Available : http://igitur-archive.library.uu.nl/dissertations/2002-1209-125604/c1.pdf.

[10] Wolfwiki. 2009. **Zeolites.** [online]. Available : http://wikis.lib.ncsu.edu/index.php/Zeolites.

[11] Wikipedia. 2008. **ZSM-5.** [online]. Available : http://en.wikipedia.org/wiki/ZSM-5.

[12] A.H. Roy, R.R. Broudy, S.M. Auerbach and W.J. Vining. 2009. **Teaching Materials that Matter: An Interactive, Multi-media Module on Zeolites in General Chemistry.** [online]. Available : http://samson.chem.umass.edu/~auerbach/pub_pdf/pap24.pdf.

[13] University of California San Diego. 2008. **ZSM-5 Catalyst.** [online]. Available : http://chemelab.ucsd.edu/methanol/memos/ZSM-5.html.

[14] Lenntech. 2008. **Zeolite Application.** [online]. Available : http://www.lenntech.com/zeolites-applications.htm.

[15] J. Wilmot. 2008. **Zeolite Adsorbents.** [online]. Available : http://www.cefic.be/Templates/shwAssocDetails.asp?NID=473&HID=429&ID=177.

[16] Wikipedia. 2008. **Low-Density Polyethylene.** [online]. Available : http://en.wikipedia.org/wiki/LDPE.

[17] The University of Southern Mississippi. 2005. **Polyethylene.** [online]. Available : http://www.pslc.ws/macrog/pe.htm.

[18] Interactive Learning Paradigms Incorporated. 2006. **Polymerization.** [online]. Available : http://www.ilpi.com/msds/ref/polymer.html.

[19] Encyclopedia Britannica Inc. 2007. **Low-Density Polyethylene.** [online]. Available : http://www.britannica.com/EBchecked/topic-art/349692/2948/The-branched-form-of-polyethylene-known-as-low-density-polyethylene#tab=active~checked%2Citems~checked.

[20] N.R. Legge, G. Holden and H.E. Schroeder. editors. 1987. **Thermoplastic Elastomers.** New York : Hanser Publishers.

[21] Eastman Chemical Company. 2008. **Block Copolymer.** [online]. Available : http://www.eastman.com/Markets/Tackifier_Center/Block_Copolymer.htm.

[22] Specialchem and Omnexus. 2008. **Block Copolymers Based on Styrene and Butadiene (TPE-S or SBS, SEBS).** [online]. Available : http://www.omnexus.com/plastics-channels/rubber-replacement/performances.aspx?id=tpes.

[23] Kraton Polymer LLC. 2006. **An Introduction to Kraton Polymer.** [online]. Available : http://www.kraton.com/content/includes/An%20Intro%20To%20Kraton.pdf.

[24] W. Soroka. 1995. **Fundamentals of Packaging Technology.** Virginia : Institute of Packaging Professionals.

[25] Global Business Hub for the Packaging Industry. 2008. **Plastic Film.** [online]. Available : http://www.packaging-films.com/plastic-films.html.

[26] M.L. Rooney. 2005. **Active Packaging Research at the Food Research Laboratory.** [online]. Available : http://www.regional.org.au/au/roc/1991food/p-15.htm.

[27] Food Science Australia. 2008. **Active Packaging.** [online]. Available : http://www.foodscience.csiro.au/actpac.htm.

[28] Dixell. 2008. **Ehtylene Gas - The Silent Killer of Produce and Flowers.** [online]. Available : http://www.dixellasia.com/index.php?tpid=0222&pgid=0223.

[29] L.Vemeiren, L.F. Devliegher, M. van Beest, N. de Kruijf and J. Debevere. 1999. "Development in the Packaging of Foods." **Trend in Food Science and Technology,** 10 : 77-86.

[30] E.M. Yahia. 2009. **Modified and Controlled Atmosphere for the Storage, Transpiration and Packaging of Horticultural Commodities.** New York : CRC Press.

[31] D. Reed. 2009. **Senescence and Post-Harvest Storage.** [online]. Available : http:// generalhorticulture.tamu.edu/HORT604/LectureSupplMex07/SenescencePostHarvest.pdf.

[32] S.V. Irtwange. 2006. "Application of Modified Atmosphere Packaging and Related Technology in Postharvest Handling of Fresh Fruits and Vegetables." **Agricultural Engineering International: the CIGR Ejournal Invited Overview.** 3(4) : 178-187.

[33] M.S. Suwandi and S. Anhar. 1987. **Membrane Technology : Proceedings of the Fourth ASEAN (Training) Workshop on Membrane Technology Held at National University of Malaysia in April 15-25.** Bangi : Asean Working Group on Food Waste Materials.

[34] Sci-Tech Encyclopedia. 2008. **Membrane Separations.** [online]. Available : http://www.answers.com/topic/membrane-separation?cat=technology.

[35] Rowan University. 2005. **Membrane Gas Separation.** [online]. Available : http://users. rowan.edu/~savelski/uol/gas.html.

[36] J. Comyn. 1985. **Polymer Permeability.** London : Elsevier Applied Science Publishers.

[37] S. Young. 2004. **Gas and Liquid Diffusion in Membranes.** [online]. Available : http:// www.psrc.usm.edu/mauritz/diffuse.html.

[38] M.L. Rooney. 1995. **Active Food Packaging.** London : Blackie Academic and Professional.

[39] T. Suslow. 1997. "Performance of Zeolite Based Products in Ethylene Removal." **Perishables Handling Quarterly.** 92 : 32-33.

[40] M.R. Domingo, F. Guillén, S. Castillo, P.J. Zapata, D. Valero and M. Serrano. 2009. "Development of a Carbon-Heat Hybrid Ethylene Scrubber for Fresh Horticultural Produce Storage Purposes." **Postharvest Biology and Technology.** 51(2) : 200-205.

[41] I. Alia-Tejacal, R. Villanueva-Arce, C. Pelayo-Zaldívar, M.T. Colinas-León, V. López-Martínez and S. Bautista-Bános. 2007. "Postharvest Physiology and Technology of Sapote Mamey Fruit." **Postharvest Biology and Technology** 45 (3) : 285–297.

[42] Evert-Fresh Inc. 2008. **Evert-Fresh Green Bags.** [online]. Available : http://www.evertfreshbags.co.uk/.

[43] Entrepreneur Inc. 2008. **New Consumer Bags Provide Longer-Life Produce.** [online]. Available : http://www.entrepreneur.com/tradejournals/article/178482503.html.

[44] Y. Wang, A.J. Easteall and X.D. Chen. 1998. "Ethylene and Oxygen Permeability through Polyethylene Packaging Films." **Packaging Technology and Science.** 11(4) : 169-178.

[45] H. Mujica-Paz and N. Gontard. 1997. "Oxygen and Carbon Dioxide Permeability of Wheat Gluten Film: Effect of Relative Humidity and Temperature." **Journal of Agricultural Food Chemistry.** 45 (10) : 4101-4105.

[46] H. Mujica-Paz, V. Guillard, M. Reynes and N. Gontard. 2005. "Ethylene Permeability of Wheat Gluten Film as a Function of Temperature and Relative Humidity." **Journal of Membrane Science.** 256 (1-2) : 108-115.

[47] Kraton Polymer LLC. 2006. **Data Document Kraton ® G1652M Polymer.** [Online]. Available : http://www.kraton.com/content/includes/An%20Intro%20To%20Kraton.pdf.

[48] Zeolyst International. 2006. **Data Sheet of ZSM-5 Type Zeolite Product (MFI).** [Online]. Available : http://www.zeolyst.com/html/zsm5.asp.

[49] ASTM D882 Committee on standard. 1998. **Standard Test Method for Tensile Properties of Thin Plastic Sheet.** New York : American Society for Testing Materials.

[50] J.C. Salamone. 1996. **Polymer Materials Encyclopedia.** New York : CRC Press.

[51] S. Jose, P.S. Thomas, S. Thomas and J. Karger-Kocsis. 2006. "Thermal and Crystallisation Behaviours of Blends of Polyamide 12 with Styrene-Ethylene/Butylenes-Styrene Rubbers." **Polymer.** 47(18) : 6328-6336.

[52] A. Mokrinia, M.A. Huneault, Z. Shib, Z. Xieb and S. Holdcroft. 2008. "Non-Fluorinated Proton-Exchange Membranes Based on Melt Extruded SEBS/HDPE Blends." **Journal of Membrane Science.** 325(2) : 749–757.

[53] H. Kim, J. Biswas and S. Choe. 2006. "Effects of Stearic Acid Coating on Zeolite in LDPE, LLDPE, and HDPE Composites." **Polymer.** 47(11) : 3981-3992.

[54] K. Soji. 2005. "Development of High Performance Elastomers with Inorganic Fillers 3 – The reinforcement Effect of Inorganic Fillers on Mechanical Properties of Vulcanizates." **Journal Society of Rubber Industry.** 78(7) : 273-279.

[55] J. Murphy. 2001. **Additive for plastic handbook.** USA : Elsevier Science.

[56] J. Biswas, H. Kim, C.S. Yim, J. Cho, G.J. Kim and S. Choe. 2004. "Structural Effect on the Tensile and Morphological Properties of Zeolite-Filled Polypropylene Derivative Composites." **Macromolecular Research.** 12(5) : 443-450.

[57] B.D. Freeman. 1999. "Basis of Permeability/Selectivity Trade off Relations in Polymeric Gas Separation Membrane." **Macromolecules.** 32(2) : 375-380.

[58] A.A. Kader and C.B.Watkins. 2000. "Modified Atmosphere Packaging Toward 2000 and Beyond." **Hort Technology.** 10(3) : 483-486.

[59] S.J. Metz, W.J.C. van de Ven, J. Potreck, M.H.V. Mulder and M. Wessling 2005. "Transport of Water Vapor and Inert Gas Mixtures through Highly Selective and Highly Permeable Polymer Membranes." **Journal of Membrane Science.** 251 (1-2) : 29-41.

[60] N. Kentaro, N. Shinji, S. Yasuhiro and N.Takanori. **Breathing film.** U.S. patent no. 6395071. May 2002.

[61] K.J. Laidler and J.H. Meiser. 1999. **Physical chemistry.** New York : Houghton Mifflin.

APPENDICES

APPENDIX A

LDPE BLOWN FILM

Table A.1 LDPE(30) film blowing process

Parameter	Data
Film blowing instrument	Single screw extruder connected with blow film unit
Extruder barrel temperature range	180-210 °C
Die zone temperature	215 °C
Blow up ratio	1.86
Cross head speed	320 rpm
Wide size of film	16 cm

Table A.2 Tensile properties of the LDPE(30) film

Blown film direction	Yield stress (MPa)	Tensile strength (MPa)	Young's modulus (MPa)	Elongation at break (%)
Machine direction (MD)	11.2 ± 0.2	16.6 ± 0.4	117 ± 9	436 ± 42
Transverse direction (TD)	11.5 ± 0.3	12.4 ± 0.3	137 ± 9	552 ± 106

APPENDIX B

WEIGHT FRACTION OF LDPE AND SEBS LAYERS

The weight fractions of LDPE and SEBS in the double-layered film were determined for the calculation of the normalized %crystallinity and the accurate zeolite contents in SEBS layer, respectively. The double-layered film was cut into a square shape with 3 × 3 cm^2 and weighed. After that, it was soaking in hot toluene (around 50 °C) for 1 hr in order to dissolve the SEBS. Then, the remained LDPE layer was cleaned with fresh toluene and then weighed. The %weight of LDPE and SEBS in the double-layered film can be calculated by following equation and was shown in Table B.2. Data presented are average of 5 replicated tests.

$$\%\text{Weight of LDPE} = \frac{\text{Weight of the remained LDPE layer}}{\text{Weight of the double-layered film}} \times 100$$

$$\%\text{Weight of SEBS layer} = 100 - \%\text{Weight of LDPE}$$

Table B.1 %Weight of LDPE and SEBS layers in the double-layered film

Sample	%Weight of LDPE layer	%Weight of SEBS layer
DB-0	38.97	61.03
DB-5SR	39.65	60.35
DB-10SR	42.13	57.87
DB-5WD	37.28	62.72
DB-10WD	38.76	61.24
DB-20WD	38.76	61.24
DB-30WD	37.41	62.59

APPENDIX C

CALCULATION

C1: Zeolite contents in SEBS layer

Table C.1 Data from TGA

Sample	%Weight of the residue (after 700 °C)
DB-0	1.871
DB-5SR	3.140
DB-10SR	8.167
DB-5WD	6.100
DB-10WD	7.884
DB-20WD	14.101
DB-30WD	21.488

From Table C.1, 1.87% weight of anti-blocking agent can be observed in the double-layered film without zeolite. Thus, it is assumed that all composite films already contain 1.87% weight of anti-blocking agent. The %weight of zeolite in SEBS layer was calculated following equation.

$$\%\text{Weight of zeolite in SEBS layer} = \frac{\%\text{Weight of the residue} - 1.871}{\%\text{Weight of SEBS layer}} \times 100$$

Example; DB-10WD

%Weight of the residue = 7.884

%Weight of SEBS layer (from Appendix B) = 61.24

$$\%\text{Weight of zeolite in SEBS layer} = \frac{(7.884 - 1.871)}{61.24} \times 100$$

$$= 9.82$$

C2: %Crystallinity

Sample	%Weight of anti-blocking agent ($W_{antiblock}$)	%Weight of LDPE layer (W_{LDPE})	ΔH_f (J/g)
DB-10WD	1.871	38.76	30.80

ΔH_f^0 (J/g) = 293 J/g (100% crystallinity of PE)

$$\%\text{Crystallinity} = \frac{\Delta H_f}{\Delta H_f^0} \times \frac{100}{W_{LDPE} - W_{antiblock}} \times 100$$

$$= \frac{30.80}{293} \times \frac{100}{38.76 - 1.871} \times 100$$

$$= 28.5$$

C3: Ethylene permeability

Peak area of standard ethylene, 530 ppm (A_S) 4024 count

Peak area of the permeated ethylene (A_E) 1100 count

$\therefore$ Concentration of the ethylene in permeated gas $= \frac{530 \times 1100}{4024}$

$= 145$ ppm or μL/L

$= 0.145$ mL/L

Flow rate of the permeated gas (F_X) 30.58 ml/min

$\therefore$ Transmission rate of ethylene (J) $= 0.145 \times 30.58$

$= 4.43$ ml · ml / L · min

$= 0.00443$ ml/min

Surface area of the film (A_F) 0.000314 m^2

Film Thickness (Δx) = 0.086 mm

Partial pressure difference of ethylene (Δp) = $Pi_{feed} - Pi_{permeate}$

= $Pi_{feed} - 0$

Partial pressure of C_2H_4 in feed (Pi_{feed}) = total absolute pressure × volume fraction of ethylene

Ethylene concentration in feed stream (%v)	20	40	60	80	100
Δp (atm)	0.202	0.404	0.606	0.808	1.01

$\therefore$ Flux of ethylene $= J / A_F$

$= 0.00443 / 0.000314$

$= 14.11 \text{ ml} / \text{min.m}^2$

$= 20318 \text{ cm}^3 / \text{m}^2\text{.day}$

$\therefore$ Ethylene transmission rate (ETR) $= J / (A_F \cdot \Delta p)$

$= \dfrac{0.00443}{0.000314 \times 1.01}$

$= 13.97 \text{ ml} / \text{min.m}^2$

$= 20115 \text{ cm}^3 / \text{m}^2\text{.day. atm}$

$\therefore$ Ethylene permeation (EP) $= (J \cdot \Delta x) / (A \cdot \Delta p)$

or $= \text{ETR} \times \text{Film thickness}$

$= 20115 \times 0.086$

$= 1738 \text{ cm}^3\text{.mm} / \text{day.m}^2\text{.atm}$

APPENDIX D

TGA THERMOGRAM

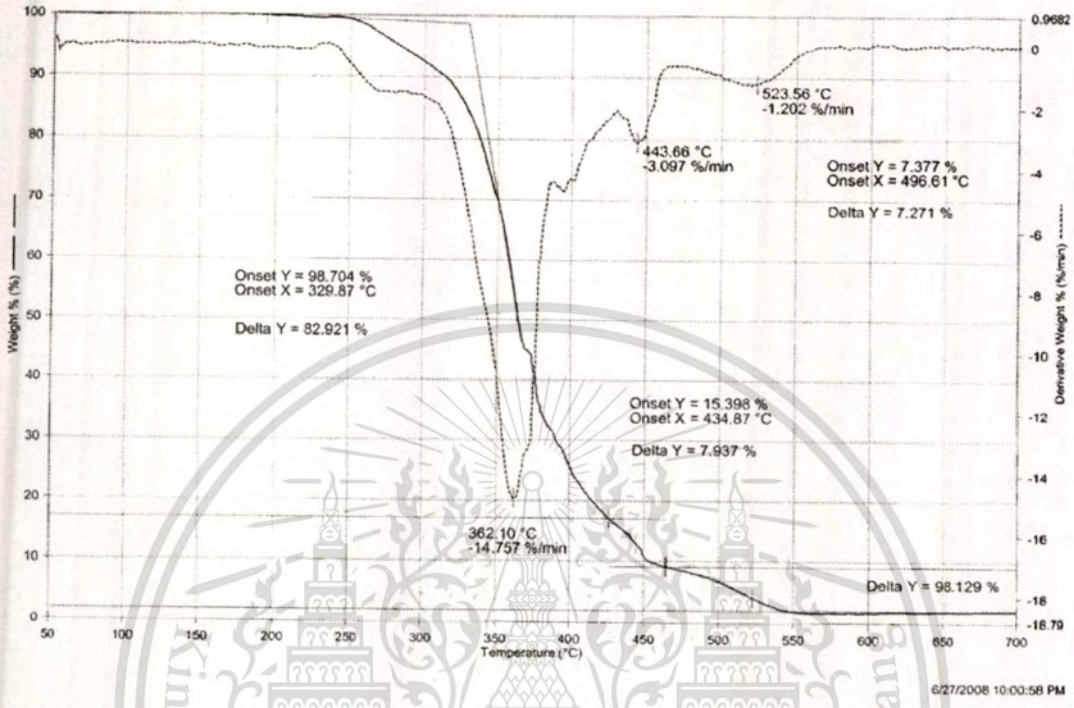

Figure D.1 Thermogram of DB-0 film

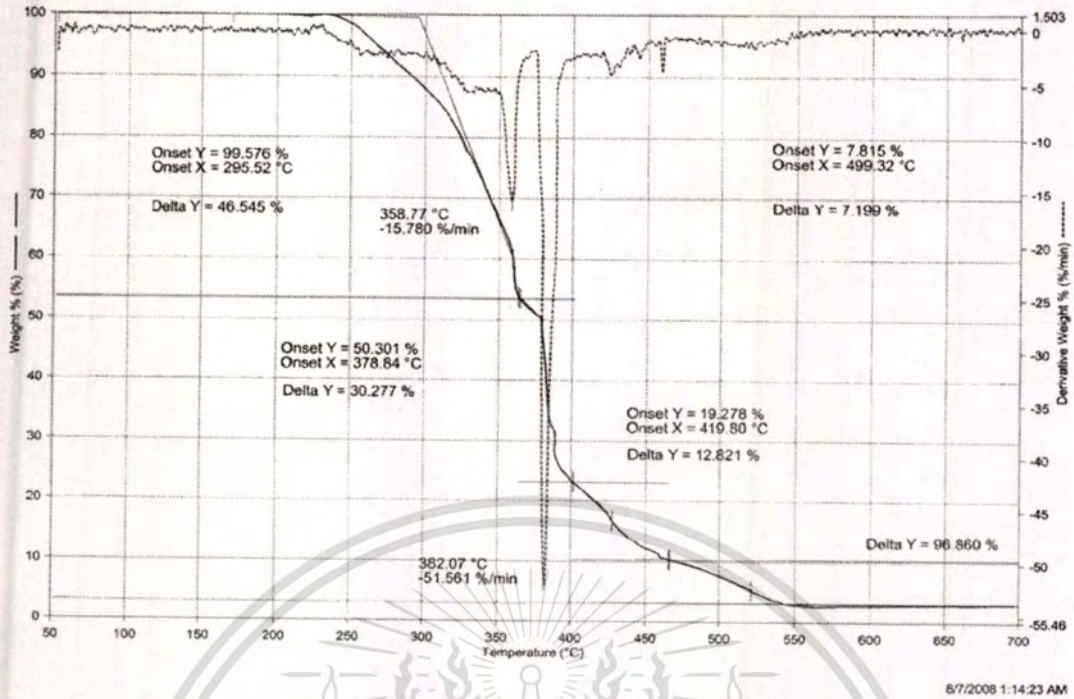

Figure D.2 Thermogram of DB-5SR film

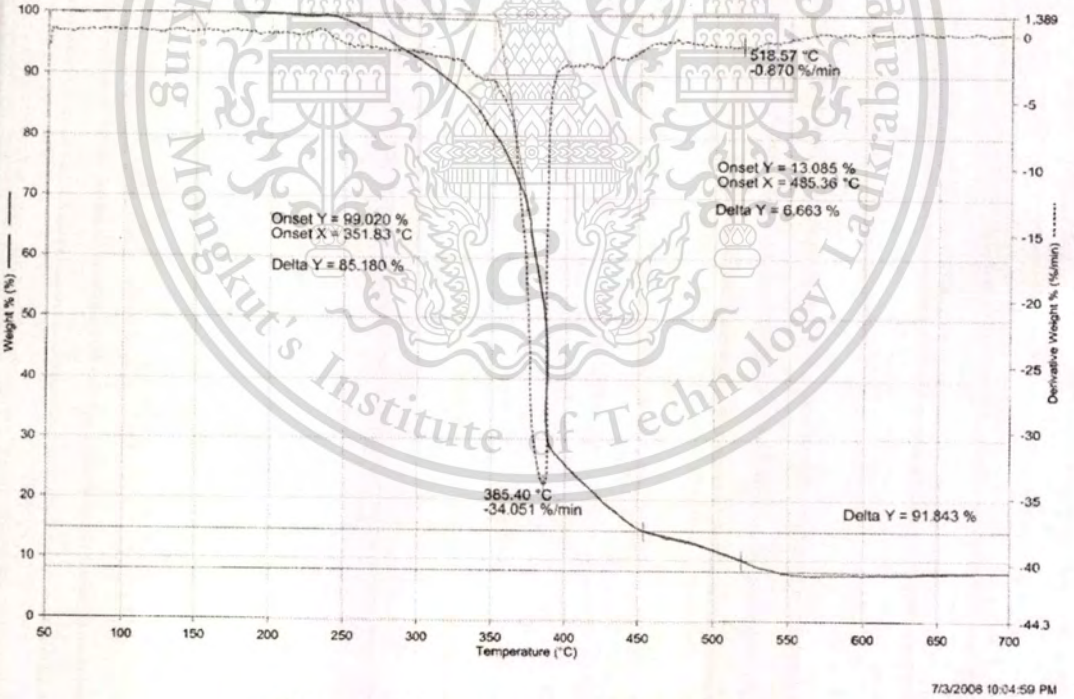

Figure D.3 Thermogram of DB-10SR film

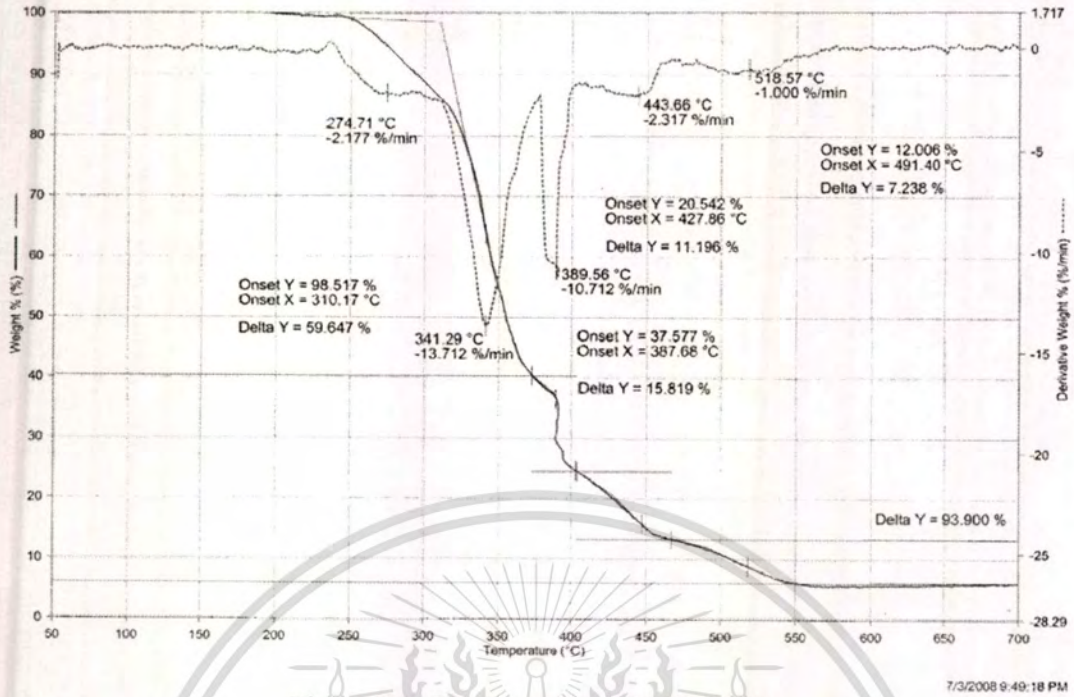

Figure D.4 Thermogram of DB-5WD film

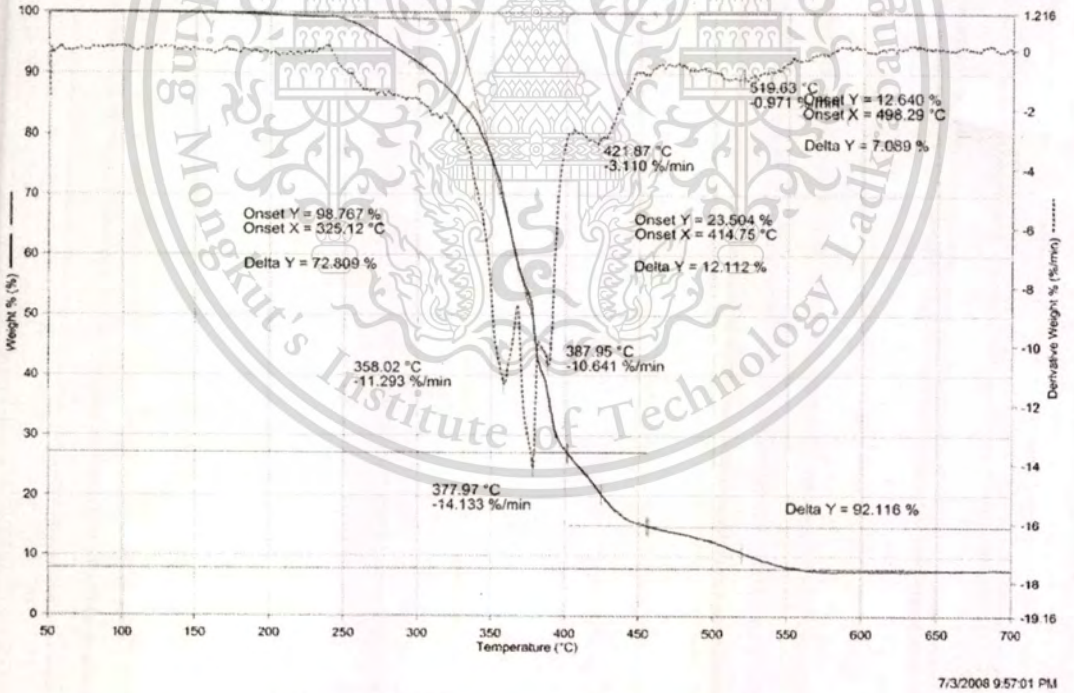

Figure D.5 Thermogram of DB-10WD film

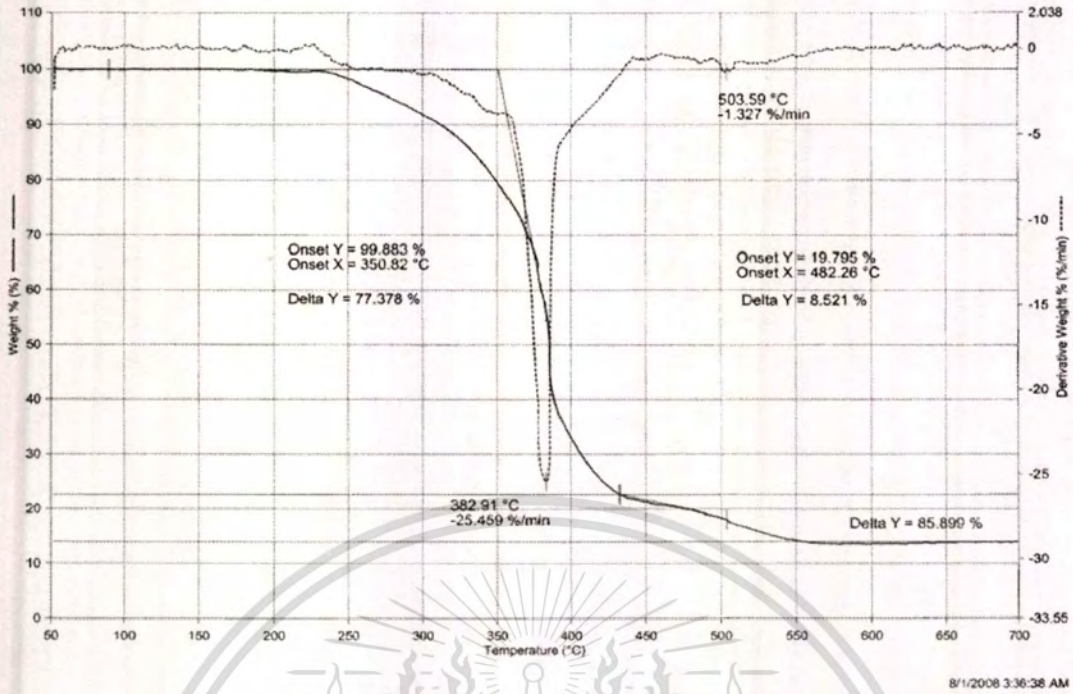

Figure D.6 Thermogram of DB-20WD film

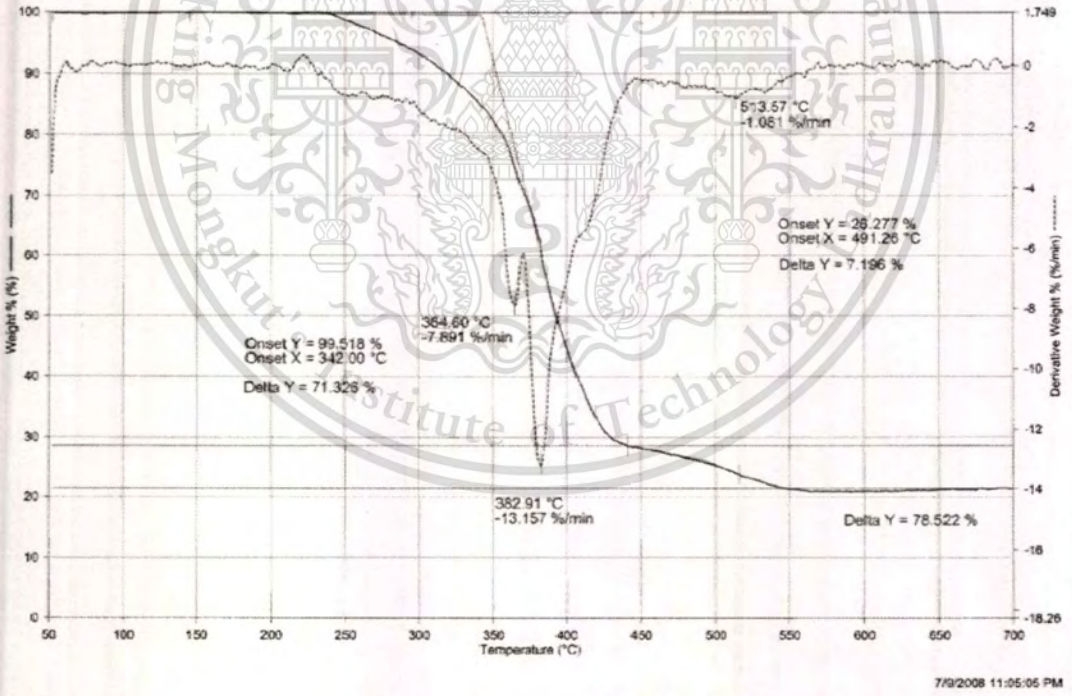

Figure D.7 Thermogram of DB-30WD film

APPENDIX E

DSC THERMOGRAM

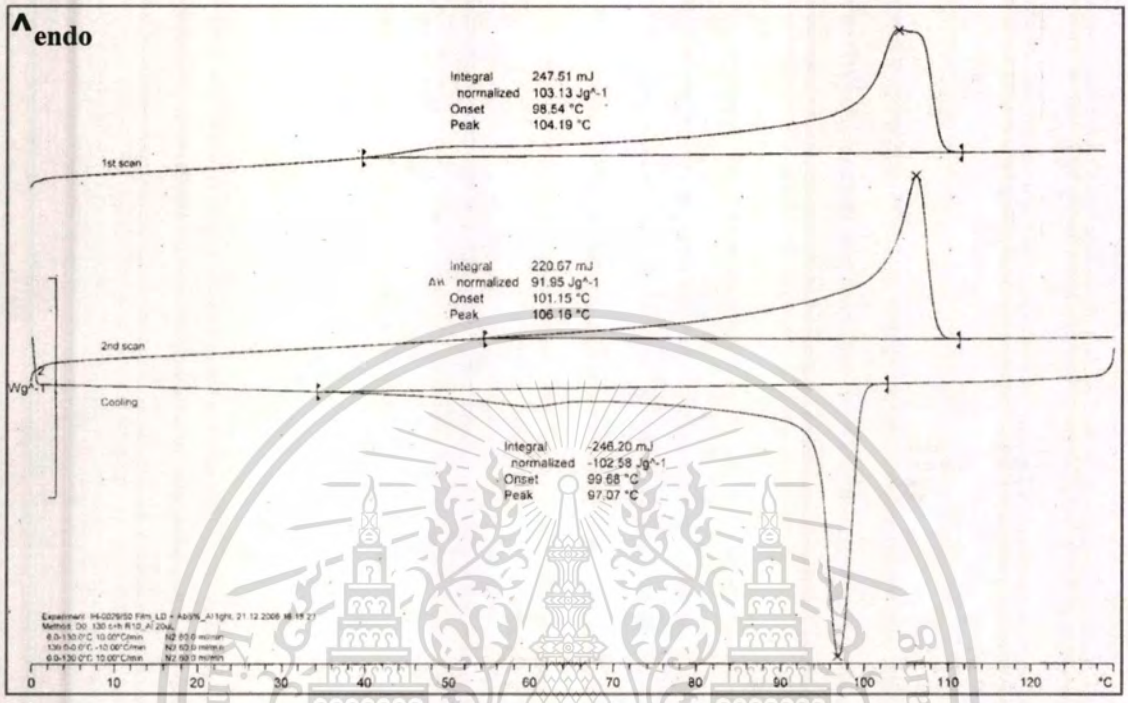

Figure E.1 Thermogram of LDPE film

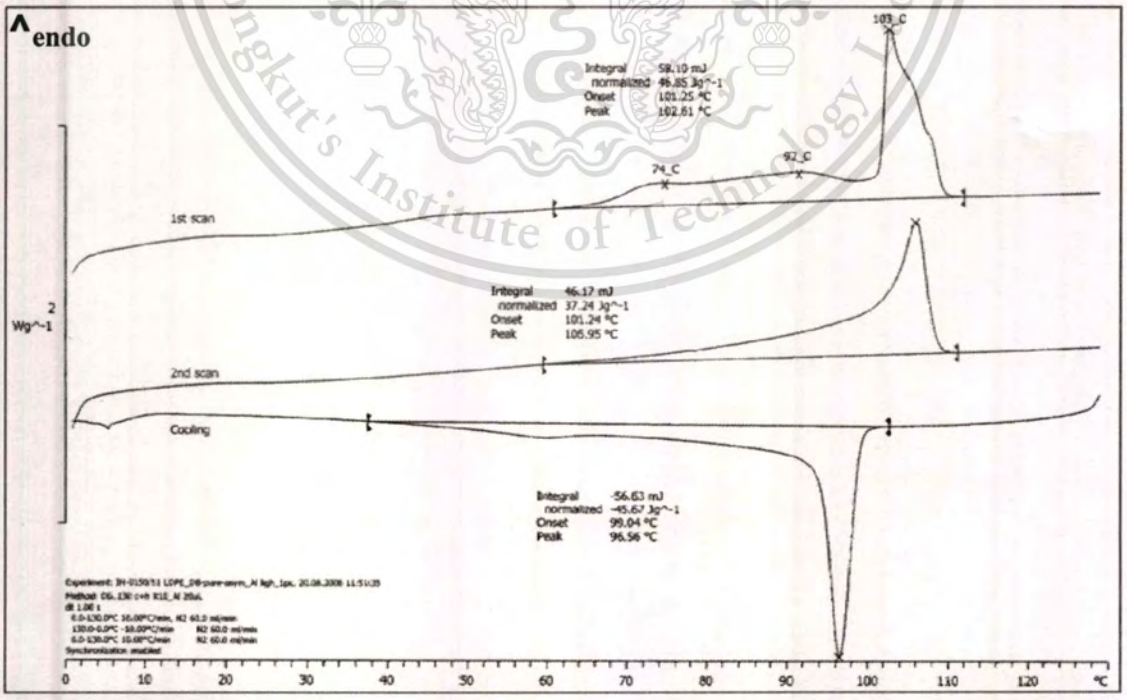

Figure E.2 Thermogram of DB-0 film

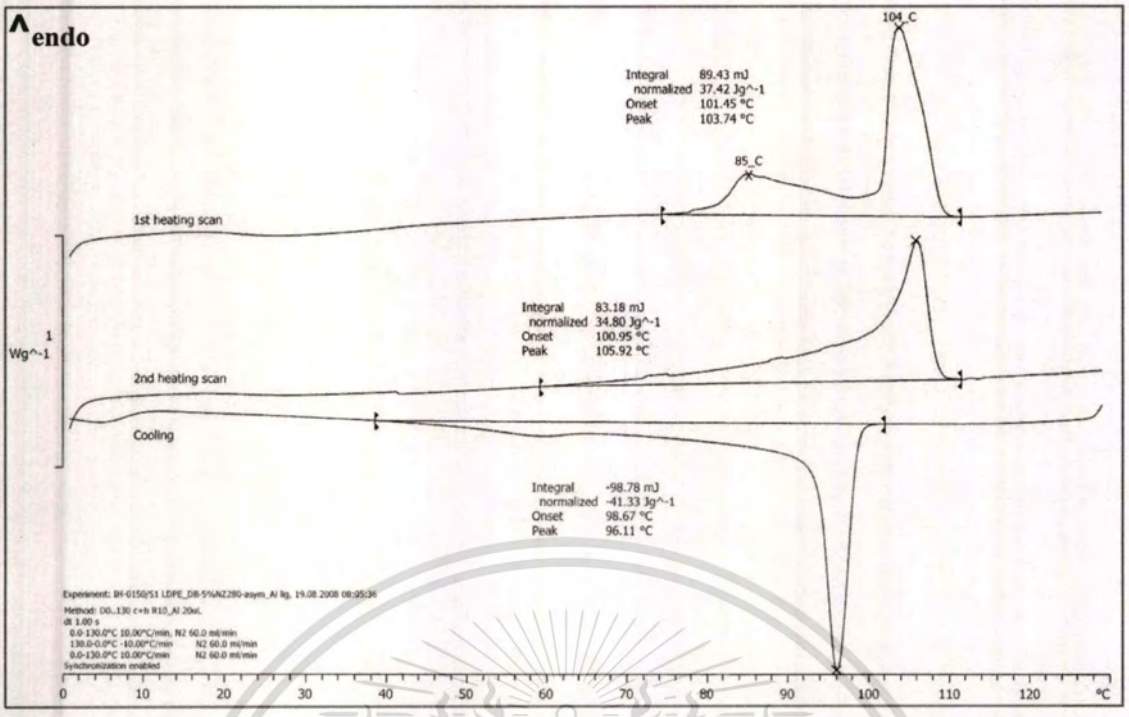

Figure E.3 Thermogram of DB-5SR film

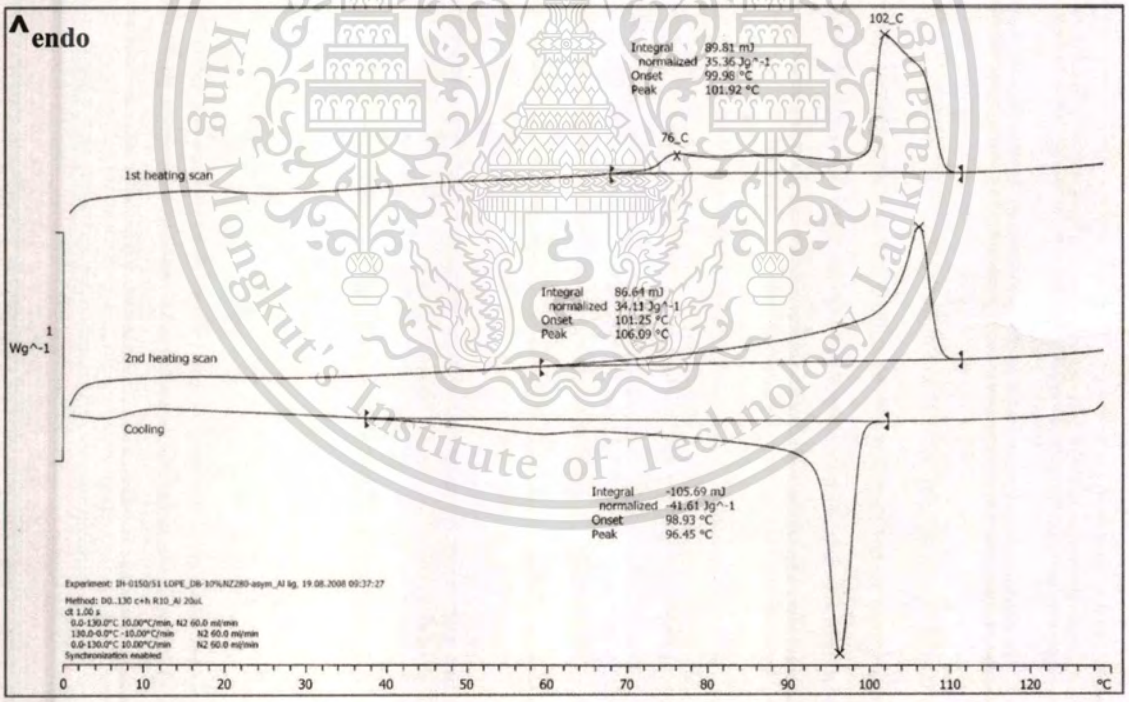

Figure E.4 Thermogram of DB-10SR film

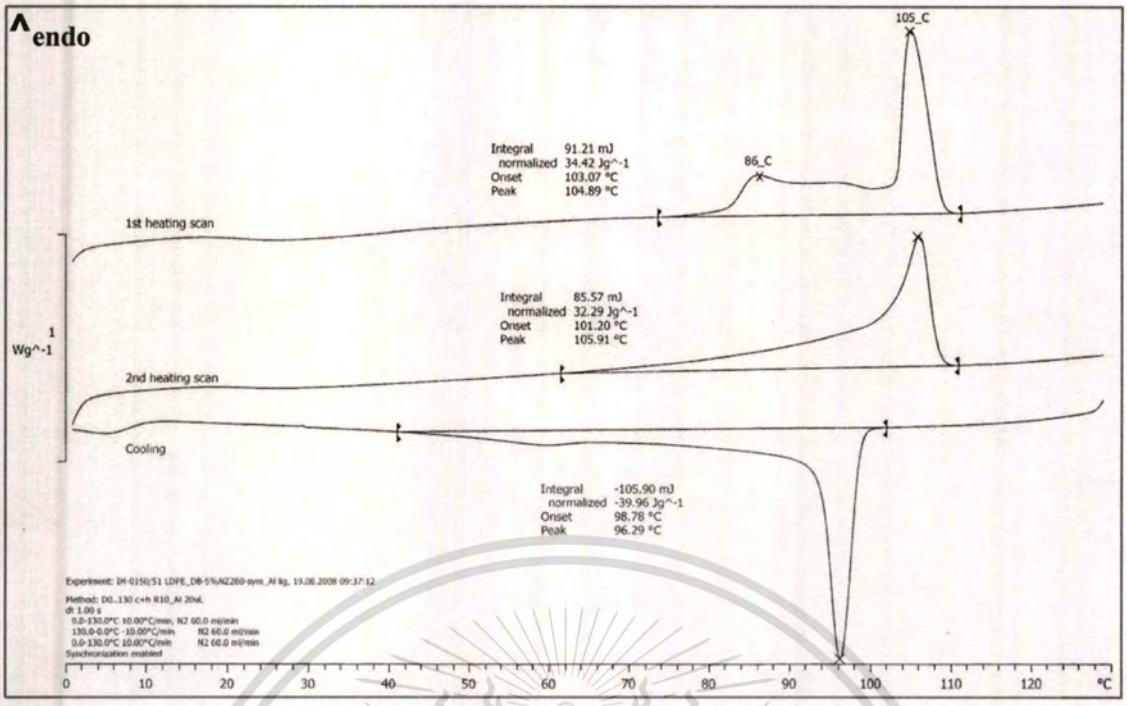

Figure E.5 Thermogram of DB-5WD film

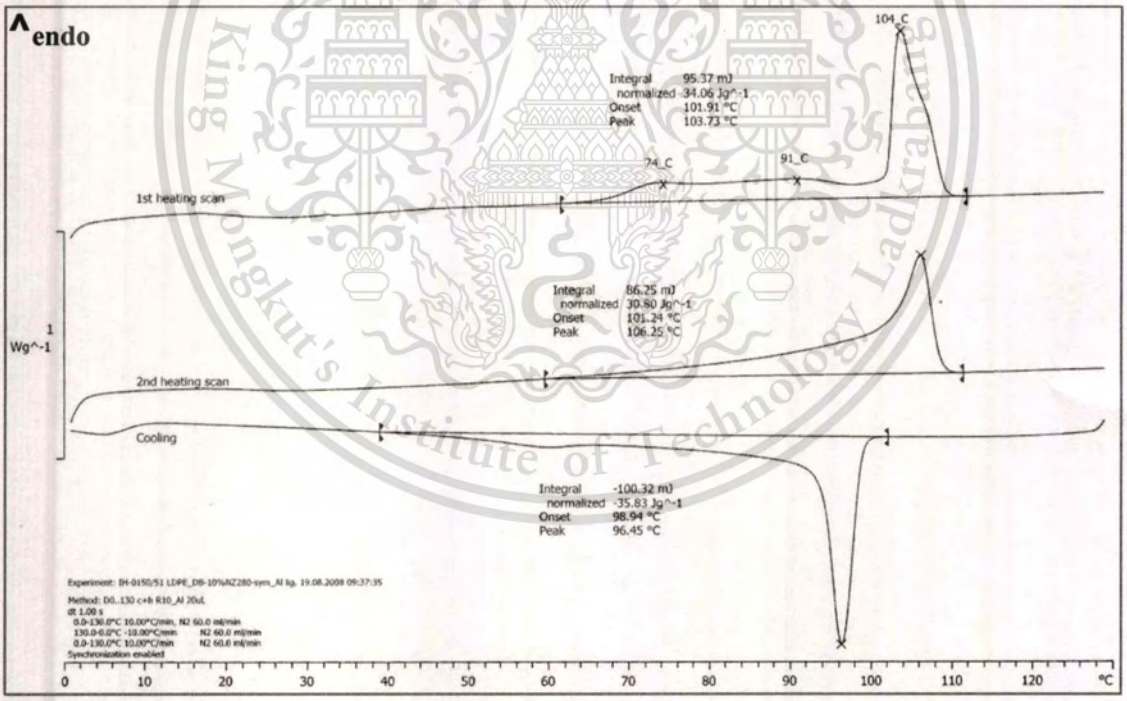

Figure E.6 Thermogram of DB-10WD film

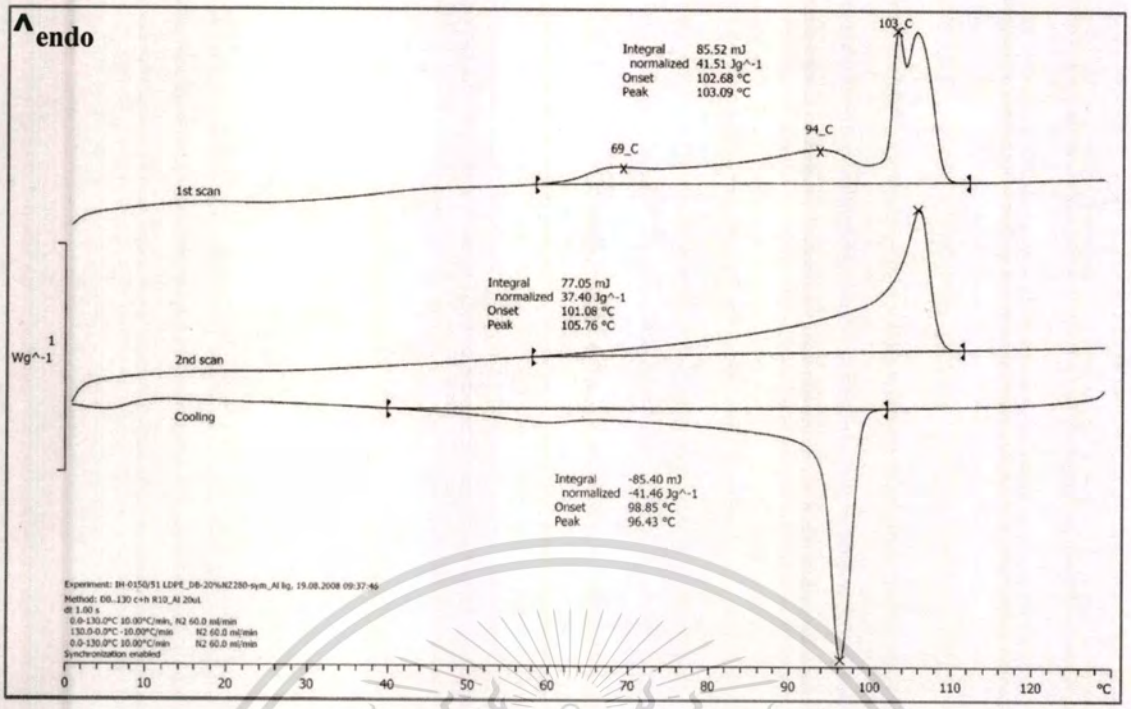

Figure E.7 Thermogram of DB-20WD film

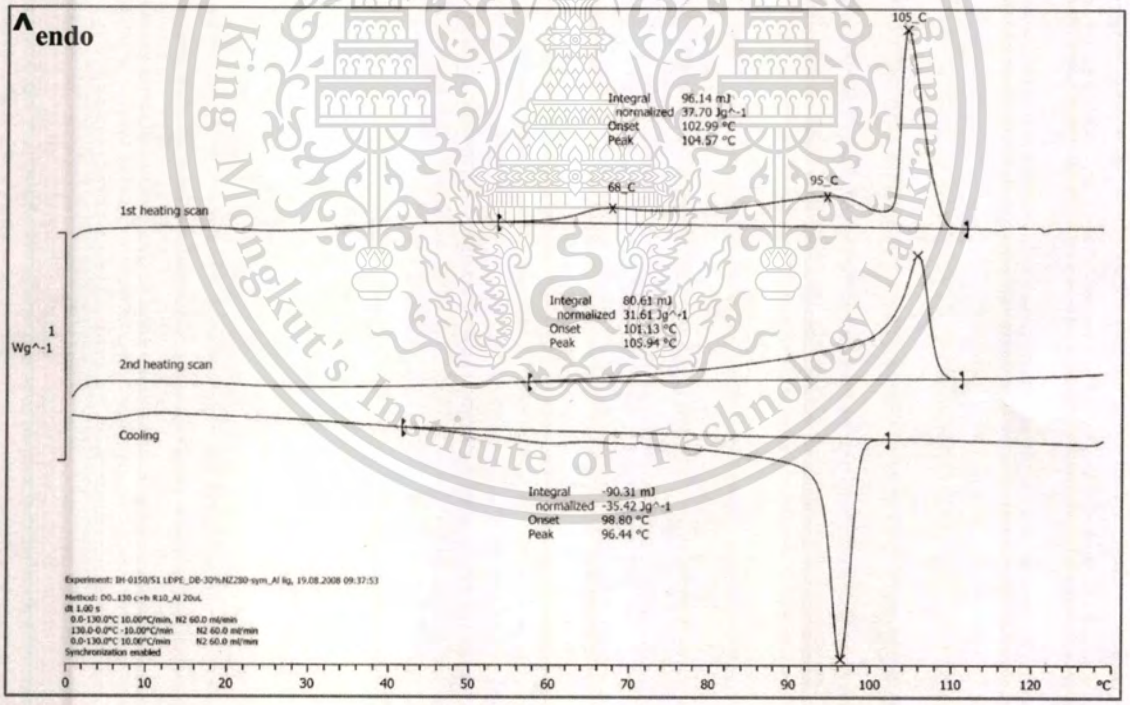

Figure E.8 Thermogram of DB-30WD film

APPENDIX F

PERMEATION

Table F.1 Ethylene permeation

Sample	Ethylene flux ($cm^3/m^2.day$)	Thickness (mm)	EP ($cm^3.mm/m^2.day.atm$)
LDPE	8663	0.083	722
	9133	0.087	798
	10112	0.079	795
			772
SEBS	61131	0.082	5037
	100758	0.072	7234
	79990	0.069	5551
			5941
DB-0	21811	0.082	1797
	21099	0.087	1844
	20113	0.086	1738
			1793
DB-5SR	28185	0.081	2283
	26587	0.075	1999
	23078	0.077	1786
			2023
DB-10SR	27449	0.069	1905
	28970	0.080	2329
	28868	0.068	1957
			2064

Table F.1 Ethylene permeation (cont)

Sample	Ethylene flux ($cc/m^2.day$)	Thickness (mm)	EP ($cm^3.mm/m^2.day.atm$)
DB-5WD	28790	0.087	2511
	29937	0.084	2509
	26418	0.090	2367
	22197	0.092	2038
			2356
DB-10WD	30274	0.088	2667
	24035	0.088	2110
	24375	0.085	2057
	29579	0.084	2476
			2328
DB-20WD	29275	0.083	2424
	28825	0.077	2231
	31046	0.080	2471
			2375
DB-30WD	28843	0.081	2331
	28608	0.082	2340
	29543	0.083	2446
			2372

Table F.2 Ethylene permeation as various ethylene concentrations in feed stream

Sample	Ethylene concentration (%v)	Ethylene flux ($cm^3/m^2.day$)		EP ($cm^3.mm/m^2.day.atm$)	
		Under N_2	Under air zero	Under N_2	Under air zero
DB-0	20	5292	3131	2096	1240
	40	9858	7030	1952	1392
	60	14438	11067	1906	1461
	80	19453	15069	1926	1492
DB-10SR	20	6065	4883	2402	1934
	40	12549	10403	2485	2060
	60	15764	15650	2081	2066
	80	22796	20816	2257	2061
DB-10WD	20	6403	4974	2536	1970
	40	13367	10156	2647	2011
	60	17710	15309	2338	2021
	80	23745	21463	2351	2125

Table F.3 Oxygen permeation

Sample	Oxygen flux ($cm^3/m^2.day$)	Thickness (mm)	OP ($cm^3.mm/m^2.day.atm$)
LDPE	3642	0.059	215
	2739	0.079	217
			216
SEBS	17033	0.072	1220
	13410	0.085	1145
			1182
DB-0	6396	0.085	544
	5635	0.082	464
			504
DB-5SR	6702	0.079	531
	6390	0.080	511
			521
DB-10SR	5860	0.069	405
	6146	0.074	457
			431
DB-5WD	5855	0.083	488
	6076	0.083	504
			496
DB-10WD	5659	0.085	483
	5452	0.086	470
			477
DB-20WD	6207	0.068	420
	5901	0.071	417
			418
DB-30WD	5967	0.082	492
	6314	0.083	523
			507

Table F.4 Carbon dioxide permeation

Sample	Carbon dioxide flux ($cm^3/m^2.day$)	Thickness (mm)	CO_2P ($cm^3.mm/m^2.day.atm$)
LDPE	5938	0.074	442
	5705	0.076	432
			437
SEBS	54621	0.080	4359
	52322	0.082	4301
			4330
DB-0	18655	0.088	1645
	18129	0.087	1574
			1690
DB-5SR	15708	0.083	1298
	16031	0.074	1180
			1239
DB-10SR	15019	0.078	1171
	16235	0.080	1295
			1233
DB-5WD	12772	0.089	1137
	15462	0.082	1268
			1202
DB-10WD	13012	0.080	1038
	16450	0.083	1375
	15591	0.083	1300
			1238
DB-20WD	15078	0.081	1227
	14229	0.085	1212
			1220
DB-30WD	16530	0.079	1303
	13894	0.081	1123
			1213

Table F.5 Water vapor permeation

Sample	WVTR ($g/m^2.day$)	Thickness (mm)	WVP ($g.mm/m^2.day$)
LDPE	6.13	0.079	0.48
	5.94	0.075	0.44
			0.46
SEBS	33.1	0.071	2.35
	35.9	0.069	2.48
			2.42
DB-0	10.93	0.080	0.88
	10.23	0.077	0.79
			0.84
DB-5SR	11.63	0.085	0.99
	11.83	0.081	0.96
			0.98
DB-10SR	13.57	0.063	0.86
	13.67	0.061	0.84
			0.85
DB-5WD	11.63	0.091	1.06
	11.83	0.089	1.06
			1.06
DB-10WD	12.03	0.086	1.03
	11.63	0.089	1.04
			1.04
DB-20WD	10.9	0.085	0.93
	10.3	0.083	0.86
			0.90
DB-30WD	10.2	0.082	0.84
	10.2	0.078	0.80
			0.82

AUTHOR BIOGRAPHY

Miss Pornpan Monprasit was born on September 24, 1984 in Rayong. She received her B.Sc. in Industrial Chemistry from King Mongkut's Institute of Technology Ladkrabang in 2006. She has been graduated student of the Polymer Technology, Faculty of science, King Mongkut's Institute of Technology Ladkrabang, since 2006.

This thesis had two publications in i) Study on ethylene gas permeability of double-layer composite film, Oral presentation in Pure and Applied Chemistry International Conference 2009 (PACCON), Naresuan university, Phitsanulok, Thailand, 14-16 January 2009, ii) Poster presentation in The 6th International Symposium on Advanced Materials in Asia – Pacific Rim (ISAMAP), Chulalongkorn University, Bangkok, Thailand, 21-23 November 2009.

SCHOLARSHIP:

2007-2008 Thailand Graduate Institute of Science and Technology, (TGIST: MTEC division) from National Science and Technology Development Agency (NSTDA), Pathumtani, Thailand (Funded Code: TG-11-12-49-001M).